Universidad Autónoma de Madrid
Programa de Doctorado en Biociencias Moleculares

Study of the effects of *in vivo* telomere elongation mechanisms in cancer and aging

DOCTORAL THESIS

Miguel Ángel Muñoz Lorente

Madrid, 2019

DEPARTAMENTO DE BIOLOGÍA MOLECULAR

FACULTAD DE CIENCIAS

UNIVERSIDAD AUTÓNOMA DE MADRID

Study of the effects of *in vivo* telomere elongation mechanisms in cancer and aging

DOCTORAL THESIS

Miguel Ángel Muñoz Lorente
BSc, MSc

The entirety of the work presented in this Thesis has been carried out at the Telomeres and Telomerase Group in the Spanish National Cancer Centre (CNIO, Madrid) under the direction and supervision of Dr. Maria Blasco Marhuenda

Madrid, 2019

Summary/ Resumen

1. English

Short and dysfunctional telomeres are sufficient to induce a persistent DNA damage response at chromosome ends, which leads to the induction of senescence and/or apoptosis and trigger age-related pathologies including a group of diseases known as “telomere syndromes”, and shorter lifespans in mice and humans. In turn, maintenance of longer telomeres owing to telomerase overexpression in adult tissues delays aging and increases mouse longevity. This opens the possibility of using telomerase activation as a potential therapeutic strategy to rescue short telomeres both in telomere syndromes and in age-related diseases. However, telomerase has been found re-activated in most of human cancers making telomerase therapy a potential risk in treating short telomere accumulation. In this regard, telomere elongation avoiding the overexpression of telomerase could be a safer answer to prevent short telomeres delaying or even avoiding short telomere related pathologies.

Based on this, the first aim of this thesis is to test the safety of telomerase gene therapy in the context of a cancer prone mouse model. To this end, we treated a well stablished K-Ras mediated lung cancer mouse model with AAV9-*Tert* for telomerase overexpression. As control, we also treated mice with AAV9 vectors carrying a catalytically inactive form of *Tert*, known to inhibit endogenous telomerase activity. We found that overexpression of *Tert* does not accelerate the onset or progression of lung carcinomas, even when in the setting of a p53-null background. These findings indicate that telomerase activation by using AAV9-mediated *Tert* gene therapy has no detectable cancer-prone effects in the context of oncogene-induced mouse tumors.

On the other hand, the second aim of this thesis is to address whether embryonic stem (ES) cells carrying telomeres elongated in the absence of genetic modifications could contribute to the formation of a healthy organism and whether these elongated telomeres may have any deleterious effects. In this regard, we generated mice in which 100% of their cells are derived from hyper-long telomere ES cells. We found that these mice have longer telomeres and less DNA damage with aging. Interestingly, they are leaner than normal due to lower body fat accumulation. They also show less metabolic aging as indicated by lower cholesterol and LDL levels, and by improved glucose and insulin tolerance. Importantly, mice with hyper-long telomeres have less cancer and show an increased longevity. These findings demonstrate that longer telomeres than normal in a given species are not deleterious but instead, show beneficial effects.

2. Español

La acumulación de telomeros cortos es suficiente para inducir una respuesta de daño persistente en el ADN, induciendo sensecencia y/o apoptosis. Este fenómeno es la principal causa de las patologías relacionadas con la edad, incluyendo un grupo de enfermedades conocidas como “síndromes teloméricos”, así como de una menor esperanza de vida tanto en ratones como en humanos. Consecuentemente, la sobreexpresión de telomerasa en adultos es capaz de retrasar el envejecimiento y aumentar la esperanza de vida en ratones, pudiendo usar esta enzima como una potencial estrategia terapéutica para tratar estas enfermedades. Sin embargo, la telomerasa se ha visto re-activada en la mayoría de cánceres humanos, haciendo de esta terapia un riesgo potencial a la hora de tratar las enfermedades relacionadas con los telómeros. A este respecto, la elongación de los telómeros evitando la sobreexpresión de telomerasa podría ser una forma más segura de tratar dichas patologías retrasando o incluso evitando la aparición de telómeros cortos.

En base a esto, el primer objetivo de esta tesis es probar la seguridad de la terapia génica con telomerasa en el contexto de un modelo animal propenso a padecer cáncer. Para ello, hemos tratado un modelo de ratón muy establecido que desarrolla cáncer de pulmón con AAV9-*Tert*. Como control, también hemos tratado estos animales con vectores virales AAV9 que contienen una forma catalíticamente inactiva de *Tert*, conocida por inhibir la actividad telomerasa endógena. Los resultados de este ensayo mostraron que la sobreexpresión de *Tert* no es capaz de acelerar la aparición ni la progresión del cáncer de pulmón, incluso en un fondo genético que carece de p53. Este descubrimiento indica que la activación de telomerasa usando la terapia génica mediada por vectores AAV9 no tiene ningún efecto oncogénico en el cáncer de pulmón en ratones.

Por otro lado, el segundo objetivo de esta tesis ha sido demostrar si células madre embrionarias poseedoras de telómeros elongados sin necesidad de modificaciones genéticas podrían contribuir a la formación de organimos sanos y si estos telómeros podrían tener algún efecto deletéreo. Por ello, fuimos capaces de generar ratones en los que el 100% de sus células derivan de las células madre con telómeros súper-largos. Encontramos que estos animales presentan telómeros más largos y menor daño en el ADN con la edad. Interesantemente, eran más delgados de lo normal debido a una menor acumulación de grasa corporal. También mostraron una menor edad metabólica indicada por bajos niveles de colesterol y LDL y por una mejorada tolerancia a la glucosa y la insulina. Importantemente, estos animales tienen menos cáncer y una mayor longevidad. Estos descrubrimientos demuestran que tener telómeros más largos de los habituales para una especie no es deletéreo, sino que presenta efectos beneficiosos.

Index

Abbreviations

a.u.f./a.u.	**A**rbitrary **U**nits (of **F**luorescence)
AC3	**A**ctive **C**aspase **3**
AKT	**AKT** Serine/Threonine Kinase
ALT	**A**lternative **L**engthening of **T**elomeres
alt-NHEJ	**alt**ernative **N**on-**H**omologous **E**nd **J**oining
APBs	**A**LT-associated-**P**ML **B**odies
ATCC	**A**merican **T**ype **C**ulture **C**ollection
ATM	**A**taxia **T**elangiectasia **M**utated
ATR	**A**taxia **T**elangiectasia **R**elated
ATRX	**A**lpha **T**halassemia/Mental **R**etardation Syndrome **X**-Linked
BLM	**Bl**oo**m**'s syndrome helicase
BSA	**B**ovine **S**erum **A**lbumin
c-NHEJ	**c**lassical **N**on-**H**omologous **E**nd **J**oining
CElyBA	**C**omite de **Ét**ica de **B**ienestar **A**nimal
Chk1	**Ch**eckpoint **k**inase 1
Chk2	**Ch**eckpoint **k**inase 2
CT	**C**omputed **T**omography
CNIO	**C**entro **N**acional de **I**nvestigaciones **O**ncológicas
D-Loop	**D**isplacement **Loop**
DAPI	4',6-**D**i**a**midino-2-**p**heny**l**indole dihydrochloride
DC	**D**yskeratosis **C**ongenita
DDR	**D**NA-**D**amage **R**esponse
DKC1	**D**ys**k**erin 1

DMEM	**D**ulbecco's **M**odified **E**agle's **M**edium
DNA-PK	**DNA**-dependent **P**rotein **K**inase
DSB	**D**ouble-**S**trand **B**reak
FBS	**F**etal **B**ovine **S**erum
FELASA	**F**ederation of **E**uropean **L**aboratory **A**nimal **S**cience **A**ssociations
G4	**G**uanine **4** (Guanine Quadruplex)
GEMM	**G**enetically **E**ngineered **M**ouse **M**odels
GFP	**G**reen **F**luorescent **P**rotein
GRO	**G**uanine-**R**ich **O**ligonucleotides
HA tag	**H**em**a**gglutinin **tag**
HDR	**H**omology-**D**irected **R**epair
iPS cells	**I**nduced **P**luripotent **S**tem cells
K-Ras^{G12V}	**K**irsten **Ra**t **S**arcoma viral oncogene, with a mutation in codon **12** that generates a **G**lycine to **V**aline transition
Kb	**K**ilo **b**ases
KO	**K**nock**o**ut
LFL	**L**i-**F**raumeni **l**ike-families
MRN	Complex formed by **M**RE11, **R**AD50 and **N**BS1
MTS	**M**ulti**t**elomeric **S**ignals
MYC	**My**elo**c**ytomatosis viral oncogene homolog
NHEJ	**N**on-**H**omologous **E**nd **J**oining
PARP1	**P**oly-**A**denosine diphosphate **R**ibose **P**olymerase **1**
PARP2	**P**oly-**A**denosine diphosphate **R**ibose **P**olymerase **1**

PBS	**P**hosphate **B**uffered **S**aline
PML	**P**ro**m**yelocytic **L**eukaemia
POT1	**P**rotection **o**f **T**elomeres **1**
PTEN	**P**hosphatase and **Ten**sin Homolog
RAD50	**RAD50** double strand break repair protein
RAP1	**R**epressor **A**ctivator **P**rotein **1**
RT	**R**oom **T**emperature
S phase	DNA **S**ynthesis phase of cell cycle
Sh	**S**hort-**H**airpin
ssDNA	**s**ingle **s**trand **DNA**
T-Loop	**T**elomere **Loop**
T-oligos	**T**elomere homolog **Oligo**nucleotide**s**
TBS	**T**ris **B**uffered **S**aline
Terc	**Te**lomerase **R**NA **C**omponent
TERT	**Te**lomerase **R**everse **T**ranscriptase
TIF	**T**elomere **I**nduced **F**oci
TIN2	**T**RF1 **In**teracting Protein **2**
TPP1	**T**INT1/**P**TOP/**P**IP**1**
TRF1	**T**elomere **R**epeat binding **F**actor **1**
TRF2	**T**elomere **R**epeat binding **F**actor **2**
Vg	**v**iral **g**enomes
WT	**W**ild **T**ype
γH2AX	Gamma-phosphorylated **H**istone **2** variant **A.X**

(c)DNA	(**c**omplementary) **D**eoxyribo**n**ucleic **A**cid
(m)RNA	(**m**essenger) **R**ibo**n**ucleic **a**cid
(p)RPA	(**p**hosphorylated) **R**eplication **P**rotein **A**
(Q-)FISH	(**Q**uantitative) **F**luorescence ***I**n **S**itu* **H**ybridization
(RT-q)PCR	(**R**eal **T**ime-**q**uantitative) **P**olymerase **C**hain **R**eaction
53BP1	p**53 B**inding **P**rotein **1**

Introduction

1. Telomeres: origin and structure

1.1 Discovery of telomeres

Telomeres are nucleoprotein structures localized at the very end of linear chromosomes. The word telomere originally derived from the Greek nouns “telos” (end) and “mere” (part). They were first described in *Drosophila* and maize cells by Hermann Müller and Barbara McClintock, respectively. They observed that the end of the chromosomes naturally lacks of chromatic fusions and therefore, they postulated the existence of a structure protecting chromosomal extremities (Muller, 1938; McClintock, 1941). Several years later, in 1978, the structure of the chromosome end was deciphered by Elizabeth Blackburn and Joe Gall showing that eukaryotic telomeres consist of tandem repeats of oligonucleotide sequences (Blackburn and Gall, 1978). This unprecedented achievement was follow by the discovery of telomerase, a ribonucleoprotein with reverse transcriptase activity, able to elongate telomeres (Greider and Blackburn, 1985; Blasco *et al.*, 1997; Hanahan and Weinberg, 2011).

In the present day, telomeres have been deeply studied and many of their functions pointed out they are key elements in two of the major concerns of our times, aging and cancer, making telomeres one of the primary hallmarks of aging (López-Otín *et al.*, 2013).

1.2 The telomeric structure

1.2.1 Primary structure: telomeres and the shelterin complex

The telomeric DNA is a highly conserved heterochromatic structure localized at the end of eukaryotic chromosomes. This region lacks the presence of protein-coding genes and in mammals is composed by tandem repeats of the 5’-TTAGGG-3’ sequence (**Figure 1**) (Meyne, Ratliff and Moyzis, 1989), ending in a guanine-rich, single stranded 3’ overhang of approximately 150-200pb, known as G-strand overhang. This structure is essential for chromosome stability as explained later (Klobutcher *et al.*, 1981; Griffith *et al.*, 1999).

Telomere length has been found to be heterogeneous across species and even within the same species, directly dependent on the developmental stage and the cell type (Flores *et al.*, 2008; Marion *et al.*, 2009). In humans, telomeres fluctuate between 5 to 15 kb (de Lange *et al.*, 1990) whereas the average of murine telomeric length spans between 15 and 40 kb, depending on the genetic background (Zijlmans *et al.*, 1997; Hemann and Greider, 2000). Within a certain species telomere length varies between organs, tissues, cell

types and even between different DNA ends in the same chromosome (Lansdorp *et al.*, 1996; Zijlmans *et al.*, 1997; Canela, Klatt and Blasco, 2007; Flores *et al.*, 2008). This remarkable heterogeneity does not alter the function of the telomere as long as their sizes remains above the critical length required for the proper protection of the chromosome and the maintenance of genomic stability (Blasco *et al.*, 1997; Lee *et al.*, 1998).

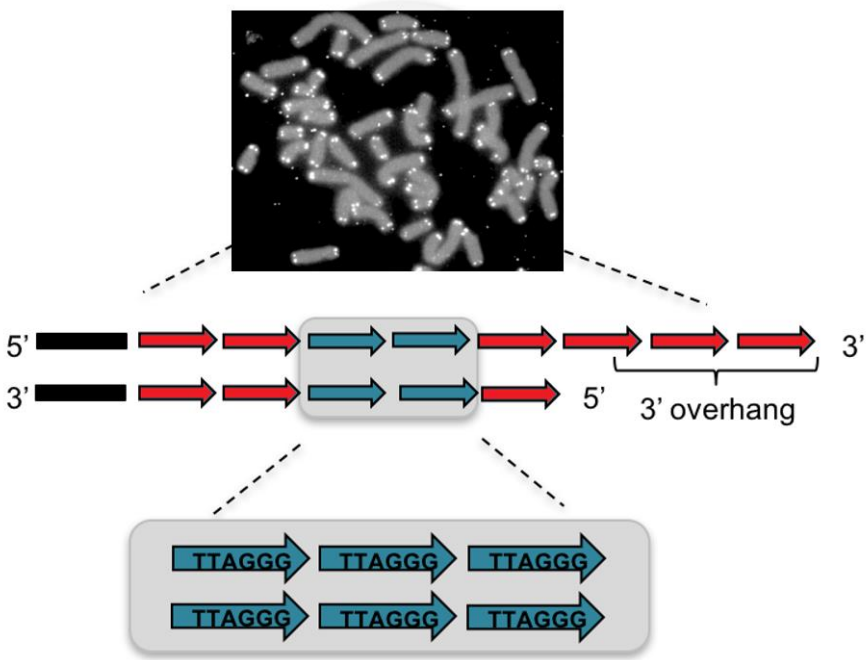

Figure 1. The telomeric structure. Schematic description of the telomere, composed by tandem repeats of the DNA sequence TTAGGG.

Telomeric DNA in mammals is bound to a set of proteins known as shelterin complex, composed by the telomere repeat factors 1 and 2 (TRF1 and TRF2), the TRF1-interacting factor 2 (TIN2), the Protection of Telomeres 1 (POT1), the POT1-TIN2 organizing protein TPP1 (also known as TINT1, PTOP or PIP1) and the repressor/activator protein 1 or RAP1 (De Lange, 2002, 2005; Liu *et al.*, 2004). Of these, TRF1 and TRF2 bind double stranded DNA repeats and interact between each other through TIN2 (Houghtaling *et al.*, 2004; Jeffrey Zheng Sheng Ye *et al.*, 2004). On the other side, POT1 binds to the single stranded G-rich overhang DNA (De Lange, 2005) and is connected with the rest of the proteins by a direct binding to TPP1 which at the same time also binds TIN2 (De Lange, 2005) (**Figure 2**).

The shelterin complex constitutes the so-called “capping” of the telomeres, being essential for their protection, preventing the degradation of the telomere and chromosomic fusions (De Lange, 2005). This complex also avoids the recognition of telomeric DNA as double strand breaks (DSB) and thus from activating DNA damage responses (DDR) (De

Lange, 2005) in the cell. Among these functions, shelterin proteins also play an essential role in telomere length regulation, as detailed below.

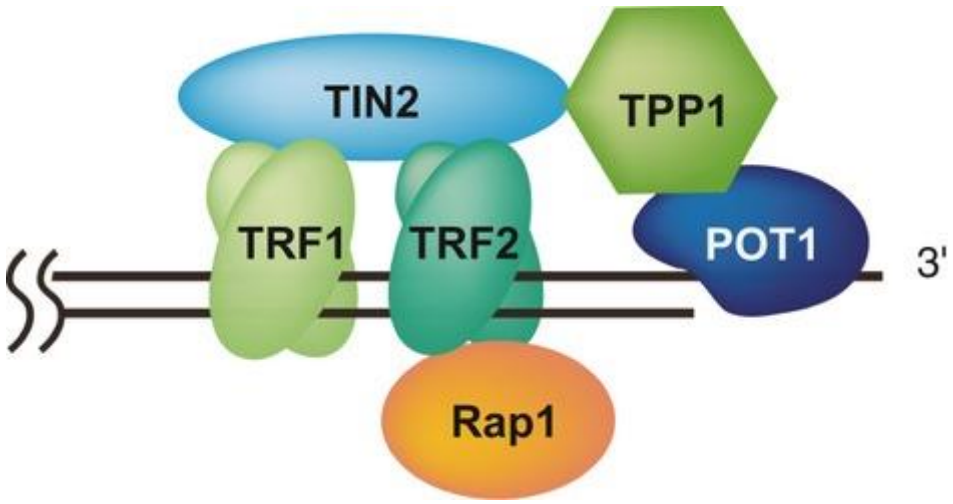

Figure 2. The shelterin complex. Schematic conformation of the different shelterin component and their interactions. From Fuyuki I., 2013.

TRF1 and TRF2

These two proteins show a high homology structure (Bianchi *et al.*, 1997; Broccoli *et al.*, 1997). They both bind the double strand repetitive DNA of the telomere as homodimers (Bianchi *et al.*, 1997; Broccoli *et al.*, 1997). Regarding their function, the main role of these two proteins consist in telomere length regulation (Smogorzewska *et al.*, 2000),. TRF2, and in lesser extent TRF1, have also an important role in telomere capping and in the prevention of DNA damage responses (Martínez *et al.*, 2009). Moreover, TRF1 plays an essential role in telomere DNA replication (Martínez *et al.*, 2009; Sfeir *et al.*, 2009).

POT1

POT1 is the only shelterin able to bind specifically the single stranded 3' overhang (De Lange, 2005). Interestingly, in mice there are two forms of this protein (POT1a and POT1b) while in humans there is only one (Hockemeyer *et al.*, 2006). It is connected with the rest of the complex through TPP1 and plays an essential and exclusive role in the protection of the single stranded telomeric DNA (Baumann and Cech, 2001). Other function of this protein regards the inhibitions of the DDR and the regulation of telomere length (Loayza and De Lange, 2003; J Z S Ye *et al.*, 2004).

TIN2

TIN2 is found connecting the homodimers of TRF1 and TRF2 (double-stranded binding proteins) and to TPP1 which binds POT1 (single-stranded binding protein). The main function of this shelterin is the stabilization of these binding proteins to the telomere, specially TRF2 (Houghtaling *et al.*, 2004; Jeffrey Zheng Sheng Ye *et al.*, 2004; Kim *et al.*, 2004). It also mediates the recruitment of POT1 via TPP1(Jeffrey Zheng Sheng Ye *et al.*, 2004). Other known functions of TIN2 involve telomere capping and telomere length regulation (Kim, Kaminker and Campisi, 1999).

TPP1

TPP1 acts as a bridge between TIN2 and POT1, allowing the recruitment of POT1 to the telomere (J Z S Ye *et al.*, 2004; Kibe *et al.*, 2010). The main function of this shelterin consists in the recruitment of the TERT subunit of the enzyme telomerase to telomeres, thus, regulating telomere elongation (Tejera *et al.*, 2010).

RAP1

RAP1 is connected with the shelterin complex through binding directly to TRF2 (Li, Oestreich and De Lange, 2000; Li, 2003). Is the only shelterin not required for telomere capping and their main functions are related to telomere length regulation and DDR inhibition (Martinez *et al.*, 2010; Sfeir *et al.*, 2010). Moreover, RAP1 plays several extratelomeric roles regulating the transcription of metabolic genes and silencing subtelomeric protein-coding genes (Martinez *et al.*, 2010; Martínez and Blasco, 2011).

To mention, in mammals there are several complementary proteins binding shelterin components. Specially, TRF1 is known to interact with Tankyrase 1 and 2 (Smith, 1998), two enzymes that regulate TRF1 binding to the telomeres; and TRF2 mainly interacts with components of DNA repair pathways such as the DNA-PKs complex (Khadka *et al.*, 2014), the MRN complex (Zhu *et al.*, 2000), the helicases WRN and BLM (Opresko *et al.*, 2002), the ADP-ribosilases PARP1 and PARP2 (Gomez, 2006) and the nucleases XPF and Apollo (Zhu *et al.*, 2003; Lenain *et al.*, 2006). Together, these proteins also play an important role in maintaining the correct function of telomeres.

1.2.2 Secondary structure: T-loop and G-quadruplex

In vivo, telomeric DNA adopts a secondary structure known as T-loop. This conformation stabilizes the telomeric structure and it is a nucleo-protein structure formed

when the single stranded 3' overhang invades the double stranded telomeric sequence, forming the mentioned T-loop and a related structure, called displacement-loop or D-loop (Greider, 1999; Griffith *et al.*, 1999; Goytisolo *et al.*, 2000) (**Figure 3A and 3B**). Thanks to this conformation, the telomeric DNA and, therefore, the chromosome ends are fully protected, preventing them from being recognized as DSB and avoiding the degradation and the activation of repair mechanisms (Greider, 1999; Griffith *et al.*, 1999). T-loop formation requires the presence of shelterins to be formed, being TRF2 the main component. This protein is key initiating and stabilizing the interactions between the 3' single stranded overhang and the invaded double stranded telomeric DNA (Griffith *et al.*, 1999; Doksani *et al.*, 2013)

Together with the T-loop and the D-loop, and thanks to the presence of guanine-rich regions, telomeric DNA is able to adopt a 3D conformation called G-quadruplex or G4 (Tang *et al.*, 2008). These structures are groups of G-quarters forms by sets of four Hoogsteen-bonded guanines formed spontaneously, not requiring the presence of any shelterin to be formed and stabilized (Sundquist and Klug, 1989; Williamson, Raghuraman and Cech, 1989) (**Figure 3C**). Although the exact function of the G-quadruplex in the telomere remains unclear, this conformation has been proposed as an alternative protective structure of the telomere, when the T-loop and shelterins are missing (Lipps and Rhodes, 2009).

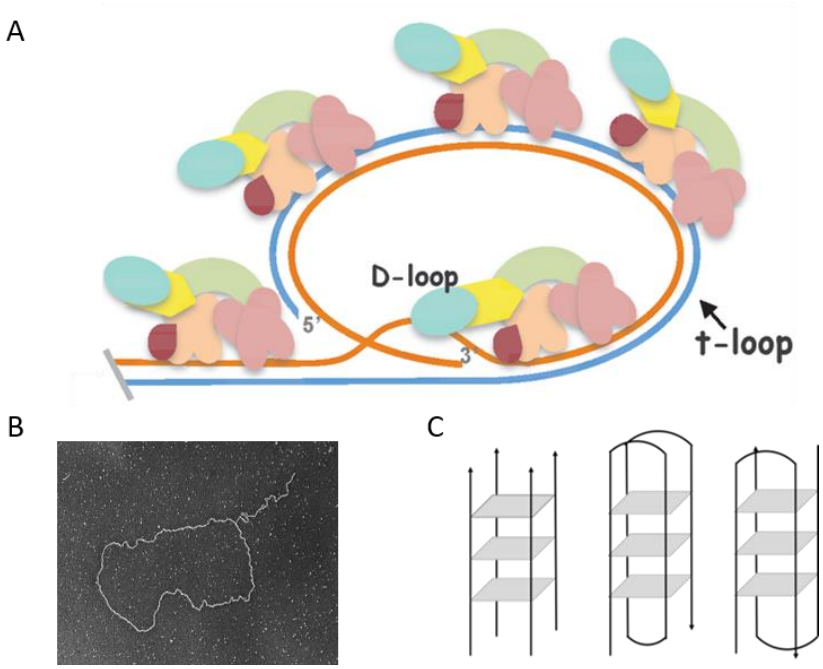

Figure 3. T-loop, D-loop and G-quadruplex. (A) Structure of the T-loop and D-loop. From DNA Repair and Telomeres – An intriguing Relationship. **(B)** Mammalian T-loop visualization by electron microscopy. From Griffith et al., 1999. **(C)** G-quadruplex structures. From Nelson et al., 2004.

2. Telomere shortening and elongation mechanisms

2.1 End-replication problem and telomere shortening

Telomeres shorten with each cell division in a rate of 50 to 200bp due to a phenomenon known as “end-replication problem” (Olovnikov, 1973). This situation is caused by the inability of the standard DNA polymerases to replicate linear DNA due to the antiparallel nature of the double stranded DNA and the characteristics of semiconservative DNA replication. During replication, DNA polymerases are only able to add bases to the 3’ end of a newly synthetized strand, moving 3’-5’ along the parental template strand. This divides the strands into leading and lagging strands. In this way, leading strand is synthetized continuously 5’-3’ direction, while lagging strand must be synthesized in a discontinuous manner generating a set of RNA primers known as Okazaki fragments (Okazaki *et al.*, 1967) (**Figure 4**). These primers are firstly synthetized by the primase, a specialized enzyme able to polymerize without the need of a primer, allowing the DNA polymerase to synthesize of the rest of the DNA molecule. RNA primers are then degraded and the gaps filled by the polymerase. Unfortunately, at the very end of the linear chromosome, this process creates a gap where the DNA polymerase is unable to synthesize due to the lack of a 3’-hydroxi end, causing telomere shortening during the replication (Harley, Futcher and Greider, 1990; Hastie *et al.*, 1990). Moreover, the fully synthesized leading strand results in a DNA molecule with a blunt end which is also digest by APOLO and EXO nucleases, shortening the telomere (Huffman *et al.*, 2000; Longhese *et al.*, 2010; Wu, Takai and De Lange, 2012).

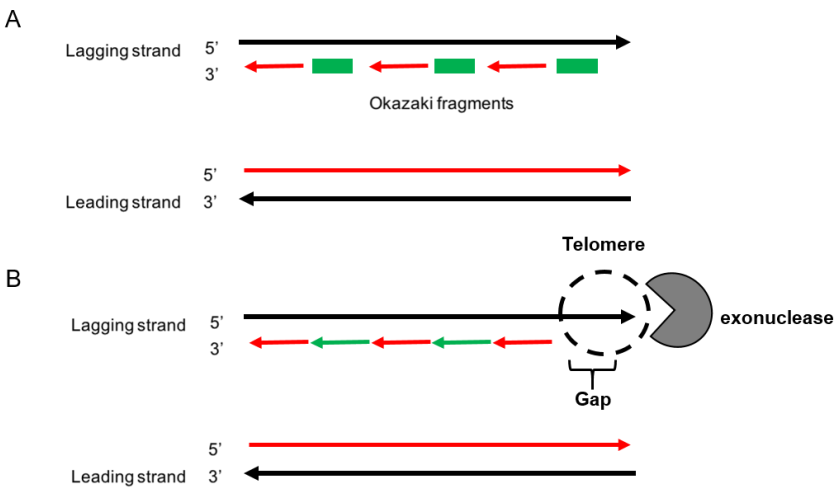

Figure 4. Linear chromosomes end replication problem. (A) The lagging strand needs Okazaki fragments to synthesize new DNA while the leading strand is continuously synthesizing. **(B)** The end of the lagging strand cannot be synthesized when the Okazaki fragment is removed, leading to a single stranded DNA recognized by exonucleases.

2.2 Telomerase

Telomeres can be elongated through *de novo* addition of telomeric repeats by a specialized DNA polymerase, the telomerase (Greider and Blackburn, 1985). This enzyme is a nucleo-protein composed by a catalytic subunit with reverse transcriptase activity (TERT) and by an RNA component (Terc) (Greider and Blackburn, 1985). Apart from these, other components are required to stabilize the complex, such as the dyskerin 1 or DKC1 (Mitchell, Wood and Collins, 1999; Cohen *et al.*, 2007) (**Figure 5**).

Telomerase binds directly to the telomeres where it recognizes the 3' overhang acting as a reverse transcriptase, using the RNA component Terc as a template for the addition of the repetitive telomeric sequence (Greider and Blackburn, 1985). This elongation is regulated by cell cycle, occurring in the late S phase during DNA replication (Marcand *et al.*, 2000) and the accessibility of telomerase to the telomeres relays on the telomere conformation. In this manner, when the telomere is short presents a low amount of shelterin proteins bound to it, T-loop is disrupted allowing the enzyme reach the telomere, constituting a mechanism of telomere length autoregulation (Marcand, Gilson and Shore, 1997).

Telomerase is only expressed in several cell types and during a short period of time during development, although some tissues and stem cell compartments maintain a certain level of expression also in the adult. It is predominantly expressed in embryonic stem cells, germ cells, adult stem cells compartments and in the majority of human cancers (Shay and Bacchetti, 1997; Greenberg *et al.*, 1998; De Lange and DePinho, 1999; Allsopp *et al.*, 2003; Montgomery *et al.*, 2011; Schepers *et al.*, 2011; Varela *et al.*, 2011; Hoffmeyer *et al.*, 2012). However, in most somatic cells of the adult organism telomerase expression is low or absent, in any case not enough to compensate for telomere loss throughout several rounds of cell division, causing one of the molecular mechanisms underlying organismal aging: telomere shortening.

2.3 Alternative Telomere Lengthening (ALT)

Besides telomerase activity, another mechanism for telomere elongation exists. It is known as ALT and it was first described in tumors and immortalized cell lines (Bryan *et al.*, 1997). This mechanism is based on homologous recombination and, as consequence, gives rise to heterogeneous telomere length, multi-telomeric clusters and associated pro-myelocytic leukemia protein bodies (PML bodies), also known as APBs (Bryan *et al.*, 1995, 1997; Dunham *et al.*, 2000; Muntoni and Reddel, 2005). This alternative mechanism is

present in 10-15% of tumors (Bryan *et al.*, 1997) but there is so far no evidence suggesting that could prevent age related telomere loss.

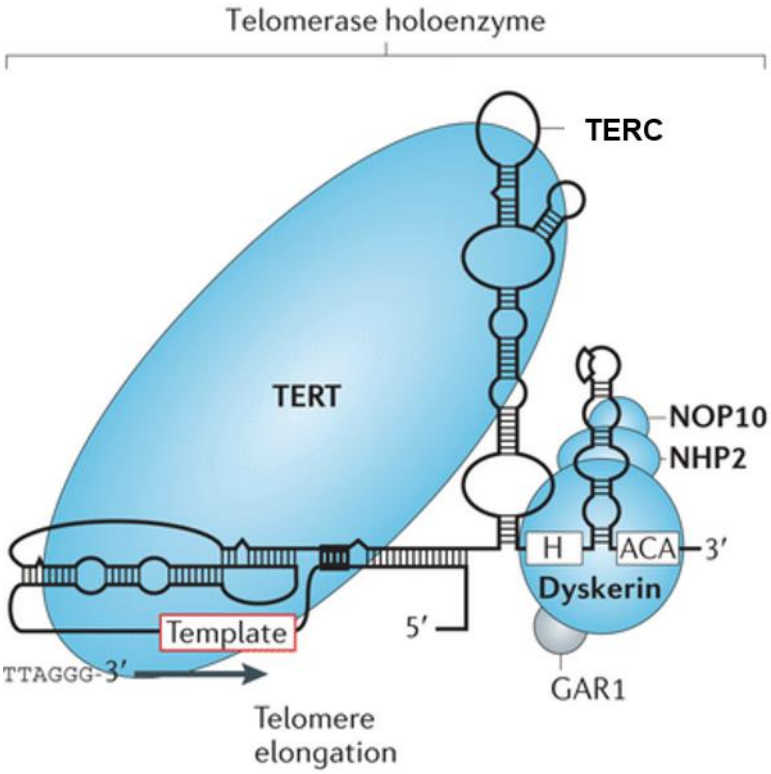

Figure 5. Structure of Telomerase. From Blackburn, 2012.

3. Telomeres and DNA damage response

When telomeres reach a critically short length or the shelterin proteins are destabilized, the T-loop is disrupted and telomeres become dysfunctional (De Lange, 2005). In this situation, telomeres are exposed and the unprotected DNA end becomes indistinguishable from a double-strand break, which actives the subsequent DNA damage response. At this point, a signaling cascade of DDR transduction-related proteins (53BP1, γH2AX, NBS1, ATM, ATR, DNA-PK) is initiated, resulting in the activation of several downstream tumor suppressor genes (*p53*, *p21*, *p16*, *Chk1* and *Chk2)* leading to senescence or apoptosis (Goytisolo *et al.*, 2000; Smogorzewska and de Lange, 2002; Artandi and Attardi, 2005; Martínez *et al.*, 2009; Sfeir *et al.*, 2009). The mayor characteristic of a dysfunctional telomere is the so-called Telomere Induce Foci (TIF), which represents the colocalization of a DDR related protein with the telomere (De Lange, 2005). The main DDR pathways activated when telomeres are recognized as DSB are the activation of the

ATM/ATR signaling, the classical non-homologous end-joining pathway and the homologous-directed repair pathway.

3.1 Activation of the ATM/ATR pathway

ATM and ATR kinases are among the earliest transducers known to initiate the DDR signaling cascade upon telomere dysfunction. This cascade ultimately results in the activation of p21 and p53, leading to cell cycle arrest and subsequently, senescence and apoptosis (Takai, Smogorzewska and De Lange, 2003).

When T-loop is disrupted, telomeric DNA is recognized as a DSB by a set of protein called MRN complex, formed by MRE11, RAD50 and NBS1 (De Jager *et al.*, 2001), activating ATM (Lee and Paull, 2007). On the other hand, ATR is activated in presence of single stranded DNA (ssDNA) (Cimprich and Cortez, 2008), and it has been proposed that the absence of POT1 leads to the recognition and binding of RPA to the G-strand overhang, recruiting ATR (Barrientos *et al.*, 2008). ATM acts through a CHK2-dependent pathway, while ATR activates CHK1. In both cases, it leads to p53 activation and the subsequent cell cycle arrest, senescence and apoptosis.

3.2 Activation of non-homologous end-joining repair pathways: c-NHEJ and alt-NHEJ

The presence of DSB also activate the non-homologous end-joining pathway which is consider an error-prone repair mechanism and elicits chromosome fusions.

Classical NHEJ (c-NHEJ) is mainly mediated by the complex DNA-PK, composed of the subunits Ku70/80 and DNA-PKcs (Yaneva, Kowalewski and Lieber, 1997). This pathway is triggered when Ku70/80 recognizes a DSB and binds to it (Calsou *et al.*, 2003). Exonucleases are then recruited to generate blunt ends followed by the ligation of the chromosome ends by ligases (Espejel, Franco, Rodr??guez-Perales, *et al.*, 2002; Espejel, Franco, Sgura, *et al.*, 2002; Smogorzewska *et al.*, 2002; Zhu *et al.*, 2003; Celli and de Lange, 2005).

The alternative-NHEJ (alt-NHEJ) is enhanced in the absence of a proficient c-NHEJ (Riballo *et al.*, 2004; Wang *et al.*, 2006; Nussenzweig and Nussenzweig, 2007). Alt-NHEJ is characterized by causing larger deletions, insertions and chromosomal translocations in the repair junctions (Nussenzweig and Nussenzweig, 2007) and exist at low levels in normal

cells, and its upregulation has been linked with cancer (Sallmyr, Tomkinson and Rassool, 2008). Indeed, some tumors, like leukemia, use alt-NHEJ related proteins to generate a higher genomic instability, leading to disease progression and resistance to treatments (Sallmyr, Tomkinson and Rassool, 2008; Li *et al.*, 2011).

3.3 Homology Directed Repair (HDR)

The activation of HDR pathway occurs in the presence of DSB in a lesser extent compared to the NHEJ. It is an error free-repair mechanism that requires the sister chromatid as template for homologous recombination. During the process, the single stranded G-rich overhang invades the sister-chromatid and uses the intact sequence as a template for DNA synthesis. HDR is not deleterious but is less frequent: it takes place at S or G2 phases of the cell cycle due to the requirement of the sister-chromatid sequence as a template for DNA synthesis (San Filippo, Sung and Klein, 2008).

4. Telomeres and aging

4.1 Telomeres and cellular senescence: Hayflick limit

Telomeres are nowadays considered one of the hallmarks of aging (López-Otín *et al.*, 2013) and their link with aging has been deeply studied. However, they were Hayflick and Moorhead who, in 1961, first suggested a possible relation between telomeres and organismal aging. They observed that *in vitro* passaging of human fibroblasts led to an irreversible growth arrest, known today as replicative senescence. They even hypothesized the existence of cellular factors (known as “Hayflick factors”), which lost would constitute the main cause of this phenomenon (Hayflick and Moorhead, 1961). Subsequent studies correlated telomere shortening as one of the main causes of this limited duplication capacity (Harley, Futcher and Greider, 1990), idea reinforced by the fact that external re-activation of telomerase is enough to prevent replicative senescence in a variety of cell types (Bodnar *et al.*, 1998; Vaziri and Benchimol, 1998; Yang *et al.*, 1999), while the opposite effects occur when telomerase is inhibited, causing proliferation arrest even in immortalized cells (Ohmura *et al.*, 1995). Furthermore, with the development of genetic mouse models the link between telomeres and aging were strongly supported *in vivo* thanks to a Terc KO mouse, deficient in functional telomerase (Blasco *et al.*, 1997). These mice are characterized by the presence of an abnormal number of short telomeres, which impairs the proper formation of the T-loop leading to activation of the DDR pathways and the loss of regenerative capacities of tissues,

finally leading to premature aging and reduced lifespan (Blasco *et al.*, 1997; Lee *et al.*, 1998; Herrera, 1999; Herrera *et al.*, 1999; Rudolph *et al.*, 1999; Herrera, Martínez-A and Blasco, 2000; Franco *et al.*, 2002; Samper *et al.*, 2002).

4.2 Telomere associated diseases

In agreement with the fact that telomere shortening underlies one of the main mechanisms of aging, mutations in both telomerase and the shelterin components have been linked to rare degenerative diseases in humans, also known as telomere syndromes (Donate and Blasco, 2011; Armanios and Blackburn, 2012). This group of rare diseases is characterized by the presence of critically short or dysfunctional telomeres, linked to the characteristic impairment of the regenerative capacities and finally resulting in premature aging and death (Donate and Blasco, 2011; Armanios and Blackburn, 2012) (**Figure 6**).

Precisely, TERT, TERC and DKC1 mutations are linked to *Dyskeratosis congenita* (DC), a severe disease that causes bone marrow deficiency. Other examples are *Aplastic anemia*, characterized by an hypocellular bone marrow; *Idiopathic pulmonary fibrosis*, a degenerative lung disease; and *liver fibrosis* (Yamaguchi *et al.*, 2005; Armanios *et al.*, 2007; Tsakiri *et al.*, 2007; Calado *et al.*, 2009).

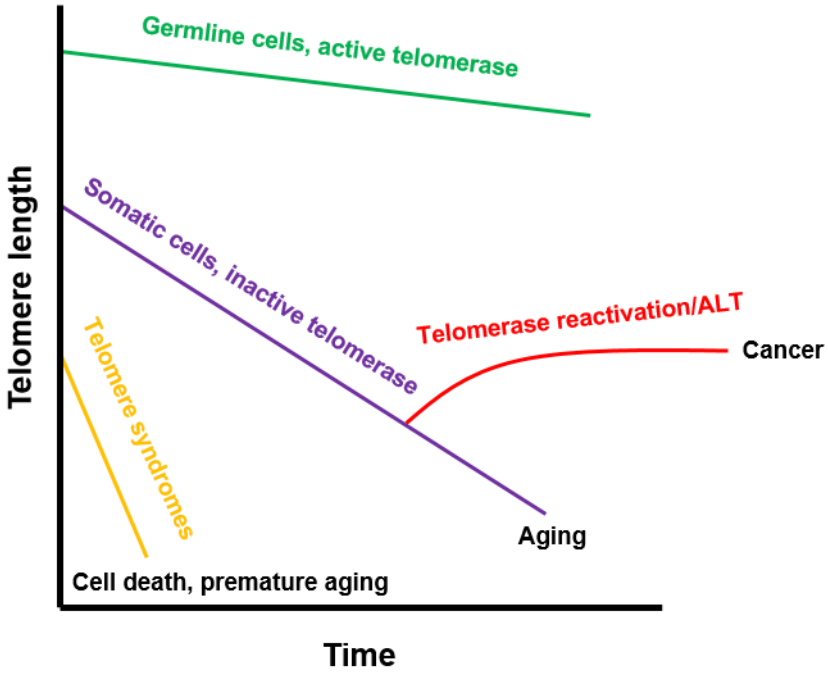

Figure 6. The connection between telomeres, aging and cancer.

4.3 Telomeres in cancer

Senescence and apoptosis constitute the two main barriers to cell proliferation. In this regard, a neoplastic cell needs to acquire the capability to overcome these barriers,

achieving unlimited replicative potential and becoming immortal. As mentioned before, telomeres constitute a key piece in replicative senescence since a minimum telomere length is essential to avoid cell crisis, making telomere and telomere maintenance mechanisms indispensable for cancer cells. In this regard, more than 90% of human cancer aberrantly re-activates and overexpress telomerase (Kim *et al.*, 1994; Shay and Bacchetti, 1997; Joseph *et al.*, 2010), while the rest of telomerase-negative tumors activates ALT (Bryan *et al.*, 1997; Barthel *et al.*, 2017). Thus, telomerase, telomeres and even shelterin proteins have been widely studied as potential anti-cancer targets.

5. Telomere elongation strategies

5.1 Telomerase mouse models

Terc and TERT telomerase subunits are required for telomere elongation and telomere lengthening functionality (Cristofari and Lingner, 2006). However, the impact of *in vivo* telomerase overexpression on aging and telomere maintenance was not easy to address due to the cancer-promoting effect already mentioned. Indeed, it has been demonstrated that constitutive overexpression of tert subunit in mouse basal skin resulted in tissue regeneration improve but also in slightly increased cancer (González-Suárez *et al.*, 2001).

In order to avoid this particular side effect and to allow the study of telomerase overexpression in aging and telomere length, Tert overexpression was combined with the overexpression of p16 and p53 tumor suppressor genes, resulting in a mouse model presenting increased lifespan, longer telomeres and reduction of aging pathologies, all without increasing cancer appearance (Tomás-Loba *et al.*, 2008).

While the overexpression of telomerase is linked to cancer promotion, telomerase deficiency in terc-deficient mouse models leads to cancer resistance (Lee *et al.*, 1998; Rudolph *et al.*, 1999; Gonzalez-Suarez *et al.*, 2000). However, telomerase abrogation in the context of cancer-prone mouse models has only shown anti-tumorigenic activity after several mouse generations of terc-deficient mice, when mouse telomeres reach a critically short length (Chin *et al.*, 1999; Greenberg *et al.*, 1999). A similar situation occurs in the case of induced chemical carcinogenic in which no differences between wild type and terc KO mice is observed until several KO generations (Gonzalez-Suarez *et al.*, 2000).

5.2 Telomerase gene therapy

Telomerase can be also reactivated in an organism throughout non-integrative gene therapy vectors which, in proliferating cells, present the advantage of allowing a temporary expression of telomerase (Bernardes de Jesus *et al.*, 2012). In particular, adeno-associated viral vectors (AAV) have been used to deliver telomerase in adult tissues in mice, allowing a temporary telomere elongation and being this overexpression sufficient to extend mouse longevity and delay many different age-related conditions, avoiding the increasing of cancer incidence produced in telomerase mouse models (Bernardes de Jesus *et al.*, 2012). This gene therapy can help not only to study transitorily the telomere length restoration but also to treat telomere related diseases, the so-called telomere syndromes, characterized for the presence of much shorter telomeres than normal with the subsequent premature loss of the regenerative capacity of tissues (Armanios and Blackburn, 2012).

AAV vectors present many desirable properties as they are non-integrative, show a poor immunogenicity and an excellent safety profile (Büning *et al.*, 2008). They are able to transduce both dividing and quiescent cells in a wide range of tissues and maintain the expression for a long time (Inagaki *et al.*, 2006). Moreover, some AAV vectors (as AAV9) have the capability of crossing the blood-brain-barrier and target brain cells upon intravenous injection in adult mice (Duque *et al.*, 2009; Foust *et al.*, 2009). In particular, expression of *Tert* using AAV9 vectors can delay physiological aging and extend longevity in wild-type mice without increasing (Bernardes de Jesus *et al.*, 2012). In fact, a single treatment with AAV9-*Tert* vectors showed therapeutics effects in preventing death by heart failure after induction of myocardial infarction in mice, as well as in preventing or reversing disease in mouse models of aplastic anemia and idiopathic pulmonary fibrosis associated to short telomeres (Bär *et al.*, 2014, 2016; Povedano *et al.*, 2018).

Importantly, AAV9-*Tert* gene therapy has not been shown to increase cancer incidence either in the context of mouse longevity studies (Bernardes de Jesus *et al.*, 2012) or in the context of the above-mentioned mouse models of disease owing to short telomeres (Bär *et al.*, 2014, 2016; Povedano *et al.*, 2018). However, mice are short lived species compared to humans, and although mice also spontaneously develop cancer with aging, a potential long-term pro-tumorigenic effect of telomerase may be missed.

5.3 "*In vitro*" telomere elongation

The enzyme telomerase is active in germ cells and during early embryogenesis (Mantell and Greider, 1994; Yang *et al.*, 1999; Xu and Yang, 2000) and is crucial for the maintenance of telomere length and germ cell viability in successive generations of a species (Hemann *et al.*, 2001; Liu *et al.*, 2002). As mentioned earlier, telomere shortening limits the regenerative capacity of cells and is correlated with the onset of cancer, aging, and chronic diseases (Rudolph *et al.*, 1999; Djojosubroto *et al.*, 2003). In this regard, the segregation of telomere length from one generation to the next is essential for normal development and well-being in mammals and this is ensured by the active elongation and maintenance of telomeres in germ cells in a telomerase-dependent manner, which elongates telomeres to a defined length, required to ensure sufficient telomere reserves for species integrity (Schaetzlein *et al.*, 2004).

ES-like pluripotent stem cells can be generated from differentiated cells (i.e., MEFs) by using defined factors, giving rise the so-called induced pluripotent stem (iPS) cells, which are considered functional equivalents of ES cells (Takahashi and Yamanaka, 2006; Okita, Ichisaka and Yamanaka, 2007; Aoi *et al.*, 2008). Interestingly, iPS cells telomeres are found to increase their telomere length during and after nuclear reprogramming until reaching ES cell telomeres. This elongation process occurs concomitantly to lower density of trimethylated histones H3K9 and H4K20 at the telomeric chromatin (Marion *et al.*, 2009). Furthermore, super-elongated telomeres were not observed in iPS cells derived from first-generation telomerase-deficient MEFs, indicating that they result from an active telomere elongation by telomerase during and after nuclear reprogramming (Marion *et al.*, 2009). Notably, early passage iPS cells had shorter telomeres than those of ES cells from the same genetic background and only acquired ES cell-like long telomeres after several passages *in vitro* (Marion *et al.*, 2009).

As reported on iPS cells, mouse ES cells are also able to elongate their telomeres. This process occurs specifically in the inner cell mass (ICM) at the blastocyst stage, and *in vitro* cultured ICM cell are able to undergo a further telomere elongation during the establishment of ES cell lines. This is due to changes in chromatin structure, specifically the loss of heterochromatic marks at early stages of ES cell establishment. In this context, a limited action of the histone metyltranferases Suv39 and Suv420 at telomeres facilitate the generation of hyper-long telomeres in established ES cell lines, similar as occurs in iPS cells (García-Cao *et al.*, 2004; Benetti *et al.*, 2008). Associated to early stages of ES-cell generation (ICM cell culture) there is a high expression of TRF1, togetherl with high Sox2

and Oct3/4 levels, and before telomere elongation and presence of high Nanog levels, suggesting a possible mechanism to ensure proficient telomere capping (Varela *et al.*, 2011).

This *in vitro* generated telomeres are referred to as hyper-long telomeres and, importantly, this elongation process by culture passage occurs in the absence of modifications in the telomerase gene. Moreover, ES cells with hyper-long telomeres can be aggregated into morulae, and can undergo development to the blastocyst stage maintaining the hyper-long telomere phenotype (Varela *et al.*, 2011), giving birth a new important tool for study telomere elongation *in vivo* avoiding the cancer risk associated to telomerase re-activation.

Objectives/Objetivos

1. To study the safety of telomerase-based gene therapy in a cancer prone environment in mice. For this purpose, we aimed:

- To overexpress *mTert* and a dominant negative form of *Tert* (*DN-mTert*) throughout AAV9 viral vectors before tumor induction in an inducible mouse lung cancer model to study their effects before the malignancy.

- To overexpress *mTert* and *DN-mTert* using AAV9 viral vectors at the same time of the tumor initiation to address their roles in the early stages of the malignancy.

- To analyze the effects of these therapies in an accelerated developing lung tumor mouse model to measure their effects in an aggressive environment.

2. To characterize the effects of telomere elongation beyond the pre-established length in mice. For this purpose, we aimed:

- To generate and study healthy mouse ES cells with hyper-long telomeres.

- To generate mice presenting hyper-long contributing cells in their tissues.

- To study the effects of whole body hyper-long telomere mice in body function and aging.

1. Estudiar la seguridad de la terapia génica basada en telomerasa en un ambiente propenso a cáncer en ratón. Para ello, nos propusimos:

- Sobreexpresar mTert y una forma dominante negativa de Tert (DN-mTert) a través de vectores virales AAV9 antes de la inducción del tumor en un modelo de ratón de cáncer de pulmón para estudiar sus efectos antes de la patología.

- Sobreexpresar mTert y DN-mTert usando los vectores virales AAV9 a la vez que se inicia el tumor para estudiar sus efectos en estadíos tempranos.

- Analizar el efecto de estas terapias en un modelo de cáncer de pulmón con desarrollo acelerado para medir sus efectos en un ambiente más agresivo.

2. Caracterizar el efecto de la elongación telomérica más allá de la longitud pre-establecida en ratones. Para ello, nos propusimos:

- Obtener células madre embrionarias dotadas de telómeros súper-largos.

- Generar ratones que presenten células con telómeros súper-largos en sus tejidos.

- Estudiar los efectos de la elongación telomérica en todas las células del animal a nivel de funciones corporales y envejecimiento.

Materials and Methods

1. Mice experimentation

1.1. Mice generation

For the telomerase gene therapy experiments, *K-Ras*$^{+/G12V}$ mice were generated as previously described (Guerra *et al.*, 2003). *K-Ras*$^{+/G12V}$ mice were crossed with *p53*$^{-/-}$ mice (Jackson Labs, http://jaxmice.jax.org/strain/002101.html) to generate the compound *K-Ras*$^{+/G12V}$ *p53*$^{-/-}$ mouse. Separated groups of mice were tail-vein injected with $2x10^{12}$ vg (viral genomes)/mouse of either AAV9-Null, AAV9-*Tert* or AAV9-*Tert-DN*, a catalytically inactive form of mouse TERT.

For the hyper-long telomere experiments, Chimeric mice were generated at the CNIO Transgenic Mice Unit by microinjection of R1-eGFP ES cells into Hsd:ICR (C57Bl6 background). Embryos were harvested from super ovulated donor females at E2.5 days of gestation. Aproximately 100 morulae at the eight-cell state were microinjected with 6-10 eGFP-expressing ES cells by laser-assisted perforation of the “zona pellucida”. After microinjection, embryos were incubated overnight in a drop of KSOM medium in a CO_2 incubator at 37ºC under oil. As a control for this study R1-eGFP 129S1 female mice were used in all the experiments.

1.2. Mice maintenance

All mice were maintained at the Spanish National Cancer Centre (CNIO) under specific pathogen-free conditions in accordance with the recommendations of the Federation of European Laboratory Animal Science Associations (FELASA). All animal experiments were approved by the Institutional Animal Care and Use Committee (IACUC) and by the Ethical Committee for animal experimentation (CEIyBA) from the CNIO and performed in accordance with the Reporting in Vivo Experiments (ARRIVE) guidelines developed by the National Centre for the Replacement, Refinement & Reduction of Animals in Research (NC3Rs). Along with those guidelines, mice were monitored in a daily or weekly basis and they were sacrificed in CO_2 chambers when the human endpoint was considered.

Mice were maintained on a 12-hour light/12-hour dark cycle. During light cycle, white light was provided by fluorescent lamps (TLD 36W/840 and TLD58W/840, Philips). Mice had free access to water and standard chow diet (18% of fat-based calorie content, Harlan Teckland 2018).

1.3 Mice genotyping

Mice genotyping was performed by Transnetyx private company (Cordova, TN 38016).

- **Transnetyx genotyping**

Transnetyx uses a RT-qPCR based system and Taqman probe technology to measure the presence or absence of a desire sequence. The following probes were used to assess the different mouse genotypes:

Kras G12V – used to test for *K-Ras*$^{+/G12V}$.

Forward Primer Sequence: GGCCTGCTGAAAATGACTGAGTATA

Reverse Primer Sequence: CTGTATCGTCAAGGCGCTCTT

Probe Sequence 1: CTACGCCACCAGCTC

Probe Sequence 2: CTACGCCTACAGCTC

p53 WT – used to test for wild type version of *p53* gene.

Forward Primer Sequence: GTGAGGTAGGGAGCGACTTC

Reverse Primer Sequence: TTGTAGTGGATGGTGGTATACTCAGA

Probe Sequence: CCTGGATCCTGTGTCTTC

p53 KO – used to test for knock out version of *p53* gene.

Forward Primer Sequence: TGTTTTGCCAAGTTCTAATTCCATCAGA

Reverse Primer Sequence: TTGTAGTGGATGGTGGTATACTCAGA

Probe Sequence: ACAGGATCCTCTAGAGTCAG

ROSA WT - used to test the presence of the wild type version of the ROSA region

Forward Primer Sequence: TTCCCTCGTGATCTGCAACTC

Reverse Primer Sequence: CTTTAAGCCTGCCCAGAAGACT

Probe Sequence: CCGCCCATCTTCTAGAAAG

eGFP-2 TG- used to test the presence of eGFP in the ROSA region

Forward Primer Sequence: GGCATCAAGGCGAACTTCAAG

Reverse Primer Sequence: ACGCCGCCGTCCTC

Probe Sequence: ATCCGCCACAACATC

1.4 Gene therapy vector production

Adeno-associated viral vectors (AAV9) were generated and purified as previously described (Ayuso *et al.*, 2014). The vectors used were (i) AAV9-Null (ii) AAV9-*Tert* that express murine catalytic subunit of telomerase (iii) AAV9-*Tert-DN* that express murine catalytically inactive telomerase (iv) AAV9-*GFP* (Bernardes de Jesus *et al.*, 2012). AAV9 particles were purified using 2 cesium chloride gradients, dialyzed against phosphate-buffered saline (PBS) and filtered. Viral genome particle titers were determined by a quantitative real-time polymerase chain reaction (PCR) method.

1.5 Adenovirus intratracheal infection

Twelve-week-old mice were treated once with intratracheal adeno-Cre vectors (Gene Vector Core, University of Iowa, $1x10^{10}$ pfu/ml) instillation with $1x10^{8}$ pfu/mouse of virus after anesthesia by intraperitoneal injection of ketamine-medetomidine (Domitor, 1mg/ml; Orion Corporation). To wake up the mice after the instillation, they were injected with 0.05 mg of atipamezole (Antisedan, 5mg/ml; Orion Corporation).

1.6 In vivo imaging by computed tomography

Eight weeks after adeno-Cre inoculation, an *in vivo* follow-up of tumor growth was achieved by four computed tomographies (CT) every 8 weeks. CT analyses were performed as previously described (Ambrogio *et al.*, 2014). Briefly, Micro-CT imaging was performed on a high resolution scanner (Locus, General Electric HealthCare, London, Ontario, Canada). The scanning protocol operates at 80 kVp and 50 mA, 400 projections and collected in one full rotation of the gantry in

approximately 10, minutes. The reconstruction was done with a modified Feldkamp cone-beam algorithm. Micro-CTimages were analyzed using MicroView Analysis + (v2.2, General Electric Healthcare, London, Ontario, Canada).

1.7 Densitometry assay

Body composition (percentage of total fat, bone densitometry and total lean) was measured using dual-energy X-ray absorptiometry (DEXA) PIXImus, Mouse Densitometer (GE Lunar co, Madison, WI, USA) using software version 1.46. Mice were anesthetized via gaseous anesthetic (isoflurane) with a continuous flow of 1% to 3% isoflurane/oxygen mixture (2 L/min), for approximately 10 min during recording. Quality control was performed using a calibrated phantom before imaging.

1.8 Subcutaneous fat thickness

Thickness of the subcutaneous fat layer was measured as previously described (Derevyanko *et al.*, 2017). Briefly, a total of 30 measurements were performed on 2 back sections of the skin for each mouse around 100 weeks old. Measurements were made using Panoramic Viewer software and ImageJ software.

1.9 Metabolic measurements

Serum levels of albumin, creatinine, bilirubin, urea, alanine aminotransferase (ALT), cholesterol, low density lipoprotein (LDL) and high density lipoprotein (HDL) were determined using ABX Pentra (Horiba Medical). To perform GTT and ITT, mice were i.p. injected with 2g of glucose/kg of body weight and 0.75 U insulin/kg of body weight (Eli Lilly; Humalog Insulin), respectively. In the case of GTT mice were previously fasted for 16h. For ITT mice were not fasted and basal levels of glucose were between 80-100 mg/dL.

1.10 Cognitive tests

To check smell capacities mice were tested by the buried food test(Yang and Crawley, 2009). Briefly, mice were fasted for 16h and they were placed in a cage with a buried pellet of food. Analysis was made by calculating the percentage of success and the total time spent to find the pellet. To measure coordination mice were tested in a Rotarod apparatus (model LE 8200). For balance mice were tested by the tightrope test, as previously described (Tomás-Loba *et al.*, 2008; Bernardes de Jesus *et al.*, 2012). In the rotarod test we measured the time mice could stay on the rod. In the tightrope test, we evaluate the ability of the mice to stay in the rope without falling, and we considered a “success” if mice were able to stay more than one minute.

2. Cell culture

R1-eGFP ES cells (obtained from A. Nagy (lunenfeld-Tanenbaum Research Institute)) from mice with a *129S1* genetic background were cultured to allow telomere elongation in complete KSR medium composed of DMEM (high glucose; Gibco) supplemented with serum replacement (KSR 15%, Gibco), LIF (1,000U/ml-1, Millipore) and 2i.

3.Histopathology, immunohistochemistry and Immunofluorescence analysis

3.1 Histopathological analysis

Histopathological analyses were performed in paraffin embedded tissue sections stained with hematoxylin and eosin (H&E), with the assistance of the CNIO Histopathology Unit.

3.2 Immunohistochemistry analyses in tissue sections

Immunohistochemistry stainings were performed by the CNIO Histopathology Unit, tissues were fixed in 10% buffered formalin, embedded in paraffin wax and sectioned at 5 μ m. For histological examination sections were stained with hematoxylin and eosin, according to standard procedures. Nuclei were counterstained with Harrys's hematoxylin. Pictures were taken using Olympus AX70 microscope.

Antibodies used for immunohistochemistry included those raised against: γH2AX Ser 139 (Millipore), Ki67 (Master diagnostica), AC3 (Cell Signaling Technology), β-GAL (3A9A; CNIO Monoclonal Antibodies Core Unit, AM(3A9A)), GFP (Cell Signaling) and p21 (291H/B5, homemade). For β-GAL and GFP double staining, the immunohistochemical reaction was developed using 3,30-diaminobenzidine tetrahydrochloride (DAB) (Chromomap DAB, Ventana, Roche) and purple chromogen (Discovery Purple Kit, Ventana, Roche), respectively.

3.3 Immunofluorescence analyses in cells and tissue sections

For immunofluorescence analyses, tissue sections were fixed in 10% buffered formalin (Sigma) and embedded in paraffin. After deparaffinization and citrate antigen retrieval, sections were permeabilized with 0.5% Triton in PBS and blocked with 1%BSA and 10% Australian FBS (GENYCELL) in PBS.

The antibodies were applied overnight in antibody diluents with background reducing agents (Invitrogen).

Primary antibodies: polyclonal rabbit anti-SFTPC (Sigma), rat polyclonal anti-TRF1 (homemade), polyclonal anti-Rap1 (BL735, Bethyl), polyclonal anti-53BP1 (Novus Biologicals).

Immunofluorescence images were obtained using a confocal ultraspectral microscope (Leica TCS-SP5) or the Opera High Content Screening (HCS) system (Perkin Elmer). Quantifications were performed with Definiens software. A double immunofluorescence using antibodies against 53BP1 to mark DNA damage foci and TRF1 to mark telomeres was performed in lung tumor sections to assay for telomeric DNA damage specifically located at telomeres.

4. Western-Blotting

Total protein extracts were obtained using RIPA extraction buffer and protein concentration was determined using the Bio-Rad DC Protein Assay (Bio-Rad). Up to 20 micrograms of protein per extract were separated in SDS–polyacrylamide gels by electrophoresis. After protein transfer onto nitrocellulose membrane (Whatman), the membranes were incubated with the indicated antibodies. Antibody binding was detected after incubation with a secondary antibody coupled to horseradish peroxidase using chemiluminescence with ECL detection KIT (GE Healthcare).

Primary antibodies: anti-RAP1 (Bethyl), anti-SMC-1 (Bethyl).

Quantifications: Protein-band intensities were measured with ImageJ software and normalized against the loading control.

5. *In situ* hybridization

5.1 Telomere measure by Quantitative Fluorescence *In situ* Hybridization (qFISH)

For quantitative telomere fluorescence in situ hybridization (Q-FISH) paraffin-embedded sections were deparaffinized and fixed with 4% formaldehyde, followed by digestion with pepsine/HCl and a second fixation with 4% formaldehyde. Slides were dehydrated with increasing concentrations of EtOH (70%, 90%, 100%) and incubated with the telomeric probe for 3.5 min at 85ºC followed by 2h RT incubation in a wet chamber. In the final steps, the slides were extensively washed with 70% formamide and 0.08% TBS-Tween. Analysis was performed by Definiens software.

5.2 Immuno-FISH

Tissue samples were fixed in 4% formaldehyde and permeabilized with 0.5% Triton in PBS. Telomeric FISH was performed as described in section 5.1 omitting the pepsin digestion step. After washing, immunofluorescence staining was performed and described in section 3.3.

5.3 FISH analysis on metaphase spreads

For metaphase preparation, cells were grown overnight in the presence of 0.1 µg/ml colcemide. Cells were incubated with hypotonic solution (0.4% KCl, 0.4% Sodium citrate) followed by cold methanol/acetic acid (3:1) fixation. On the final steps, cells were spread on glass slides and telomeric FISH was performed as described in 5.1. Analysis of MTS signals was performed by superposing the FISH telomere image and the DAPI image.

6. TRAP

ES cells were trypsinized and washed in PBS, spleen was washed in PBS after isolation, and then S-100 extracts were prepared as described in (Blasco *et al.*, 1997)**.** Three protein concentrations were used for each sample (5, 2.5, and 1 µg) for the ES cells, and two protein concentrations were used for each sample (5 and 1 µg) of spleen. Extension and amplification reactions and electrophoresis were performed as described in (Blasco *et al.*, 1997). A negative control was included by pre-incubating each spleen extract with RNase for 10 min at 30°C before the extension reaction and internal control for PCR efficiency was also included.

7. Real-time qPCR

Total RNA from cells was extracted with the RNeasy kit (QIAGEN) and reverse transcribed was using the iSCRIPT cDNA synthesis kit (BIO-RAD) according to manufacturer's protocols.

Quantitative real-time PCR was performed with the QuantStudio 6 Flex (Applied Biosystems, Life Technologies) using Go-Taq qPCR master mix (Promega) according to the manufacturers protocol. All values were obtained in triplicates.

Primers for mouse and samples are listed below:

TBP1-F 5'-ACCCTTCACCAATGACTCCTATG-3'

TBP1-R 5'-TGACTGCAGCAAATCGCTTGG-3'

TRF1-F 5'-GTCTCTGTGCCGAGCCTTC-3',

TRF1-R 5'-TCAATTGGTAAGCTGTAAGTCTGTG-3'

TRF2-F 5'-AGAGCCAGTGGAAAAACCAC-3'

TRF2-R 5'-ATGATGGGGATGCCAGATTA-3'

POT1A-F 5'-AAACTATGAAGCCCTCCCCA-3'

POT1A-R 5'-CGAAGCCAGAGCAGTTGATT-3'

POT1B-F 5'-AGTTATGGTCGTGGGATCAGAG -3'

POT1B-R 5'-GAGGTCTGAATGGCTTCCAA -3'

RAP1-F 5'-AAGGACCGCTACCTCAAGCA-3'

RAP1-R 5'-TGTTGTCTGCCTCTCCATTC-3'

TPP1-F 5'-ACTTGTGTCAGACGGAACCC-3'

TPP1-R 5'-CAACCAGTCACCTGTATCC-3'

TIN2-F 5'-TCGGTTGCTTTGCACCAGTAT-3'

TIN2-R 5'-GCTTAGCTTTAGGCAGAGGAC-3'

TERT-F 5'-GGATTGCCACTGGCTCCG-3'

TERT-R 5’-TGCCTGACCTCCTCTTGTGAC-3’

TERC-F 5’-TCATTAGCTGTGGGTTCTGGT-3’

TERC-R 5’-TGGAGCTCCTGCGCTGACGTT-3’

Cytochrome C-F 5'-ACCAAATCTCCACGGTCTGTT-3'

Cytochrome C-R 5'-GGATTCTCCAAATACTCCATCAG-3'

ATP Synthase-F 5'-TCTCGGCCAGAGACTAGGAC-3'

ATP Synthase-R 5'-GCACCTGCACCAATGAATTT-3'

Cytochrome c oxidase subunit 6-F 5'-GTAACGCTACTCCGGGACAA-3'

Cytochrome c oxidase subunit 6-R 5'-TCCAGGTAGTTCTGCCAACA-3'

Cytochrome c oxidase subunit 5a-F 5'-CTCGTCAGCCTCAGCCAGT-3'

Cytochrome c oxidase subunit 5a-R - 5'-TAGCAGCGAATGGAACAGAC-3'

PGC1α-F 5'-CCCTGCCATTGTTAAGACC-3'

PGC1α-R 5'-TGCTGCTGTTCCTGTTTTC-3'

PGC1β-F 5'-GGACGCCAGTGACTTTGACT-3'

PGC1β-R 5'-TTCATCCAGTTCTGGGAAGG-3'

ERRα-F 5'-CCTCTTGAAGAAGGCTTTGCA-3'

ERRα-R 5'-GCAGGGCAGTGGGAAGCTA-3'

PPARα-F 5’-TCGGCGAACTATTCGGCTG-3’

PPARα-F 5’-GCACTTGTGAAAACGGCAGT-3’

P16-F 5’-TACCCCGATTCAGGTGAT

P16-R 5’-TTGAGCAGAAGAGCTGCTACGT-3’

CMV-F 5’-CAATTACGGGGTCATTAGTTCATAGC-3’

8. Mitochondrial copy number

Relative mtDNA content were obtained by the comparative Ct method (Venegas and Halberg, 2012; Gonzalez-Hunt *et al.*, 2016). Briefly, we measured by qPCR the mtDNA genes *Cox1*, *Cytb* and *Nd1* and the nuclear DNA (nucDNA) gene *H19*. Then we subtracted the mtDNA averaged Ct values from the nucDNA averaged Ct values obtaining the ΔCt. We finally calculated the relative mitochondrial DNA content by raising 2 to the power of ΔCt and then multiplying by 2.

Expressed as equations:

ΔCt = nucDNA Ct − mtDNA Ct.

Relative mitochondrial DNA content = $2 \times 2^{\Delta Ct}$.

Primers were used as follows:

COX1-F 5'-CTGAGCGGGAATAGTGGGTA-3'

COX1-R 5'-TGGGGCTCCGATTATTAGTG-3'

CYTB-F 5'-ATTCCTTCATGTCGGACGAG-3'

CYTB-R 5'-ACTGAGAAGCCCCCTCAAAT-3'

ND1-F 5-'AATCGCCATAGCCTTCCTAACAT-3'

ND1-R 5'-GGCGTCTGCAAATGGTTGTAA-3'

H19-F 5'-GTACCCACCTGTCGTCC-3'

H19-R 5'-GTCCACGAGACCAATGACTG-3'

9. RNA seq

1 µg of total RNA per sample was used. Sample RNA Integrity Numbers were 10 when assayed on an Agilent 2100 Bioanalyzer. PolyA+ fraction was purified and randomly fragmented, converted to double stranded cDNA and processed through subsequent enzymatic treatments of end-repair, dA-tailing, and ligation to adapters as in Illumina's "TruSeq Stranded mRNA Sample Preparation Part # 15031047 Rev. D" kit (this kit incorporates dUTP during 2nd strand cDNA synthesis, which implies that only the cDNA

strand generated during 1st strand synthesis is eventually sequenced). Adapter-ligated library was completed by PCR with Illumina PE primers (8 cycles). The resulting purified cDNA library was applied to an Illumina flow cell for cluster generation and sequenced on an Illumina instrument (see below) by following manufacturer's protocols.

10. Quantification and statistical analysis

Survival data were analyzed by Kaplan Meier survival curves, and comparisons were performed by Log Rank test. Statistical analysis was performed using GraphPad Prism software version 5. Comparison of the percentage of mice with tumors was performed by Chi-Square test.

Fluorescence quantifications were performed with Definiens software and immunohistochemistry quantifications were performed by direct cell counting. Western Blot protein-band intensities were measured with ImageJ software and normalized against the loading control. Unpaired Student's t test (two-tailed) was used to determine statistical significance. P values of less than 0.05 were considered significant. *$p<0.05$, **$p<0.01$, ***$p<0.001$. Statistical analysis was performed using GraphPad Prism software version 5.

Results

PART 1. Effects of telomerase gene therapy in cancer prone mice

As mentioned before, AAV9-*Tert* gene therapy has not been shown to increase cancer incidence in the context of mouse longevity studies (Bernardes de Jesus *et al.*, 2012) or in the case of mouse models of diseases owing to short telomeres (Bär *et al.*, 2014, 2016; Povedano *et al.*, 2018). However, mice are short lived species compared to humans and that could make us to miss a potential long-term pro-tumorigenic effect of telomerase, even though telomerase is transitorily expressed due to the nature of the system. To circumvent this, here we set to study the safety of *AAV9-Tert* treatment in the context of cancer prone mouse models. In particular, we tested the long-term effects of AAV9-*Tert* gene therapy in an oncogene-induced lung cancer mouse model. To this end, we tested our AAV9-*Tert* gene therapy vectors in the well-established *lox-stop-lox-K-Ras^{G12V} knock-in* mouse model in which endogenous expression of the *K-Ras^{G12V}* oncogene is induced upon Cre expression (Guerra *et al.*, 2003).

1.1 Effects of telomerase activation in cancer onset, development and malignancy

In this regard, we set out to address the impact of telomerase activation by using *Tert* gene therapy in the well-established oncogenic *K-Ras* lung carcinogenesis model (Guerra *et al.*, 2003). This mouse model harbors one copy of the *K-Ras^{G12V}* oncogene *(K-Ras$^{+/LSLG12Vgeo}$)* containing a STOP codon flanked by loxP sites. Expression of the Cre recombinase leads to the excision of the stop cassette and consequent expression of *K-Ras^{G12V}* and its β-galactosidase (*β-geo*) reporter (**Figure 7A**). The Cre recombinase is delivered by intratracheal instillation with replication-defective adenoviruses encoding the Cre recombinase (Adeno-Cre) (García-Beccaria *et al.*, 2015). The telomerase gene is packaged in adeno-associated virus type 9 (AAV9) and is delivered systemically by intravenous tail injection (Bernardes de Jesus *et al.*, 2012). First, we checked whether lung cells could be co-infected with adeno-Cre and with AAV9 viruses. To this end, we simultaneously transduced mice with adeno-Cre and with AAV9 carrying GFP (AAV9-eGFP). One week after the viral transductions, mice were sacrificed and lung samples were taken for immunohistochemistry staining of β-galactosidase (β-geo), a surrogate marker co-expressed with the *K-Ras^{G12V}*, and GFP (**Figure 7C,D**). One week after induction of oncogenic *K-Ras*, β-Gal positive cells appear in small clusters of 4-8 cells that show a cytoplasmic foci staining (Mainardi *et al.*, 2014) (**Figure 7C**). Double staining with anti-β-Gal (brown) and with anti-GFP (purple) of these samples revealed that these cell clusters were

also positive for GFP, demonstrating that lung cells can be co-infected with adeno and adeno-associated viruses (**Figure 7D**).

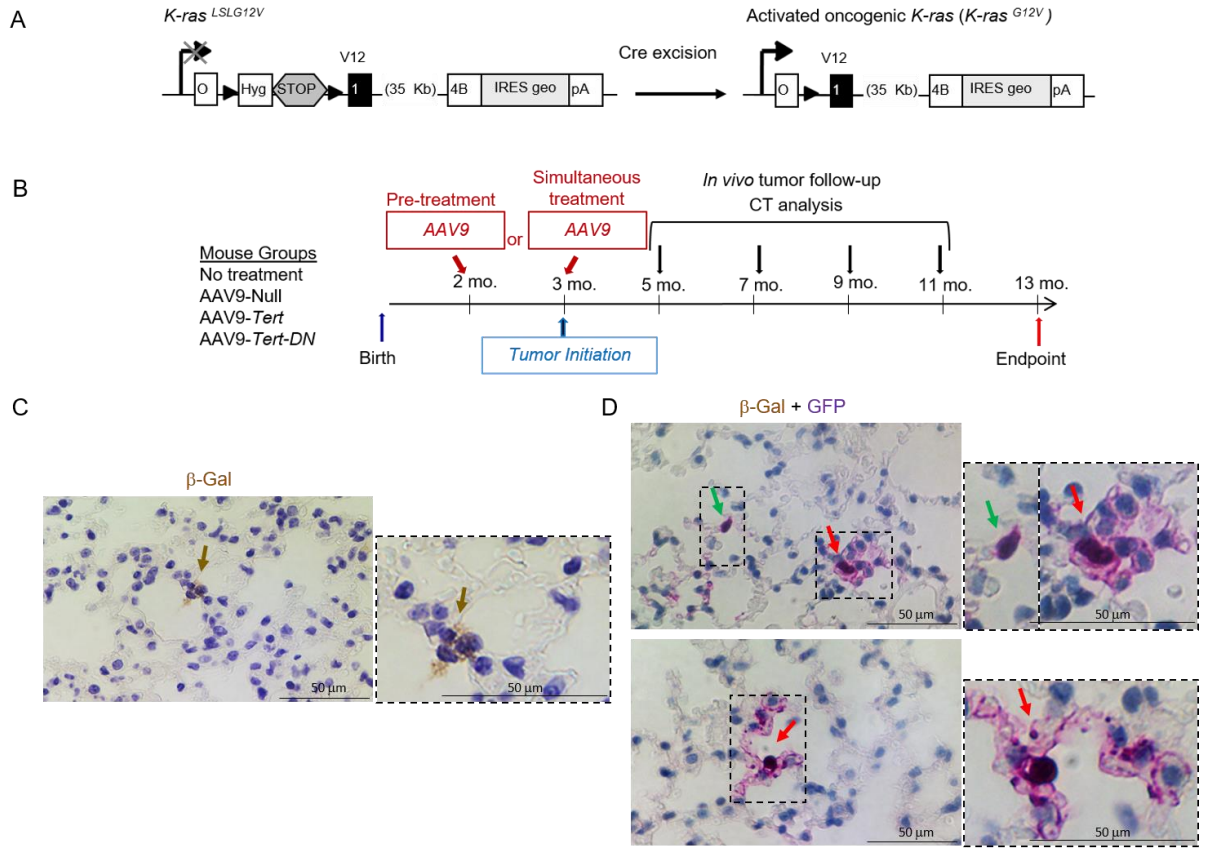

Figure 7. Oncogenic *K-Ras* expression. (A) Genetic model. The *K-Ras*^{G12V} oncogene is activated after Cre-mediated excision of the STOP cassette. **(B)** *In vivo* approaches and imaging follow up. **(C)** Representative images of β-Gal (brown) immunohistochemistry staining of lungs one week after double infection with adeno-cre and AAV9-GFP. **(D)** Representative images of β-Gal (brown) and GFP (purple) immunohistochemistry double staining of lungs one week after double infection with adeno-cre and AAV9-GFP. Brown arrow marks β-gal positive cell cluster. Green arrow marks a single AAV9-GFP positive cell. Red arrows mark cluster of cells double positive for β-Gal and GFP.

1.1.1 Telomerase activation mediated by AAV9 vectors does not favor *K-Ras*^{G12V}-induced lung carcinogenesis

Next, to address the impact of AAV9-*Tert* treatment in the context of oncogenic *K-Ras* expression, we tested two possible scenarios. First, we used a “pre-treatment” strategy in which young 8-week-old mice were first infected by tail vein injection with either AAV9-Null, AAV9-*Tert* or a catalytically inactive AAV9-*Tert-DN* vectors. TERT-DN acts as a dominant

negative and has been previously described to inhibit endogenous telomerase activity and to impair the growth of cancer cell lines (Martín-Rivera and Blasco, 2001; Sachsinger *et al.*, 2001). Four weeks after treatment with the viral vectors, we induced the expression of the oncogenic *K-Ras* by intratracheal instillation with replication-defective adenoviruses encoding the Cre recombinase (Adeno-Cre) (**Figure 7B**). In a second experimental setting, we used a "simultaneous treatment" strategy in which 12-week-old mice were treated with either one of the three AAV9 vectors (AAV9-Null, AAV9-*Tert* and AAV9-*Tert-DN*) by tail injection at the same time that they were intratracheally treated with Adeno-Cre to activate *K-Ras* (**Figure 7B**). In both strategies, we included a group of 12-weeks old mice that were not infected with any of the AAV9 vectors but were treated with adeno-Cre, as positive control for oncogenic *K-Ras* tumorigenesis in the absence of AAV9 viral vectors. Two months after oncogene activation by adeno-Cre inoculation, tumor growth was longitudinally followed by using computed tomography (CT) every two months (**Figure 7B**). Mice were sacrificed 40 weeks after oncogene activation and samples were taken for histological analysis (**Figure 7B**).

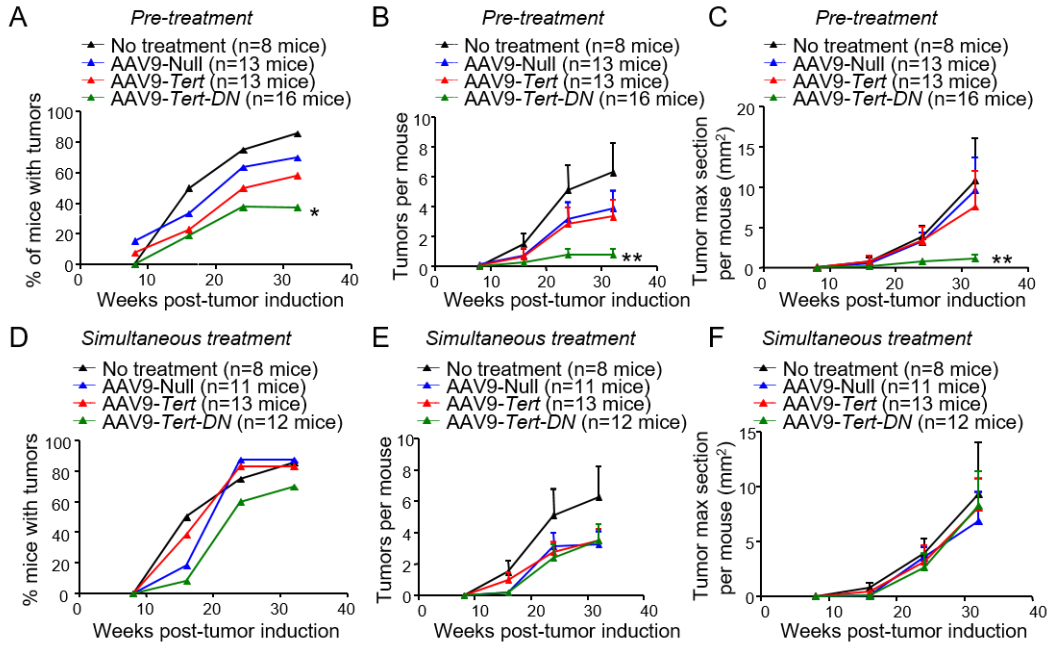

Figure 8. Tumor follow up. (A-F) CT quantification of the percentage of mice developing tumors **(A, D)**, the number of tumors **(B, E)** and the area of the tumors **(C, F)** in both, pre-treated and simultaneously treated mice. Error bars represent standard error. *t*-test was used for statistical analysis. The number of mice are indicated in each case. Indicated p-values correspond to 32-weeks-old measurements. *, p<0.05. **, p<0,01.

In vivo tumor follow-up by CT showed that AAV9-*Tert* treated mice had the same number of mice affected with tumors as well as the same number of tumors per mouse and the same tumor area as the AAV9-Null treated mice and the untreated control group both in the "pre-treatment" and "simultaneous treatment" experimental settings (**Figure 8A-F**). Interestingly, mice pre-treated with AAV9-*Tert-DN* vectors before oncogene activation ("pre-treatment group"), showed a significant decrease in the percentage of mice developing tumors at 32 weeks post-oncogene activation (**Figure 8A**). In addition, pre-treated AAV9-*Tert-DN* mice showed less number of tumors per mouse and a reduced tumor area compared to either AAV9-*Tert* treated, AAV9-Null treated mice or to the untreated control group at 32 weeks post-oncogene activation (**Figure 8B,C**). In contrast, in the "simultaneous treatment" group, we observed no significant differences between the AAV9-*Tert-DN* and the other groups both in the percentage of mice with tumors, in the number of tumors per mice or in the tumor area (**Figure 8D-F**).

We also studied the impact of AAV9-*Tert* gene therapy in *K-Ras*-induced lung tumorigenesis in a p53-deficient background, a more aggressive scenario in which lung tumors develop even more rapidly (García-Beccaria *et al.*, 2015). To this end, we first treated the mice with the AAV9 viruses and then activated oncogenic K-Ras. Mice were sacrificed 5 months post-adeno-cre infection for macroscopic quantification of tumor burden (**Figure 9A**). In this p53-deficient genetic background, 100% of the experimental mouse groups developed lung tumors and no significant differences in the number of tumors and in tumor size were detected between AAV9-*Tert* treated group as compared to AAV9-null and untreated control groups (**Figure 9B,C**).

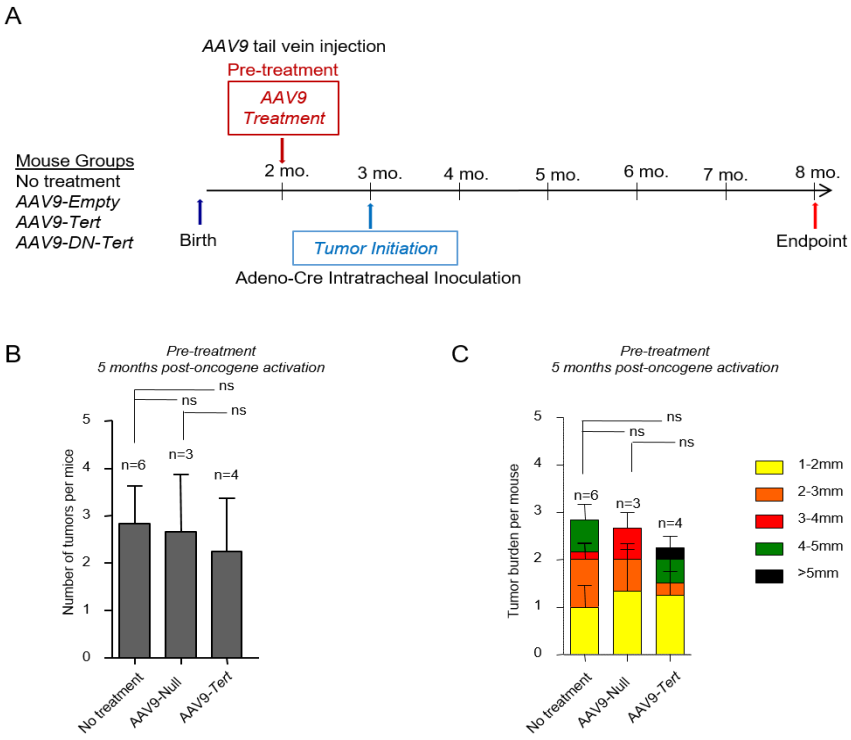

Figure 9. Oncogenic *K-Ras* expression and tumor quantification in a p53-deficient background. (A) Eight weeks old *K-Ras*$^{+/G12V}$ *p53*$^{-/-}$ mice were transduced with AAV9 (Null or *Tert*) vectors by tail vein injection and four weeks after they were infected with Adeno-cre intratracheally. Mice were sacrificed 5 months post-oncogene activation for pathological analysis. **(B-C)** Macroscopic quantification of total number of tumors per mouse **(B)** and tumor burden according to tumor diameter per mouse **(C)**. Error bars represent standard error. *t*-test was used for statistical analysis. The number of mice are indicated in each case.

All together, these results indicate that telomerase gene therapy has no effect in tumor onset or in tumor development in a context of oncogenic K-Ras lung tumorigenesis even in a p53-deficient background, in mice. In contrast, telomerase inhibition by using a dominant negative *Tert* gene, administered previously but not simultaneously to oncogene activation, significantly impairs tumor growth.

1.1.2 Telomerase activation mediated by AAV9 vectors does not increase malignancy in *K-Ras*^{G12V}-mediated lung cancer

To analyze the degree of malignancy of the *K-Ras*^{G12V} lung tumors in the different experimental cohorts, we performed hematoxylin and eosin staining in serial sections of paraffin embedded lungs at 40 weeks post-oncogene activation in the “pre-treatment” group, which was the one that showed significant differences in tumor growth in the AAV9-*Tert-DN* cohort. Lesions were classified either as hyperplasias, adenomas, or carcinomas. Hyperplasic lesions showed alveolar-like structures with uniform nuclei and similar to healthy lung tissue. Adenomas contained cells with slightly enlarged nuclei with prominent nucleoli and disturbed the adjacent tissue. Carcinomas presented cells with very large, pleomorphic nuclei, high mitotic index with aberrant mitosis, and hyperchromatism (**Figure 10A-C**). We observed no significant differences in the total number of hyperplasic lesions between the different mouse cohorts (**Figure 10A**). Similarly, mice pre-treated with AAV9-*Tert* did not show any significant differences in the incidence of adenomas and carcinomas compared to mice treated with the AAV9-Null or to mice not treated with viruses (mock) (**Figure 10B-C**). However, and interestingly, we observed a significant reduction in the number of adenomas in the AAV9-*Tert-DN* pre-treated mice compared to mock and AAV9-Null pre-treated mice (**Figure 10B**). Furthermore, the total number of carcinomas was also lower in mice pre-treated with AAV9-*Tert-DN* compared to mock, AAV9-Null and AAV9-*Tert* treated mice (**Figure 10C**). These results demonstrate that AAV9-*Tert* gene therapy does not increase the malignancy of K-Ras induced lung tumors. Again, telomerase inhibition by using AAV9-*Tert-DN* gene therapy vector previous to oncogene-induction had a significant impact in decreasing both tumor onset and tumor malignancy.

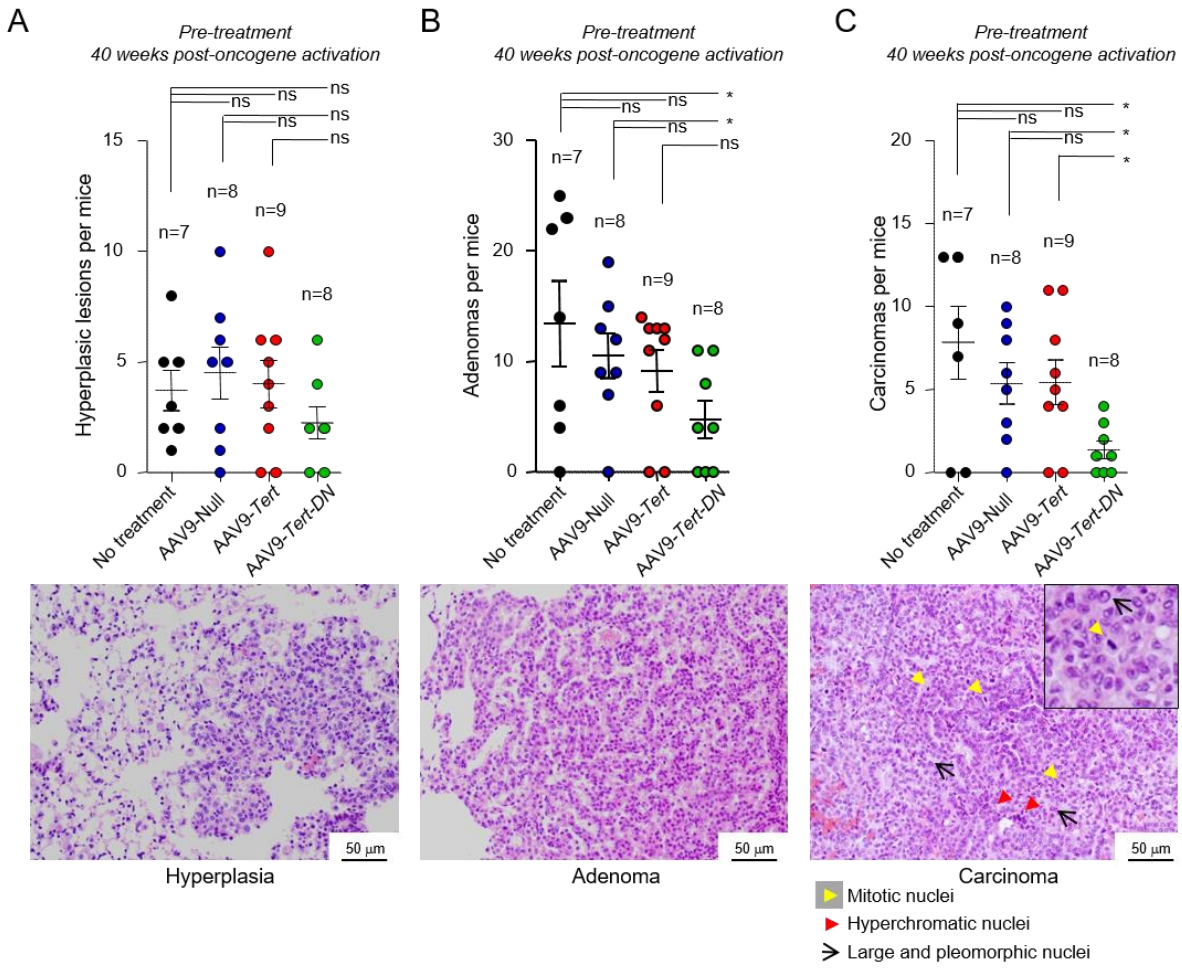
A
Pre-treatment
40 weeks post-oncogene activation
Hyperplasic lesions per mice
n=7
n=8
n=9
n=8
ns
No treatment
AAV9-Null
AAV9-Tert
AAV9-Tert-DN
B
Pre-treatment
40 weeks post-oncogene activation
Adenomas per mice
n=7
n=8
n=9
n=8
ns
*
C
Pre-treatment
40 weeks post-oncogene activation
Carcinomas per mice
n=7
n=8
n=9
n=8
ns
*
50 µm
Hyperplasia
Adenoma
Carcinoma
Mitotic nuclei
Hyperchromatic nuclei
Large and pleomorphic nuclei

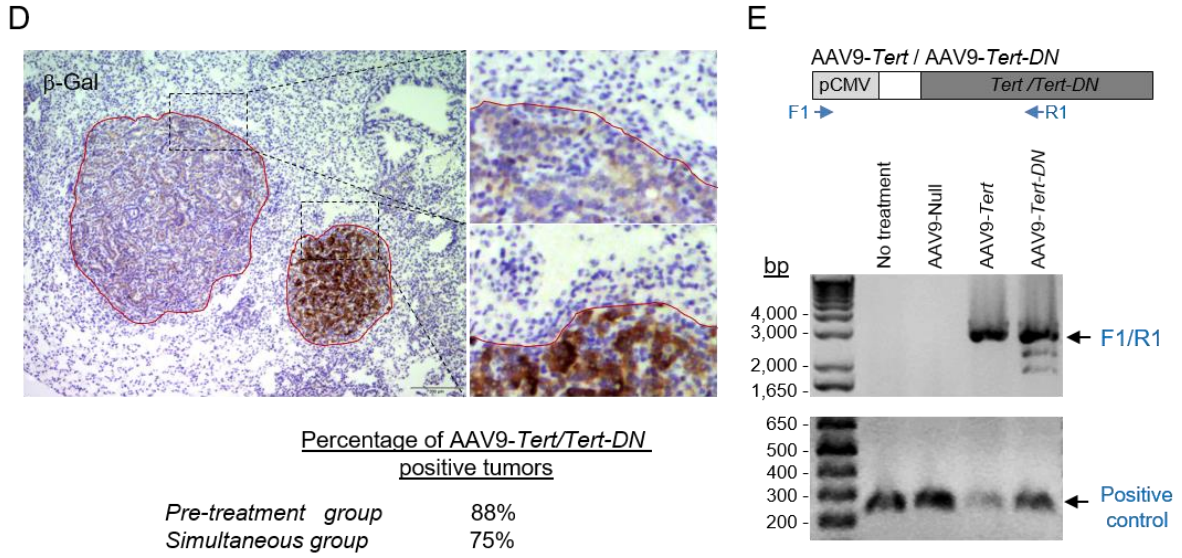
D
β-Gal
Percentage of AAV9-Tert/Tert-DN positive tumors
Pre-treatment group 88%
Simultaneous group 75%
E
AAV9-Tert / AAV9-Tert-DN
pCMV
Tert /Tert-DN
F1
R1
No treatment
AAV9-Null
AAV9-Tert
AAV9-Tert-DN
bp
4,000
3,000
2,000
1,650
F1/R1
650
500
400
300
200
Positive control

Figure 10. AAV9-*Tert* therapy does not aggravate *K-Ras*-mediated lung tumor progression. **(A-C)** Quantification of total number of hyperplasia **(A)**, adenomas **(B)** and carcinomas **(C)** in pre-treated 40 weeks old mice. A representative image of each lesions is shown in the panels below. Hyperplasic lesions show alveolar-like structures with uniform nuclei and similar to healthy lung tissue. Adenomas contain cells with slightly enlarged nuclei with prominent nucleoli and disturb the adjacent tissue. Carcinomas present cells with very large, pleomorphic nuclei (black arrows), high mitotic index (yellow arrow head) and hyperchromatism (red arrow head). Error bars represent standard error. *t*-test was used for statistical analysis. The number of mice are indicated in each case. *, $p<0.05$. **(D)** Detection of β-galactosidase expression by immunohistochemistry in the lungs as a surrogate marker of oncogenic *K-Ras*^{G12V} expression. Note that β-Gal positive areas coincide with tumors (within the red line). **(E)** PCR detection of AAV9-*Tert* and AAV9-*Tert-DN* viral genome. The PCR reaction was performed with total tumor DNA as template and primers annealing at the 5'-end within the CMV promoter (F1) at the 3'-end within the *Tert*/*Tert-DN* ORF (R1) that renders a 2.905 kb DNA fragment. A representative agarose gel image of the PCR product from the untreated, AAV9-Null, AAV9-*Tert* and AAV9-*Tert-DN* treated tumors is shown. A PCR with primers annealing to a mouse genomic 0.3 kb DNA fragment was run as a PCR positive control. The DNA ladder is shown to the left.

To confirm that the tumors originated from cells simultaneously infected with adeno-cre and the AAV9 vectors, we first determined *K-Ras*^{G12V} expression in tumors by detecting the expression of its surrogate β-galactosidase marker by immunohistochemistry and we found that all tumors were originated from adeno-cre infected cells (**Figure 10D**). We next determined the presence of the AAV9-*Tert*/AAV9-*Tert-DN* viral genomes (vg) in the tumors at the end-point from the different experimental groups. We performed a PCR from total tumor DNA as template and using primers annealing at the 5'-end within the CMV promoter that drives the expression of the *Tert* transgene and at the 3'-end within the *Tert*/*Tert-DN* ORF (**Figure 10E**). We analyze a total of 26 tumors belonging to AAV9-Null, AAV9-*Tert* and AAV9-*Tert-DN* treated mice from the "pre-treatment" and from the "simultaneous" group. We found that the AAV9-*Tert*/*Tert-DN* vg was detected in 88% of all the tumors analyzed from the "pre-treatment" and in 75% of the tumors analyzed from the "simultaneous" group (**Figure 10E**). These results confirmed that K-Ras^{G12V} induced tumors aroused from cells also infected with the AAV9 vectors.

1.2 AAV9-*Tert* treatment results in *Tert* mRNA over-expression in the lung and reduces mRNA levels of the p16 senescence marker

Next, to study whether the effects of the different viral vectors carrying the wild-type and mutant *Tert* genes could be related to their expression levels, we studied the transcriptional

expression levels of both *Tert* and *Tert-DN* mRNAs in treated lungs both at 8 weeks and 40 weeks post-oncogene activation by using quantitative PCR (qPCR) analysis. We found a similar upregulation of both *Tert* and *Tert-DN* mRNA levels at 8 weeks after oncogene activation and this up-regulation was maintained, although to lower levels, at 40 weeks after oncogene activation in both the "pre-treatment" and "simultaneously treatment" cohorts (**Figure 11A-C**).

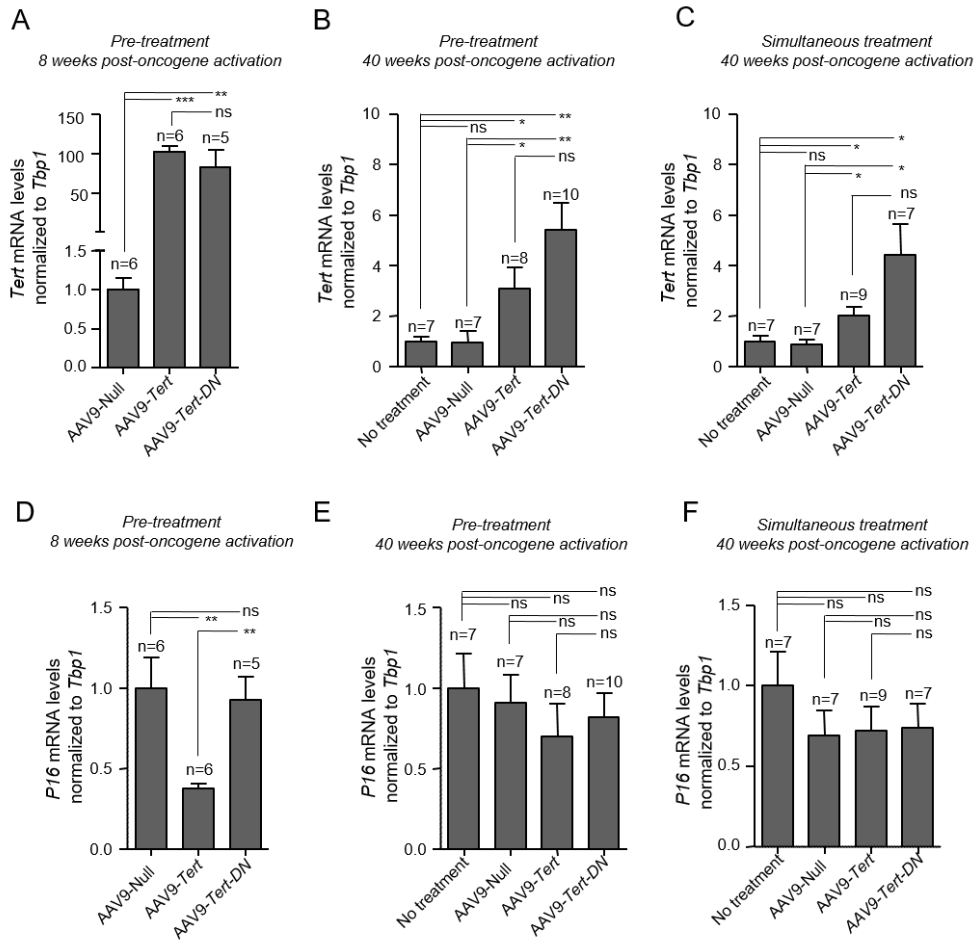

Figure 11. *Tert*, *Tert-DN* and *p16* gene expression after AAV9 injection. (A-C) *Tert* expression levels measured by qPCR in healthy lungs of pre-treated mice at 8 weeks post-oncogene activation **(A)** and pre-treated **(B)** and simultaneously treated **(C)** mice 40 weeks post-oncogene activation. **(D-F)** *p16* expression levels measured by qPCR in healthy lungs of pre-treated mice at 8 weeks post-oncogene activation **(D)** and at 40 weeks post-oncogene activation in the pre-treated **(E)** and in simultaneously treated **(F)** mice. Error bars represent standard error. *t*-test was used for statistical analysis. The number of mice are indicated in each case. *, p<0.05. **, p<0,01.

Previous studies showed that K-ras mediated lung carcinogenesis induces senescence in the pre-neoplastic lesions (adenomas) and that this senescence is overcome in the more aggressive lesions (Serrano *et al.*, 1997; Collado *et al.*, 2005; DiMauro and David, 2010). Interestingly, short/dysfunctional telomeres have been proposed to be at the origin of this oncogene-induced senescence (D'Adda Di Fagagna *et al.*, 2003; Suram *et al.*, 2012). We set to assess whether treatment with the AAV9-*Tert* and AAV9-*Tert-DN* vectors had any effects on the levels of the senescence marker p16 compared to untreated mice and to mice treated with AAV9-Null. To this end, we determined p16 mRNA levels at 8 and at 40 weeks post-oncogene activation by using qPCR (**Figure 11D-F**) (Collado, Blasco and Serrano, 2007). Interestingly, in the "pre-treatment" group, AAV9-*Tert* treated lungs showed significantly lower p16 expression compared to AAV9-*Tert-DN* treated mice and to both untreated and AAV9-Null treated mice at 8 weeks post-oncogene activation (**Figure 11D**), suggesting that telomerase expression previous to oncogene activation inhibits senescence induction at early times during K-Ras induced lung carcinogenesis. However, at 40 weeks post-oncogene activation these differences were lost and we observed similar p16 mRNA expression levels in the different mouse cohorts both in the "pre-treatment" and in the "simultaneous" group (**Figure 11E,F**), most likely owing to the more advanced tumor stage. These results indicate that pre-treatment with AAV9-*Tert* leads to reduced senescence associated to oncogene-activation, however, this does not seem to be important for overall tumor progression and aggressiveness.

1.3 AAV9-*Tert* treatment results in longer telomeres in lung cells

It has been previously demonstrated that AAV9 vectors target preferentially alveolar type II cells (ATII) in mouse lungs (80% of AAV9-infected lung cells are ATII cells) (Povedano *et al.*, 2018). To address the effects of treatment with AAV9-*Tert* and AAV9-*Tert-DN* viral vectors in telomere length in whole lung tissue and specifically in ATII cells, we performed an immuno-telomereFISH using an anti-Sftpc antibody as a marker for ATII cells and a telomeric quantitative FISH probe to measure telomere fluorescence on lung sections (Povedano *et al.*, 2018). Telomere fluorescence was measured in healthy whole-lung tissue and in ATII cells at 8 weeks post-oncogene activation in the "pre-treatment" group, which was the one that showed differences in tumor growth between the different viral treatments (**Figure 12**). The results show that AAV9-*Tert* treated lungs presented significantly higher telomere fluorescence and a lower percentage of short telomeres (telomeres below 25th percentile of telomere fluorescence) in both healthy whole-lung tissue and in ATII cells compared to AAV9-Null and AAV9-*Tert-DN* treated lungs (**Figure 12 A-C**).

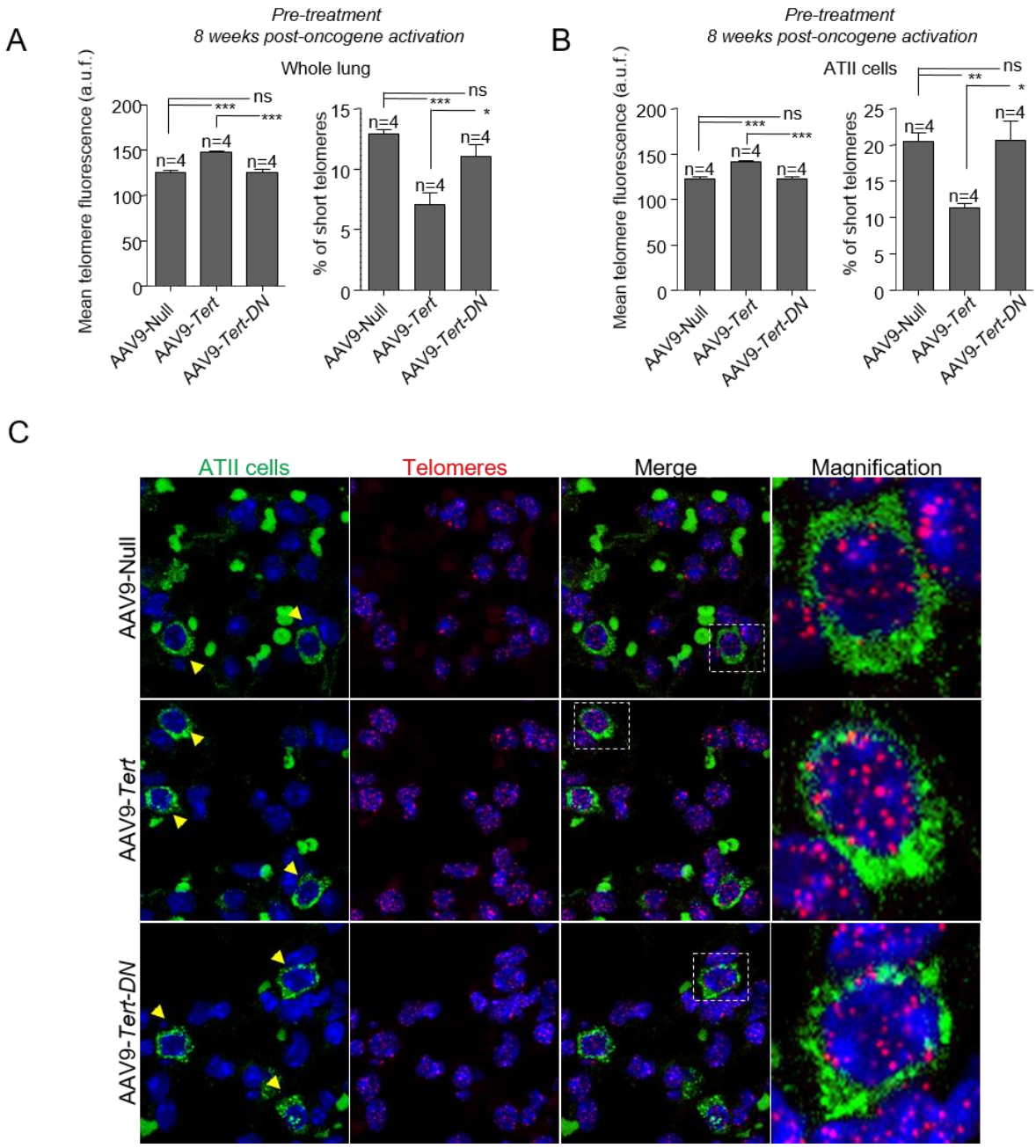

Figure 12. Telomerase gene therapy results in longer telomeres in lung cells. **(A-B)** Mean telomere fluorescence and percentage of short telomeres in whole lung **(A)** and in ATII cells **(B)** at 8 weeks post-oncogene activation in the pre-treated mice. **(C)** Representative images showing ATII cells stained with anti-SFTPC (green cytoplasm, yellow arrow heads) by IF and telomeres stained in red by FISH. Auto-fluorescent red blood cells lacking nuclei are observed in the images. Magnification images are shown to the right. Error bars represent standard error. *t*-test was used for statistical analysis. The number of mice are indicated in each case. *, p<0.05. **, p<0,01. ***, p<0,001.

Telomere fluorescence was also measured in healthy whole-lung tissue, in ATII cells, and in tumors at the experimental end-point (40 weeks post-oncogene activation) in both pre-treated (**Figure 13**) and simultaneously treated groups (**Figure 14**). At the end-point, AAV9-*Tert* treated mice in both groups, "pre-treatment" and "simultaneous", showed longer telomeres and lower percentage of short telomeres both in the whole lung and in ATII cells compared to untreated, AAV9-Null and to AAV9-*Tert-DN* control groups (**Figures 13A-C and 14A-C**). When telomere length was determined in tumors, we also observed a significant increase in average telomere length and a decrease in the percentage of short telomeres in AAV9-*Tert* treated samples compared to untreated, AAV9-Null and to AAV9-*Tert-DN* control groups (**Figures 13D,E and 14D,E**).

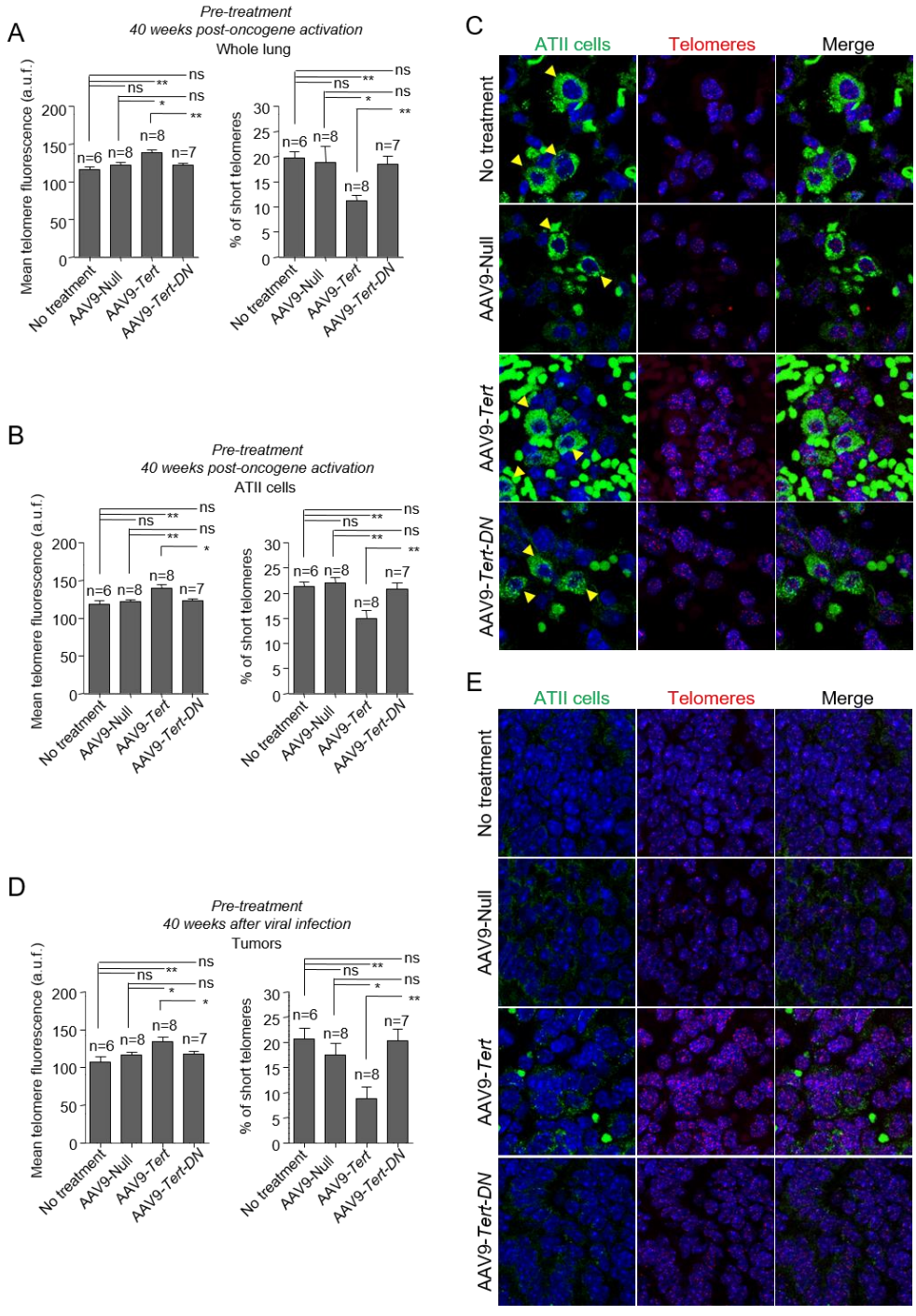

Figure 13. Telomerase gene therapy results in longer telomeres in lung cells and tumors in the "pre-treatment" group. (A-E) Mean telomere fluorescence and percentage of short telomeres in whole lung **(A)**, in ATII cells **(B)** and in tumors **(D)** at 40 weeks post-oncogene activation in the pre-treated mice. **(C,E)** Representative images showing ATII cells stained with anti-SFTPC (green cytoplasm, yellow arrow heads) by IF and telomeres stained in red by FISH in healthy lung tissue **(C)** and in tumors **(E).** Auto-fluorescent red blood cells lacking nuclei are observed in the images. Tumor samples do not show any SFTPC positive cells. Error bars represent standard error. *t*-test was used for statistical analysis. The number of mice are indicated in each case. *, p<0.05. **, p<0,01.

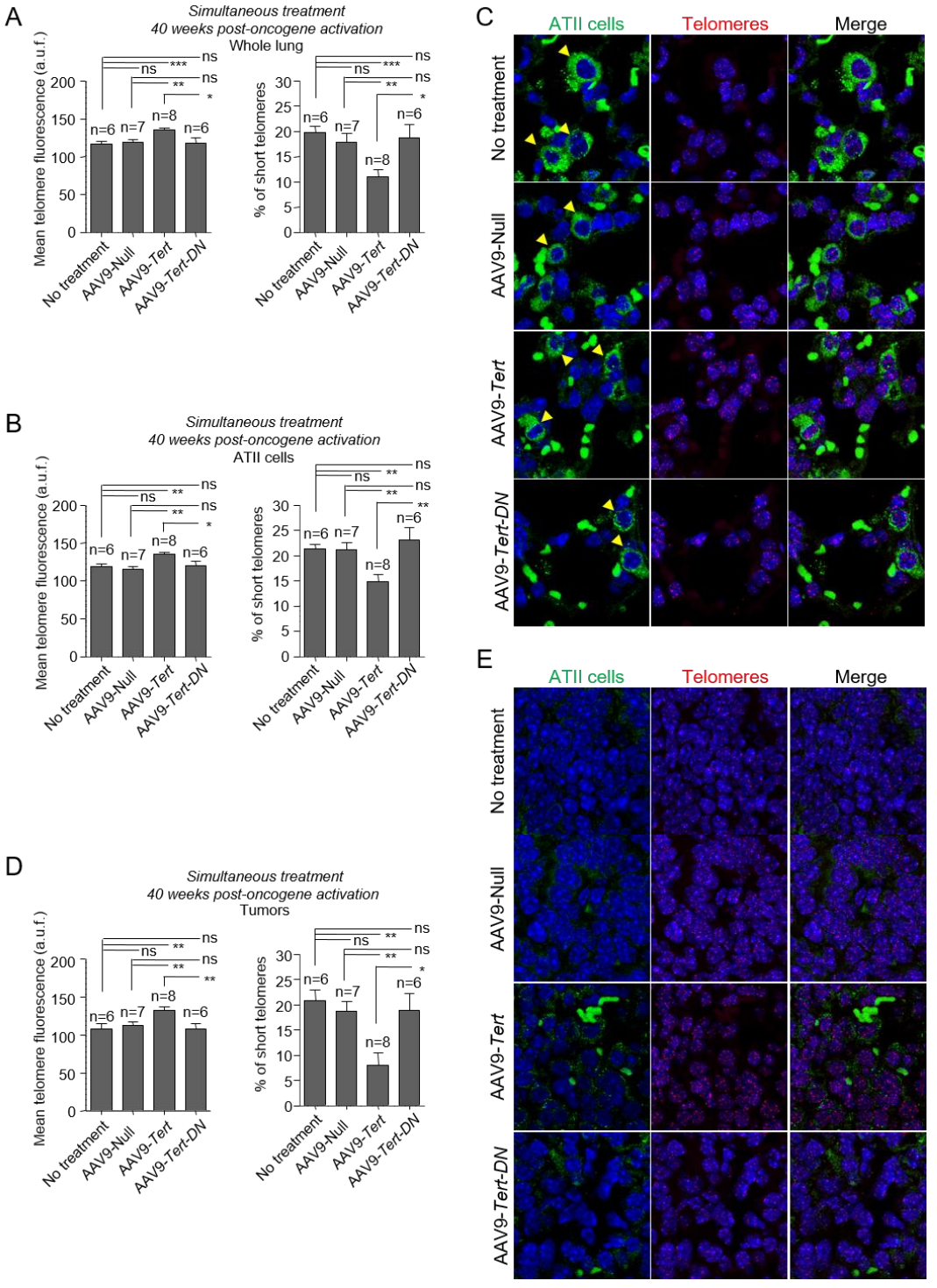

Figure 14. Telomerase gene therapy results in longer telomeres in lung cells and tumors in the simultaneous treatment group. (A-E) Mean telomere fluorescence and percentage of short telomeres in whole lung **(A)**, in ATII cells **(B)** and in tumors **(D)** at 40 weeks post-oncogene activation in simultaneously treated mice. **(C,E)** Representative images showing ATII cells stained with anti-SFTPC (green cytoplasm, yellow arrow heads) by IF and telomeres stained in red by FISH in healthy lung tissue **(C)** and in tumors **(E)**. Auto-fluorescent red blood cells lacking nuclei are observed in the images. Tumor samples do not show any SFTPC positive cells. Error bars represent standard error. *t*-test was used for statistical analysis. The number of mice are indicated in each case. *, p<0.05. **, p<0,01.

1.4 Effects of dominant negative version of telomerase activation in tumor environment

1.4.1 AAV9-*Tert-DN* treatment induces DNA damage and apoptosis and blocks proliferation in lung tumors

To understand, at the molecular level, the impact of different AAV9 treatments on lung tumorigenesis, we next determined DNA damage (γH2AX-positive cells), apoptosis (C3A-positive cells), and proliferation (Ki67-positive cells) in tumors at 40 weeks post-oncogene activation both in the "pre-treatment" and "simultaneous treatment" groups by using immunohistochemistry. Interestingly, in both experimental settings, tumors appearing in the AAV9-*Tert-DN* treated mice showed significantly less Ki67-positive cells compared to AAV9-*Tert* treated and to control groups (no viral treatment and mice treated with AAV9-Null) (**Figure 15A**), which is in agreement with significantly less tumors in this group (**Figure 8A-C**). Importantly, no significant differences in Ki67-positive cells were observed between AAV9-*Tert* treated and control mice (no viral treatment and mice treated with AAV9-Null) neither in the "pre-treatment" nor in the "simultaneous" groups (**Figure 15A-C**), which is in agreement with similar tumor burdens in these groups (**Figure 8D-F**).

Next, we determined the impact of different AAV9 treatments on DNA damage induction by quantifying the percentage of γH2AX positive cells in the tumors at 40 weeks after oncogene-induction both in the "pre-treatment" and "simultaneous treatment" groups. We found that lung tumors appearing in the mice with AAV9-*Tert-DN* presented increased number of cells with DNA damage compared to AAV9-*Tert* treated and control mice (no viral treatment and treated with AAV9-Null). Again, the tumors appearing in mice treated with AAV9-*Tert* showed a similarly low abundance of cells positive for γH2AX to the untreated and AAV9-Null treated cohorts (**Figure 15D-F**).

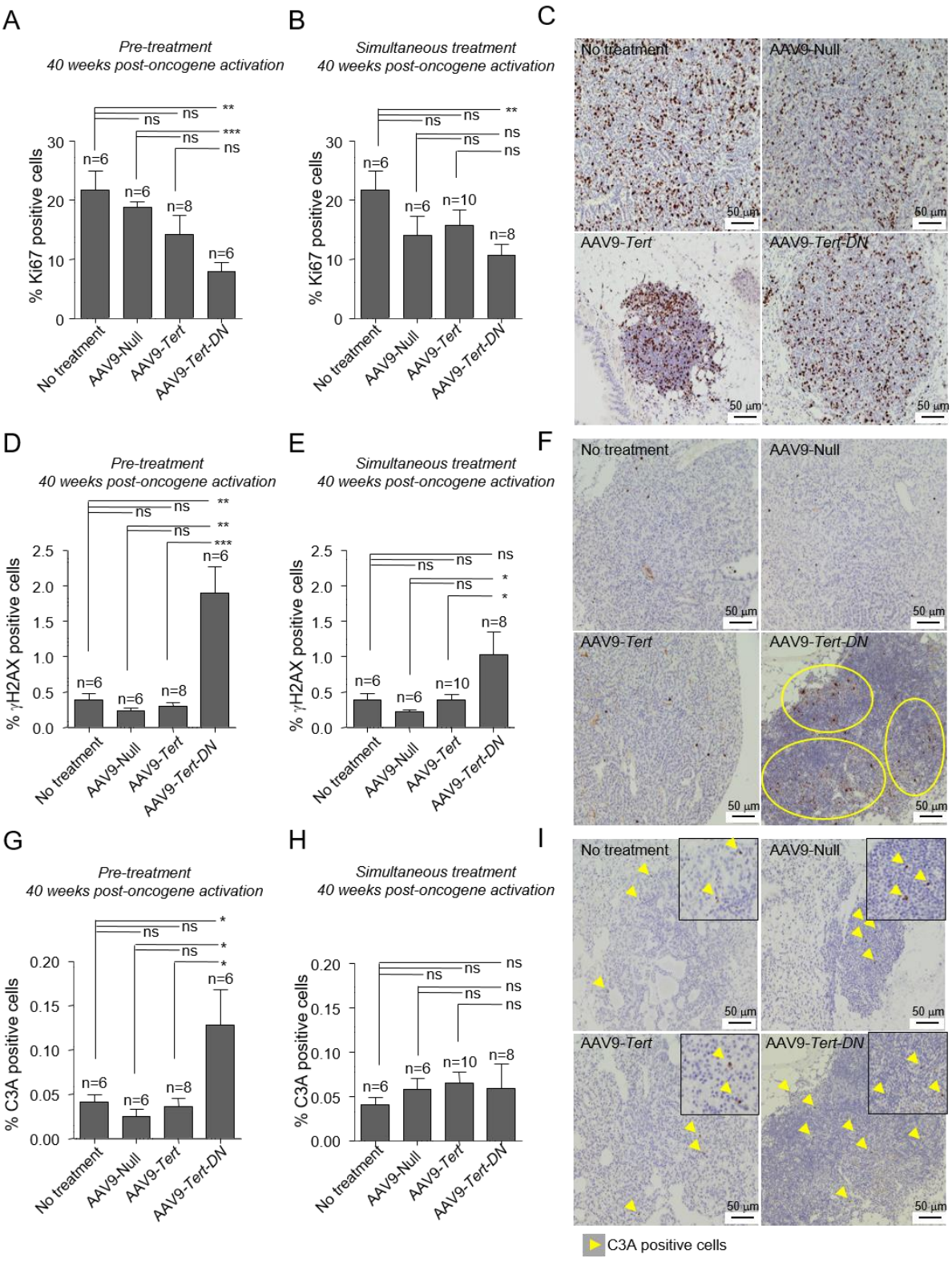
A
Pre-treatment
40 weeks post-oncogene activation
% Ki67 positive cells
B
Simultaneous treatment
40 weeks post-oncogene activation
% Ki67 positive cells
C
No treatment
AAV9-Null
AAV9-Tert
AAV9-Tert-DN
50 µm
D
Pre-treatment
40 weeks post-oncogene activation
% γH2AX positive cells
E
Simultaneous treatment
40 weeks post-oncogene activation
% γH2AX positive cells
F
G
Pre-treatment
40 weeks post-oncogene activation
% C3A positive cells
H
Simultaneous treatment
40 weeks post-oncogene activation
% C3A positive cells
I
C3A positive cells

Figure 15. Effect of AAV9 treatments on tumor proliferation DNA damage burden and apoptosis. (A-C) Quantification of the percentage of Ki67 positive cells in pre-treated **(A)** and simultaneously treated mice **(B)** at 40 weeks post-oncogene activation; Ki67 representative images correspond to pre-treated mice lung tumors **(C)**. **(D-F)** Quantification of the percentage of γ-H2AX positive cells in the pre-treated **(D)** and simultaneously treated **(E)** mice at 40 weeks post-oncogene activation; γ-H2AX representative pictures correspond to pre-treated mice lung tumors **(F)**. **(G-I)** Quantification of the percentage of active caspase-3 (C3A) positive cells in pre-treated **(G)** and simultaneously treated mice **(H)** at 40 weeks post-oncogene activation; C3A positive cells (yellow arrow heads) in representative images corresponding to pre-treated lung tumors **(I)**. Error bars represent standard error. *t*-test was used for statistical analysis. The number of mice is indicated in each case. *, p<0.05. **, p<0,01. ***, p<0,001.

In accordance with higher DNA damage in tumors from mice pre-treated with AAV9-*Tert-DN* vectors, we observed increased numbers of apoptotic cells in the AAV9-*Tert-DN* treated mice compared to AAV9-*Tert* treated mice and control mice (untreated and AAV9-Null treated cohorts) (**Figure 15G,I**). Again, in the "pre-treatment" group we found no significant differences in the number of apoptotic cells between the AAV9-*Tert* and control mice (**Figure 15G,I**). However, no differences in the number of apoptotic cells were observed in the "simultaneous treatment" among the different mouse cohorts (**Figure 15H,I**), in agreement with similar tumor burden in all cohorts within the simultaneous treatment group (**Figure 8D-F**)

Altogether, these results indicate that tumor burden in the different cohorts correlates with proliferation, DNA damage and apoptosis, namely tumors appearing in the AAV9-*Tert-DN* "pre-treatment" group have less proliferation and more DNA damage and apoptosis. Importantly, telomerase overexpression in the AAV9-*Tert* treated mice did not influence any of these parameters either in the "pre-treatment" or in the "simultaneous treatment" groups, in agreement with the fact that AAV9-*Tert* treatment did not increase lung tumorigenesis.

1.4.2 AAV9-*Tert-DN* treatment induces telomeric DNA damage in KRas-induced lung tumors

In order to study the effects of the different gene therapy vectors on DNA damage specifically located at telomeres, we performed a double immunofluorescence using antibodies against 53BP1 to mark DNA damage foci and TRF1 to mark telomeres in lung tumor sections. To this end, we quantified the number of cells presenting ≥4 53BP1 foci within the tumor in the "pre-treatment" and "simultaneous treatment" groups (**Figure 16A-C**).

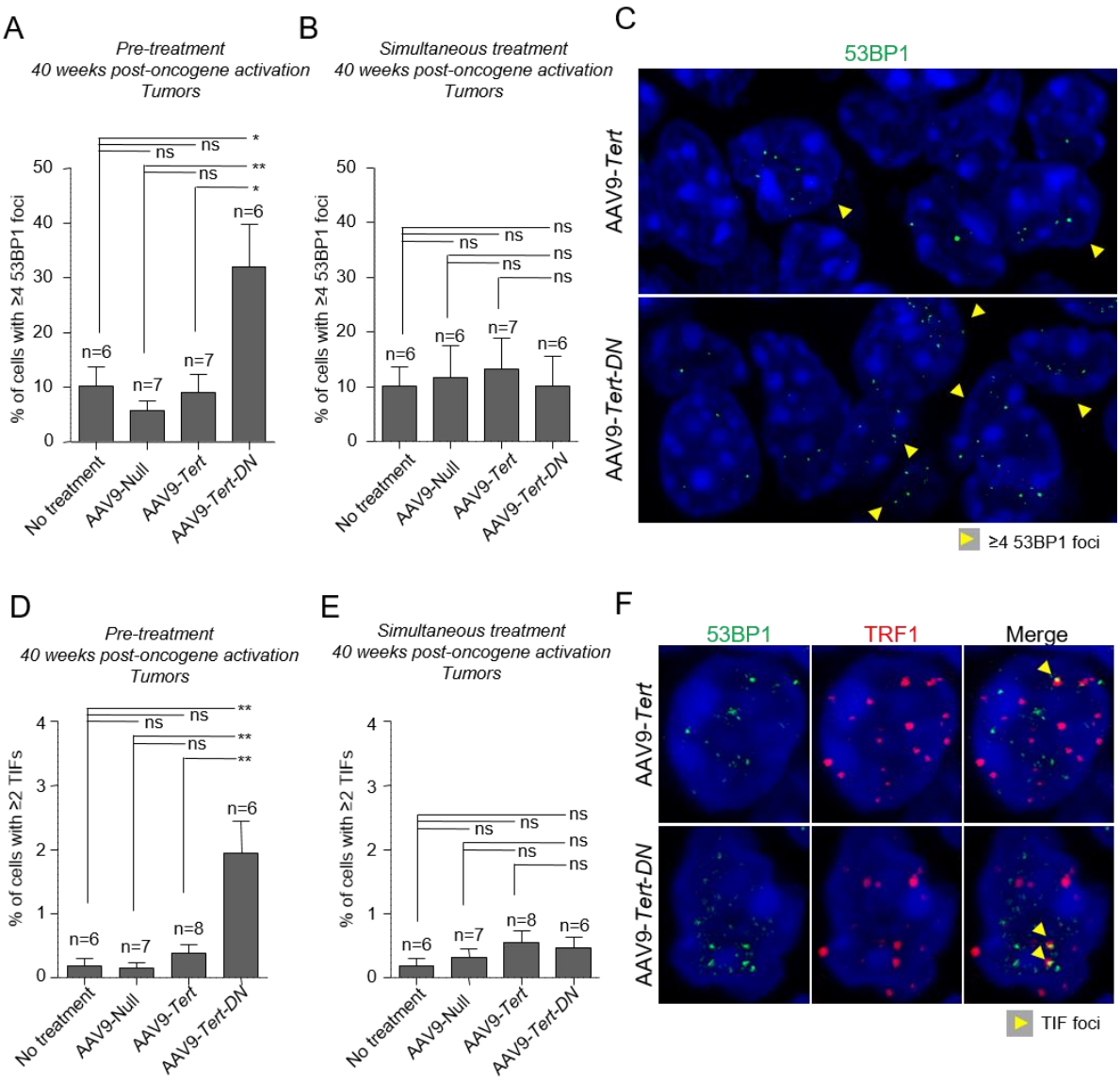

Figure 16. Increased DNA damage after AAV9-*Tert-DN* gene therapy correlate with more telomeric DNA damage. (A-B) Quantification of percentage of cells with more than 3 53BP1 foci by IF, 40 weeks post-oncogene activation in the "pre-treatment" group **(A)** and in the "simultaneous" group **(B)**. **(C)** Representative images of 53BP1 staining. Cells with more than 3 53BP1 foci corresponding to pre-treated mice are marked with a yellow arrow head. **(D-E)** Quantification of percentage of cells with more than 1 telomeric induced foci (TIF) by IF, 40 weeks post-oncogene activation in the "pre-treatment" group **(D)** and in the "simultaneous" group **(E)**. **(F)** Representative images of TIF (yellow arrow heads) positive cells corresponding to pre-treated mice. DNA damage and telomeric foci were labeled with antibody against 53BP1 (green) and antibody against TRF1 (red). Error bars represent standard error. *t*-test was used for statistical analysis. The number of mice is indicated in each case. *, p<0.05. **, p<0,01.

In the “pre-treatment” group, tumors appearing in the AAV9-*Tert-DN* treated mice showed a 5-fold increase in 53BP1-positive cells compared to tumors appearing in untreated mice or mice treated with AAV9-Null and AAV9-*Tert* vectors (**Figure 16A,C**). In the “simultaneous” group, however, no differences in the percentage of damaged cells among the four mouse cohorts were detected (**Figure 16B**). In addition, the percentage of damaged cells presenting ≥ 2 telomere induced foci (TIF) was 5-fold higher in tumors from the AAV9-*Tert-DN* treated group compared to untreated, AAV9-Null and AAV9-*Tert* treated cohorts in the “pre-treatment” group (**Figure 16D,F**). In the “simultaneous treated group”, however, no differences in the percentage of cells presenting ≥ 2 TIFs among the four mouse cohorts were detected (**Figure 16E**). These results suggest that telomerase inhibition by using AAV9-*Tert-DN* gene therapy vectors previous to oncogene activation results in increased telomere damage associated to oncogenic K-Ras tumorigenesis. This is in agreement with the reduced tumor burden observed in mice in which telomerase activity was inhibited by AAV9-*Tert-DN* before oncogene activation (**Figure 8A-C and 10C**). The observation that AAV9-*Tert* treatment leads to similar numbers of tumor cells with telomere damage (TIFs) than the AAV9-Null controls, underlies the non-oncogenic effects of telomerase gene therapy.

PART 2. Characterization of the effects of telomere elongation beyond the pre-established length in mice.

As told in the introduction, *in vitro* expansion of mouse ES cells derived from the ICM results in a further telomere lengthening until doubling the normal telomere length of the ICM of the blastocyst. These telomeres are referred to as hyper-long telomeres (Varela *et al.*, 2011). Interestingly, these cells can be aggregated in morulae, and can undergo development to the blastocyst stage maintaining the hyper-long telomere phenotype (Varela *et al.*, 2011). Here, we set to address the hypothesis of whether it would be possible to modify the normal telomere length of the *Mus musculus* species by altering telomere length in ESC in the absence of genetic manipulations. Thus, we set to study whether ES cells with hyper-long telomeres were able to give rise to chimeric mice composed of cells with hyper-long telomeres, and to study telomere length dynamics with aging in these mice.

2.1 Mouse ES cells requires few passages to elongate their telomeres

It has been previously described that ES cells lengthen their telomeres upon *in vitro* expansion (Varela *et al.*, 2011). Thus, here we first addressed whether there was a limit to telomere lengthening during expansion. To this end, we subjected ES cells to over 60 passages *in vitro* and analyzed telomere length by quantitative FISH (Q-FISH) on metaphase spreads at different passages. Mean telomere length was increased until passage 24 and then, was maintained until passage 60 (**Figure 17**), suggesting that a few passages are sufficient to reach maximum telomere length in ES cells.

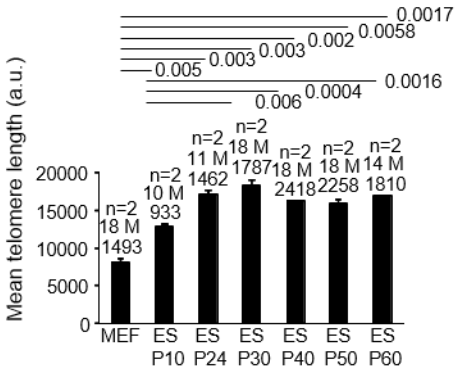

Figure 17. Analysis of ES cells bearing hyper-long telomeres. Mean telomere length analyzed on metaphase spreads in primary MEF (passage 2) and ES cells at the indicated passages. The "M" in the graph indicates the number of metaphases studied. Student T-test with the Bonferroni correction was used to calculate the p values.

2.1.1 Hyper-long ES cells show similar gene expression patterns and no increased telomerase activity compared to normal ES cells

To study whether other changes might occur during *in vitro* expansion of ES cells we subjected four independent clones of ES cells at passage 6 and passage 16 to RNA-deep sequencing and found only five genes (out of 19555 genes analyzed) significantly differentially expressed for an FDR below 0,05 analyzed using DESeq (Methods). These genes were *Sox18* (upregulated 20-fold compared to ES cells at passage 6) and *Sox17*, *Zbtb48*, *Chst15* and *Jph4* (downregulated less than 2-fold compared to ES cells at passage 6) (**Table 1**). Thus, RNA-seq analysis showed very few changes in gene expression between ES cells at passage 4 and 16. Importantly, we did not observe alterations in mRNA expression of telomerase genes or in components of shelterin. We confirmed similar TRAP telomerase activity in passage 4 and passage 16 ES cells (**Figure 18**).

RNA sequencing of ES cells at passage 16 versus passage 6

Gene name	Log2 fold change	P value	Function
Sox18	4.455160405	1.73E-224	Embryonic and postnatal angiogenesis (1)
Sox17	-1.185658886	5.18913E-12	Embryonic and postnatal angiogenesis (2)
Zbtb48	-0.969303187	4.3873E-08	POK family protein (3)
Chst15	-0.8167311010.16707432	1.01643E-06	Sulfotransferase (4)
Jph4	-0.6540687230.13873356	2.42225E-06	Junctional membrane complexes (5)

In red genes that were upregulated at passage 16 compared to passage 6 and in green genes that were downregulated at passage 16 compared to passage 6.

Table 1. RNA sequencing of ES cells at different passages.

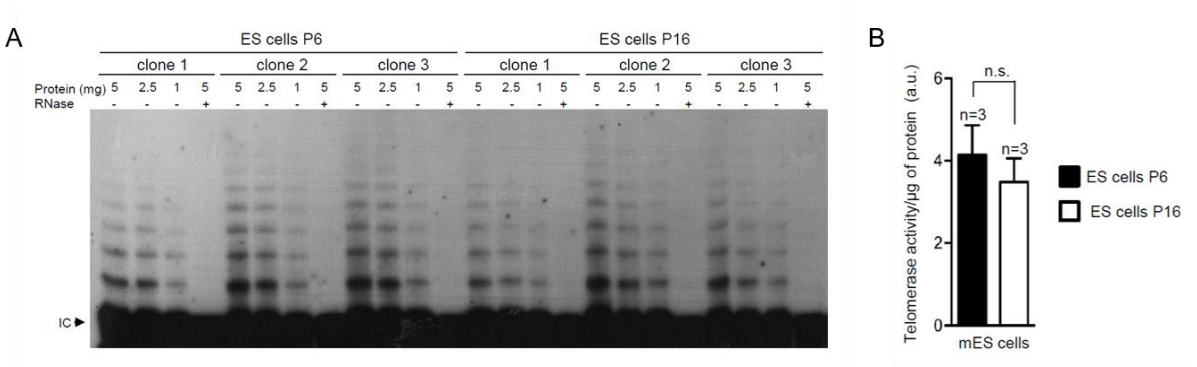

Figure 18. Telomerase activity in early and late passage ES cells. (A) Telomerase activity assay from extracts of three independent clones of mouse ES cells at passage 6 and passage 16. **(B)** Quantification of the telomerase activity.

2.1.2 Hyper-long telomere ES cells do not present increased levels of specific telomere damage and telomeric aberrations

We next asked whether continuous telomere lengthening associated to *in vitro* ES cell expansion would cause DNA damage, particularly at regions difficult to replicate such as telomeres. To assess DNA damage specifically at telomeric chromatin, we performed double immunofluorescence with anti-γH2AX and TRF1 antibodies to quantify TIFs (**Figure 19A-C**). We found very few ESCs with DNA damage (> 3 γH2AX foci per cell) up to passage 24, but this percentage significantly increased at later passages with more than 40% of the cells showing DNA damage (**Figure 19A**). In the case of telomere-specific damage, we also observed low numbers of telomere-induced DNA damage foci (TIF)-positive cells until passage 24, and this was significantly increased at later passages (**Figure 19B,C**).

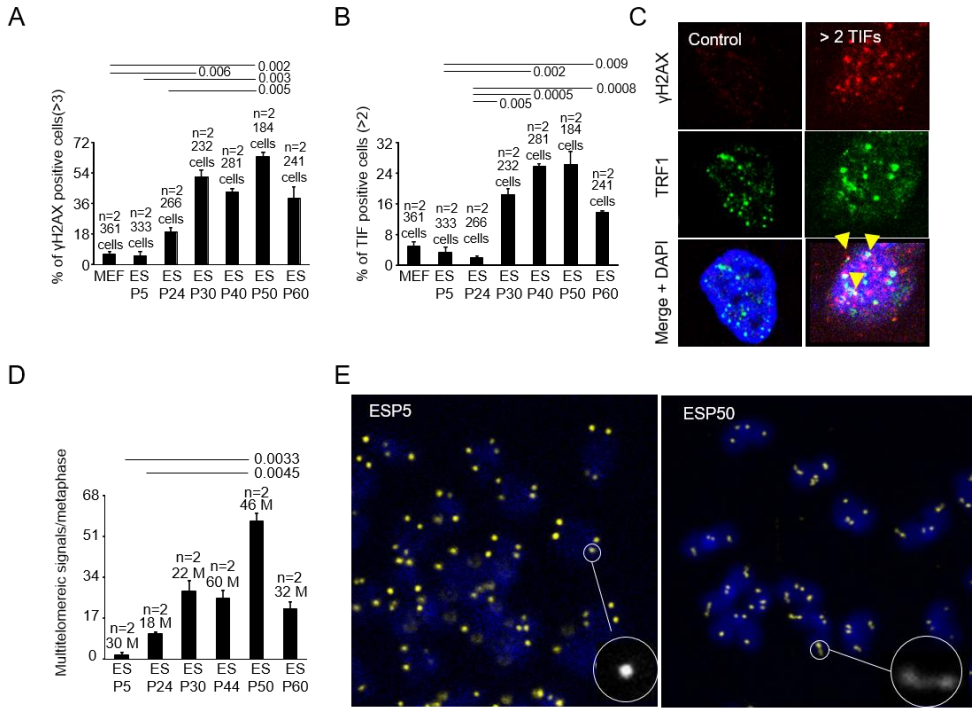

Figure 19. (A) Percent of cells with DNA damage measured by IF with anti γH2AX antibody in primary MEFs (passage 2) and ES cells at the indicated passages. We show a representative graph of three independent experiments. **(B)** Percent of cells with more than 2 TIFs, analyzed by IF with anti γH2AX and TRF1 antibodies in primary MEFs (passage 2) and ES cells at the indicated passages. We show a representative graph of three independent experiments. **(C)** Representative micrographs of control or damaged cells. Cells were subjected to IF with anti γH2AX and TRF1 antibodies. Colocalization of γH2AX and TRF1 is indicated with yellow arrows. **(D)** Mean number of multitelomeric signal in metaphases from ES cells at the indicated passages, analyzed by telomere FISH. Representative graph of two independent experiments. **(E)** Representative images of metaphases at passages 5 and 50. A representative telomere shape is highlighted in each micrograph. Student T-test with the Bonferroni correction was used to calculate the p values.

In order to study the specific type of DNA damage present at later passages in cells with hyper-long telomeres, we arrested cells with colcemid and performed telomere Q-FISH on metaphase spreads. We found that the only telomere aberration increased with ESC passaging was the presence of multitelomeric signals (MTS) (**Figure 19D,E**), a type of aberration previously associated to increased telomere fragility as the result of replication stress at telomeres (Marion *et al.*, 2009; Sfeir *et al.*, 2009).

Taken together these results demonstrate that hyper-long telomeres after moderate ES cell passaging (up to 24 passages) are well capped and do not show increased DNA damage.

2.2 ES cells with hyper-long telomeres are able to generate 100% contributing chimeric mice

We previously showed that it is possible to generate mouse ES cells with hyper-long telomeres in the absence of any genetic manipulations. In order to address the impact of excessively long telomeres in a given species, next, we addressed the capability of ES cells bearing hyper-long telomeres to contribute to chimaera formation *in vivo* and to retain hyper-long telomeres in the adult organism. They were not only able to contribute in the formation of chimeric mice but also they allow us to generate a cohort of chimeric mice with a 100% contribution from ES cells with hyper-long telomeres ES cells. To this end, approximately 100 morulae at the eight-cell state were microinjected with 6-10 GFP-positive female ES cells with hyper-long telomeres at passage 16 by laser-assisted perforation of the “zona pellucida” obtaining chimeric mice which were 100% contributed by the GFP-positive ES cells (**Figure 20A**). In particular, adult mice (1.5 to 2 years of age) mice showed 100% of their cells positive for eGFP as determined by immunohistochemistry (IHC) with anti GFP antibodies in different mouse tissues (**Figure 20B**). The fact that, even at old age, chimeric mice show 100% of the cells that are GFP-positive, and therefore are derived from ES cells with hyper-long telomeres, indicates that these cells with hyper-long telomeres are not negatively selected during aging. Further supporting that cells with hyper-long telomeres are not deleterious, all mouse tissues showed a normal histology even at older ages (**Figure 20B**).

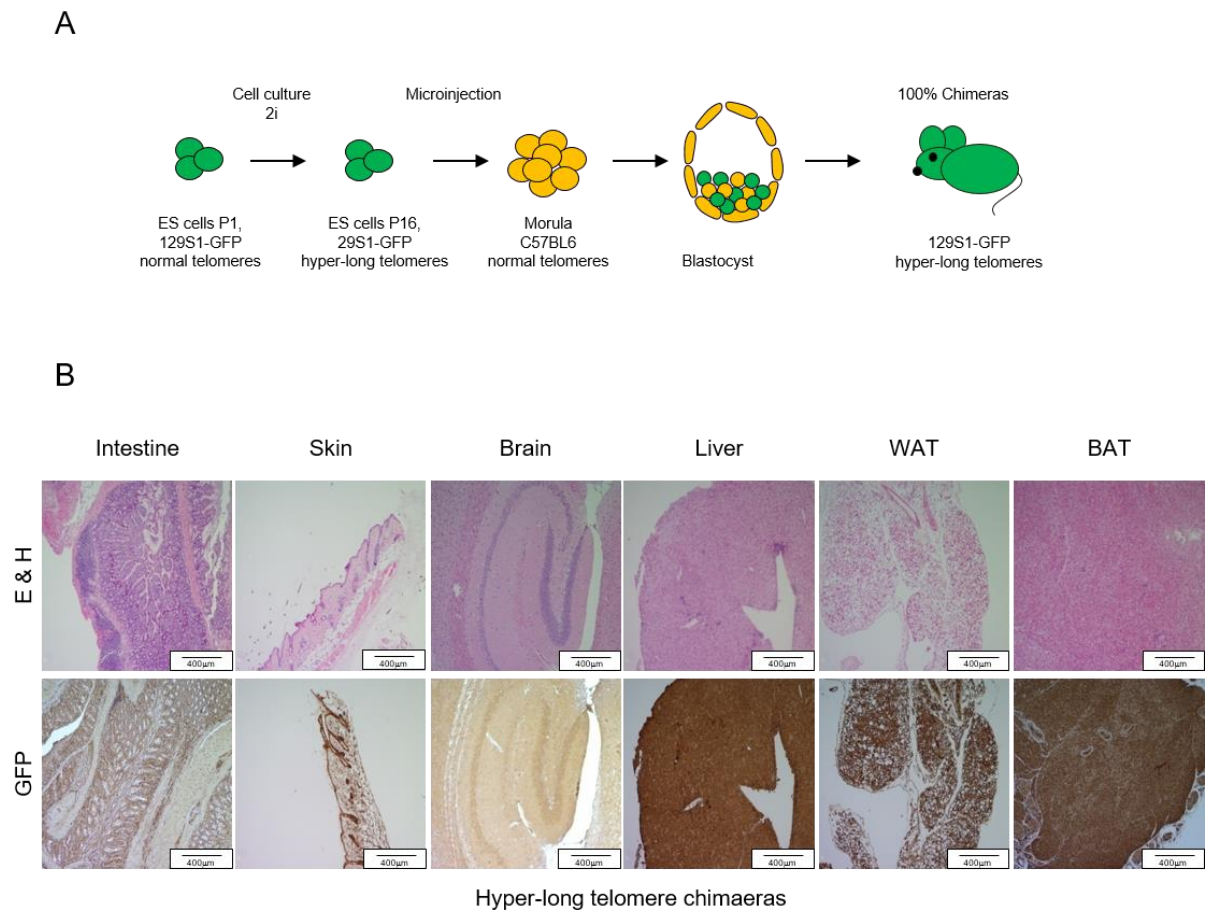

Figure 20. Hyper-long ES cells contribute to form 100% healthy chimeric mice. (A) Scheme showing generation of mice with hyper-long telomeres. eGFP ES cells are cultured in 2i medium until passage 16 and they are microinjected into morulae to obtain 100% contributing chimaeras. **(B)** Representative images showing 100% eGFP ES cell contribution in different organs and tissues.

2.3 Differential phenotypic effects in Hyper-long telomere mice

2.3.1 Hyper-long telomere mice present lower weight rates due to less fat accumulation

Strikingly, these mice 100% contributed by ES cells with hyper-long telomeres were significantly reduced size than control mice from the same genetic background (**Figure 21A**). To further study this unexpected phenotype, we carried out a longitudinal follow-up of mouse weight throughout their entire lifespan and found that hyper-long telomere mice showed a significant reduction in body weight which started from 40 weeks of age onwards (**Figure 21B**).

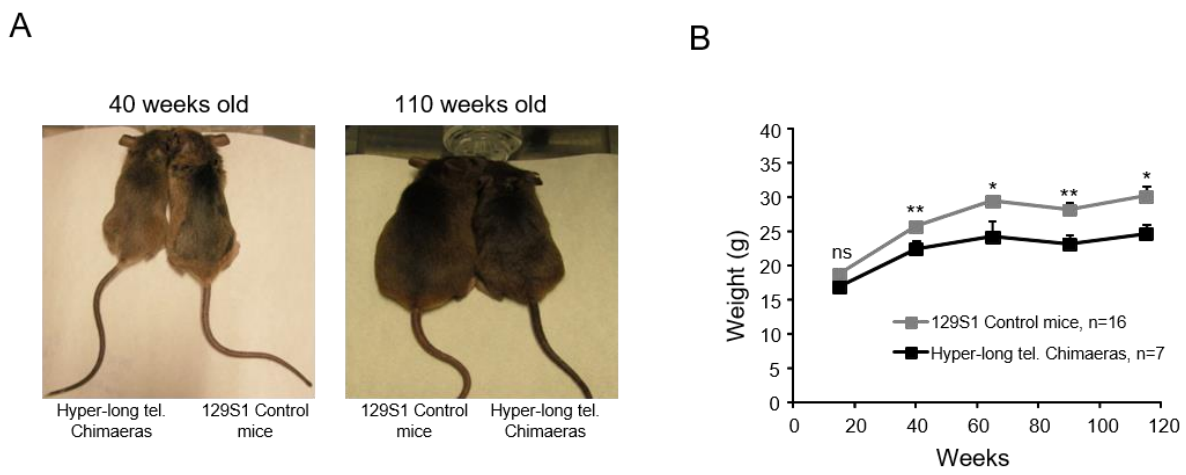

Figure 21. Hyper-long telomere mice are leaner than normal mice. (A,B) Longitudinal follow up of weight in the indicated cohorts. Hyper-long telomere mice show a significant reduction in body weight from 40 weeks onwards **(A)** and this body size reduction is maintained until the last timepoint measured **(A,B)**. Error bars represent standard error. *t*-test was used for statistical analysis. The number of mice is indicated in each case. *, p<0.05. **, p<0,01.

In order to investigate the small-body size phenotype of hyper-long telomere mice, we performed densitometry assays at 75 and 100 weeks of age in both hyper-long telomere mice and normal telomere length controls from the same genetic background. We found that hyper-long telomere mice showed significantly lower fat content than age-matched control mice at two different ages (75 and 100 weeks-old) (**Figure 22A**). In contrast, no differences were observed in either bone mineral density (BMD) (**Figure 22B**) or in total lean mass between hyper-long telomere mice and the normal telomere length controls (**Figure 22C**). In agreement with lower fat accumulation, hyper-long telomere mice also showed a significantly reduced skin subcutaneous fat layer compared to age-matched control mice (100 weeks of age) (**Figure 22D, E**). These results indicate that the reduced body size of hyper-long telomere mice is due to a lower accumulation of fat.

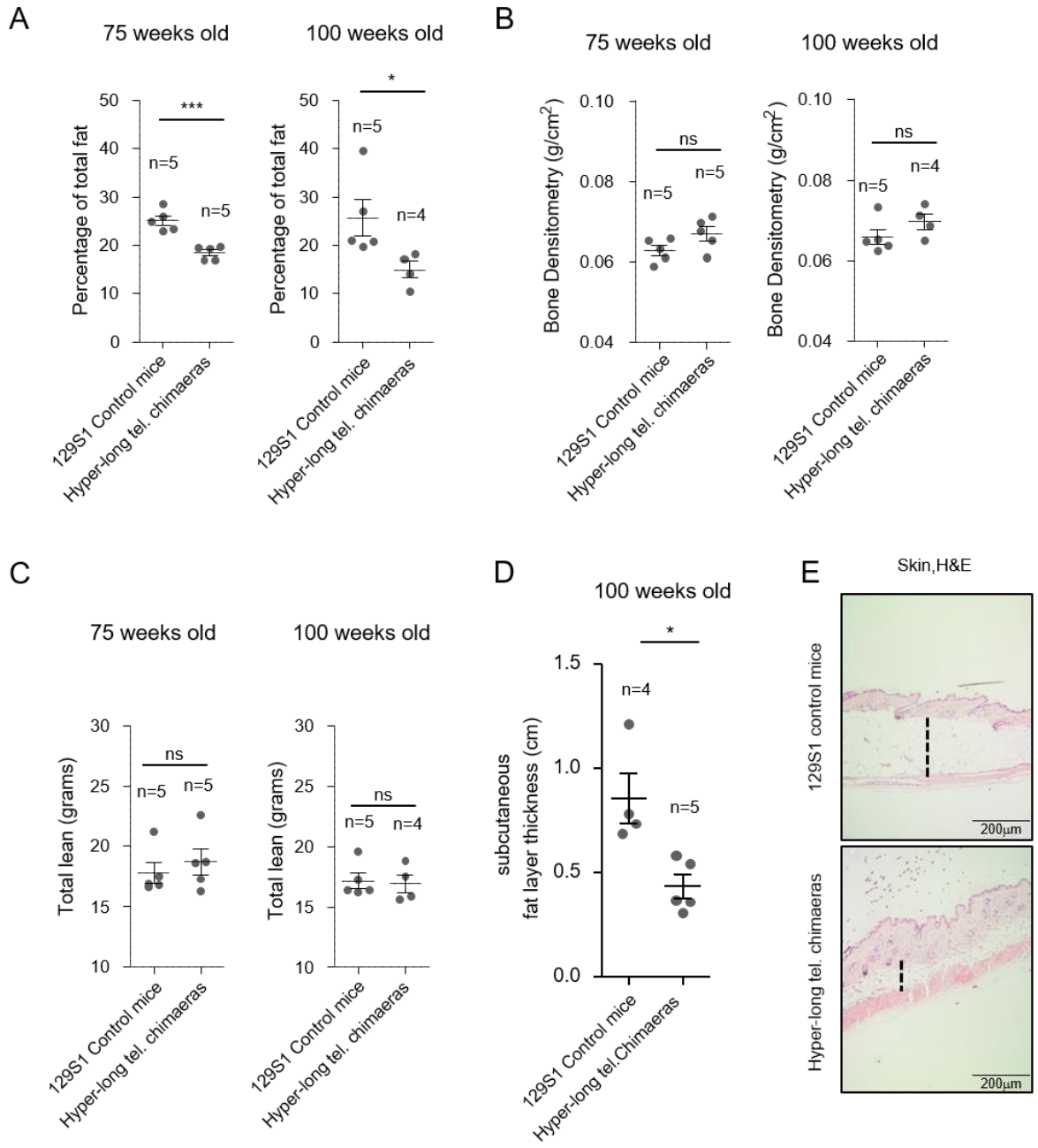

Figure 22. Reduced body size in hyper-long telomere mice is due to lower fat accumulation. **(A-C)** Densitometry analysis of hyper-long telomere mice and normal mice at two different ages. **(A)** Quantification of percentage of total fat. **(B)** Quantification of bone density. **(C)** Quantification of total lean mass. **(D-E)** Quantification of the skin subcutaneous fat layer in 100 weeks-old hyper-long mice and age-matched controls **(D)**, and representative image showing skin subcutaneous fat layer thickness **(E)**. Measurements were done by ImageJ software and calculated by the mean value of 30 to 40 different measurements all over the skin subcutaneous fat layer. Error bars represent standard error. *t*-test was used for statistical analysis. The number of mice is indicated in each case. *, p<0.05. ***, p<0,001.

2.3.2 Hyper-long telomere mice show improved metabolic parameters

As mice with hyper-long telomeres showed reduced fat accumulation, we next set to determine different metabolic parameters. First, we measured the levels of albumin, creatinine, bilirubin, urea, alanine aminotransferase (ALT), cholesterol, the low-density lipoprotein (LDL), and the high-density lipoprotein (HDL) in blood serum from both hyper-long telomere mice and age-matched controls at 50, 75 and 100 weeks of age. We found no significant differences in the levels of creatinine, bilirubin, albumin, urea and HDL at any of the time points between hyper-long telomere mice and control mice (**Figure 23A-E**). Interestingly, hyper-long telomere mice showed significantly lower levels of the "bad cholesterol", LDL, compared to control mice at the three time points studied (**Figure 23F**). Hyper-long telomere mice also showed significantly lower levels of cholesterol and of the hepatic damage marker ALT compared with control mice (**Figure 23G,H**). Thus, we found lower cholesterol levels, including LDL levels, and decreased liver damage in hyper-long telomere mice compared to control mice.

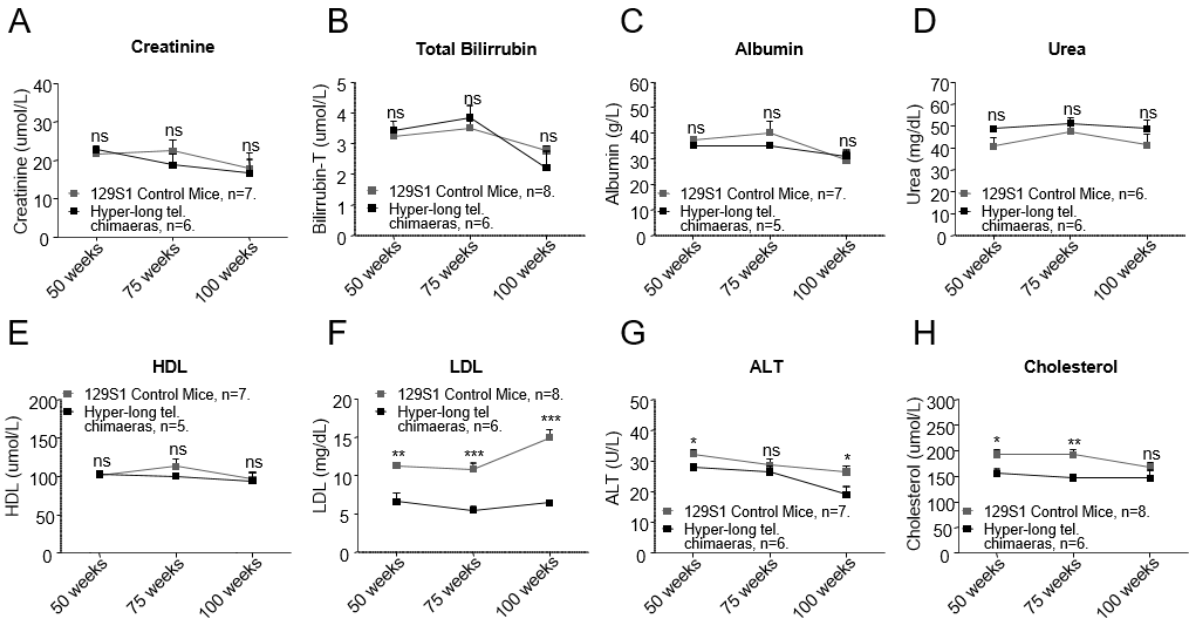

Figure 23. Hyper-long telomere mice show improved metabolic parameters. (A-H) Pentra quantification of different serum metabolites at 50,75 and 100 weeks-old. Metabolites were measured in serum obtained from blood extracts using ABX Pentra, **(A)** quantification of creatinine levels, **(B)** quantification of total bilirubin levels, **(C)** quantification of albumin levels, **(D)** quantification of urea levels, **(E)** quantification of HDL (High Density Lipoprotein) levels, **(F)** quantification of LDL (Low Density Lipoprotein) levels, **(G)** quantification of ALT (Alanine aminotransferase) levels and **(H)** quantification of cholesterol levels. Error bars represent standard error. *t*-test was used for statistical analysis. The number of mice is indicated in each case. *, p<0.05. **, p<0,01. ***, p<0,001.

To further asses the metabolic effects of hyper-long telomeres, we next studied glucose metabolism by performing a glucose tolerance test (GTT). To this end, glucose was injected intraperitoneally in age-matched hyper-long telomere mice and normal telomere mice at 50, 75 and 100 weeks of age previously fasted for 16 hours. At all timepoints, hyper-long telomere mice showed an increased glucose sensitivity (**Figure 24A-C**). We obtained similar results when we performed an insulin tolerance test (ITT). In this case, hyper-long telomere mice showed a better insulin tolerance at both 75 and 100 weeks of age compared to the normal telomere length controls (**Figure 24D-F**).

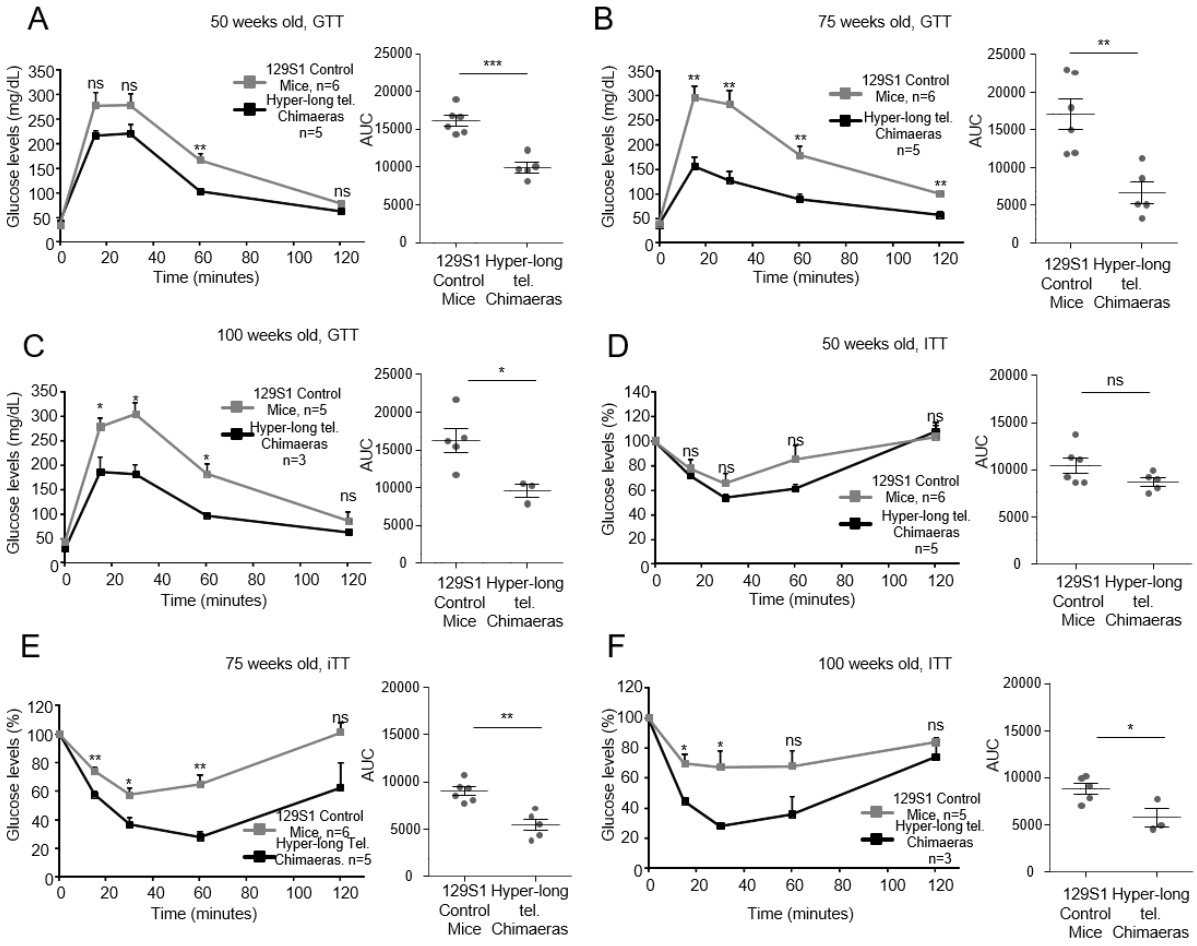

Figure 24. Hyper-long telomere mice show less metabolic aging. (A-C) Glucose tolerance test (GTT). GTT was performed in hyper-long telomere mice and age-matched controls at 50 **(A)**, 75 **(B)** and 100 **(C)** weeks of age by intraperitoneal glucose injection after 16h fasting. **(D-F)** Insulin tolerance test (ITT). ITT was performed in hyper-long telomere mice and age-matched controls at 50 **(D)**, 75 **(E)** and 100 **(F)** weeks of age by intraperitoneal insulin injection. Error bars represent standard error. *t*-test was used for statistical analysis. The number of mice is indicated in each case. *, p<0.05. **, p<0,01. ***, p<0,001.

In summary, these results indicate that hyper-long telomere mice have an improved metabolic fitness compared to normal telomere length mice. In particular, they show lower levels of LDL, cholesterol, and ALT in blood, as well as are more sensitive to glucose and insulin even at old age (100-weeks old), suggesting less metabolic aging compared to age-matched control mice.

2.3.3 Enhanced mitochondrial function in hyper-long telomere mice

Since previous works have reported a relation between telomere and mitochondrial homeostasis (Sahin *et al.*, 2011; Sahin and DePinho, 2012), here we next addressed whether hyper-long telomeres could be also affecting mitochondrial function. To this end, we first performed a qPCR-based assay in order to determine the relative mitochondrial DNA (mtDNA) copy number in WAT of 100-110-week old mice using three different mitochondrial genes (*Cox1*, *Cytb* and *Nd1).* Interestingly, we found that relative mtDNA copy number in WAT of hyper-long telomere mice were double than control mice from the same background in the three genes analyzed (**Figure 25A-C**).

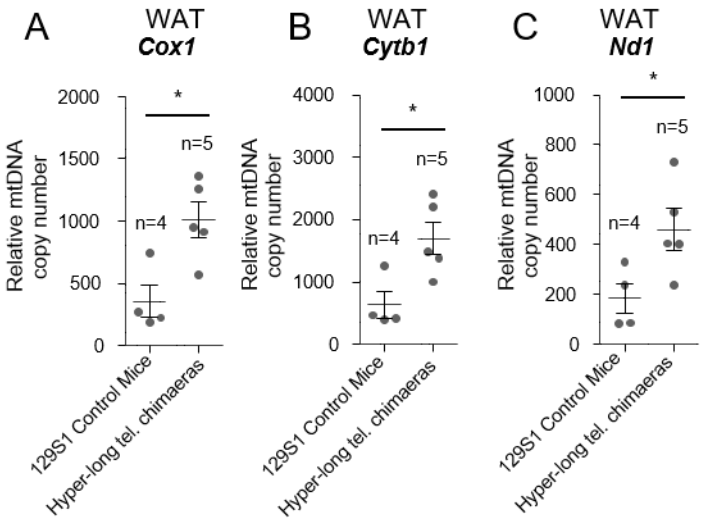

Figure 25. Increased mitochondrial DNA in mice with hyper-long telomeres. (A-C) Relative mtDNA content was calculated by the comparative Ct method of the mitochondrial genes *Cox1* **(A)**, *Cytb1* **(B)** and *Nd1* **(C)** compared to the nuclear gene *H19* in WAT of 100-110 weeks old hyper-long telomere mice and age-matched controls. The number of mice is indicated in each case. *, $p<0.05$.

Next, we also measured mRNA expression levels of the different oxidative phosphorylation genes (OXPHOS) Cytochrome C, ATP synthase, Cytochrome C subunit 6 and Cytochrome C subunit 5a as well as mitochondrial regulators PGC-1α and PGC-1β and critical targets such as ERRα and PPARα. Concomitant with our previous result, we found a significant upregulation in all these genes in hyper-long telomere mice compared to the normal length age-matched controls (**Figure 26A-H**).

Taken together, these data suggest that mice with hyper-long telomeres have an improved mitochondrial function, which could be also contributing to their delayed aging phenotype and improved metabolic function.

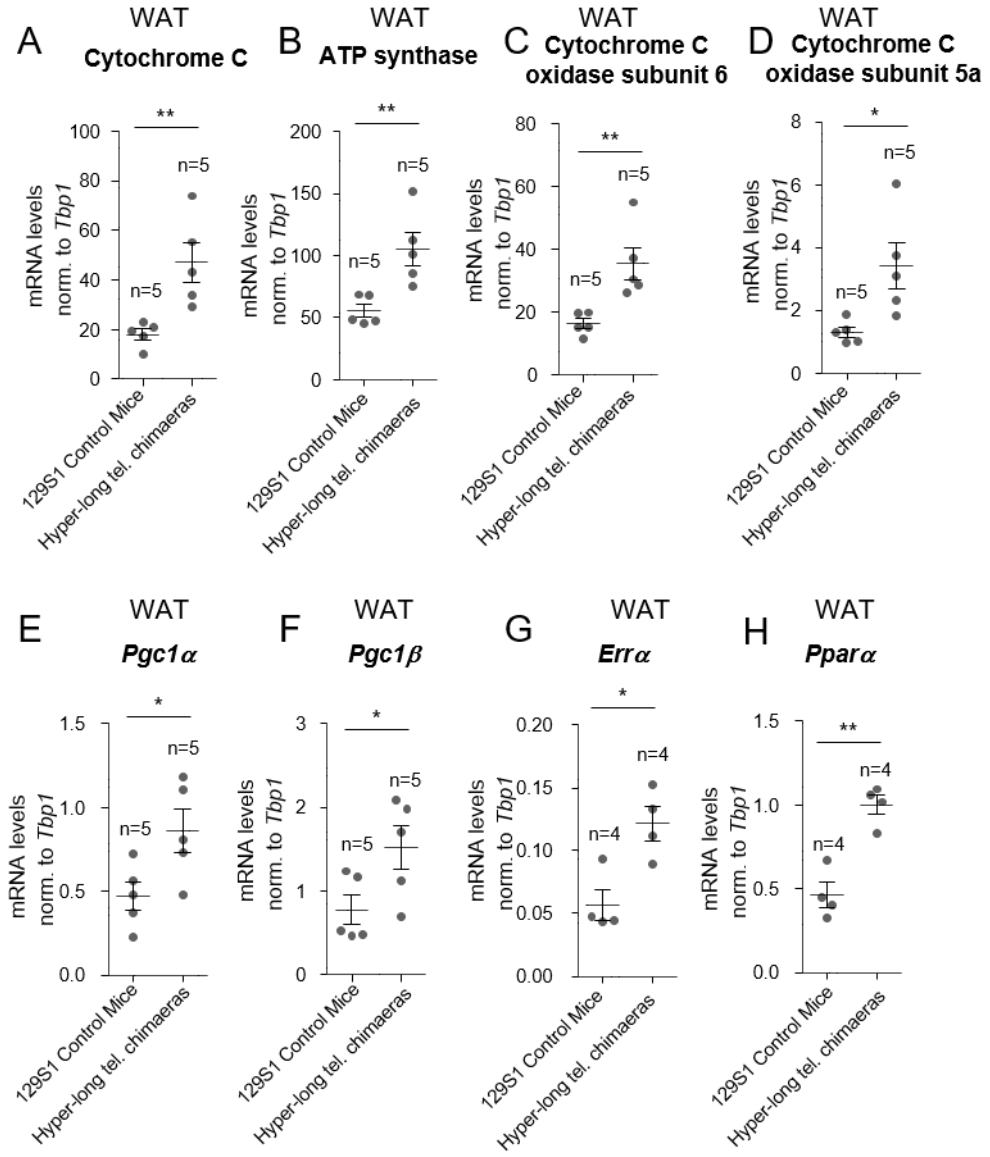

Figure 26. Improved mitochondrial function in mice with hyper-long telomeres. (A-H) mRNA levels from WAT of the OXPHOS genes Cytochrome C **(A)**, ATP synthase **(B)**, Cytochrome C subunit 6 **(C)** and Cytochrome C subunit 5a **(D)** as well as mitochondrial regulators PGC-1a **(E)** and PGC-1b **(F)** and critical targets such as ERRa **(G)** and PPARa **(H)**. Error bars represent standard error. *t*-test was used for statistical analysis. The number of mice is indicated in each case. *, p<0.05. **, p<0,01.

2.3.4 Longer telomeres do not affect cognitive capabilities

Next, we wondered whether having longer telomeres than normal could affect cognitive capabilities in these mice. To address this, we performed different cognitive tests at 50, 75 and 100 weeks of age. To evaluate neuromuscular endurance, we performed a rotarod test, which measures the time that mice are able to stay on a rotating platform with accelerated movement without falling (**Figure 27A**). We observed no differences between the hyper-long telomere mice and the control mice at the different time points (**Figure 27B**).

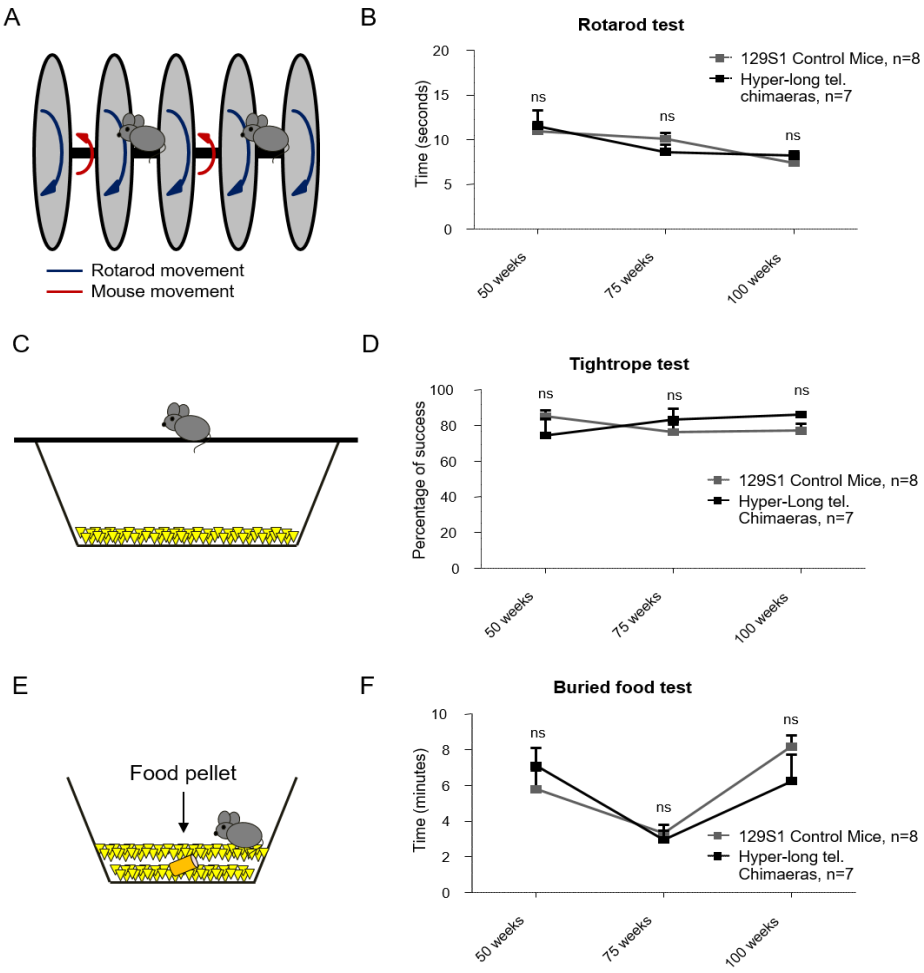

Figure 27. Mice with hyper-long telomeres have normal cognitive capabilities. (A-F) Different cognitive assays were performed in hyper-long telomere mice and age-matched controls at 50, 75 and 100 weeks of age. In order to evaluate neuromuscular endurance we performed the rotarod test **(A-B)** which measures the time that mice are able to stay on a rotating platform with accelerated movement without falling, for coordination we performed tightrope test which evaluates the capability of the mice to stay on a rope without falling during at least 1 minute **(C-D)** and for sensory perception we performed the buried food test **(E-F)** in which we measured the ability of mice to find a buried food pellet after 16h fasting. Error bars represent standard error. *t*-test was used for statistical analysis. The number of mice is indicated in each case.

In order to study mouse coordination, we performed a tightrope test, which evaluates the capability of the mice to stay on a rope without falling during at least 1 minute (**Figure 27C**). Again, we did not see any significance difference in performance between the hyper-long telomere mice and the controls (**Figure 27D**). Finally, to measure the sensory perception of mice we used a buried food test, in which we measured the ability of mice to find a buried food pellet after 16h fasting (**Figure27E**). Again, we found no differences between hyper-long telomere mice and controls (**Figure27F**).

Together, these results suggest that hyper-long telomere mice show normal cognitive capabilities, such as normal coordination, balance and smell.

2.4 Hyper-long telomere mice live longer and have less spontaneous cancer

Critically short telomeres in humans and mice can lead to premature aging and shorter lifespans by limiting the ability of stem cells to regenerate tissues (Flores, Cayuela and Blasco, 2005; Marion and Blasco, 2010; Armanios and Blackburn, 2012). In turn, we previously showed that longer telomeres owing to telomerase over-expression in adult mice can increase mouse longevity (Tomás-Loba *et al.*, 2008; Bernardes de Jesus *et al.*, 2012). Thus, here we set to address whether longer telomeres than normal in the adult organism, in the absence of telomerase over-expression, were sufficient to increase longevity. Strikingly, we found that hyper-long telomere mice showed a significant increase of 12.75% in median longevity as well as an increase in maximum longevity of 8.40% compared to normal telomere length controls (**Figure 28A**). These findings indicate that long telomeres *per se*, even in the absence of telomerase overexpression, are sufficient to increase mouse longevity.

The fact that hyper-long telomere mice had an increased longevity also suggested that they are unlikely to have any deleterious effects, as promoting cancer. This question is

of particular importance because previous works have correlated presence of long telomeres in humans with increased cancer incidence (Wentzensen *et al.*, 2011; Horn *et al.*, 2013; Blackburn, Epel and Lin, 2015; Naxerova and Elledge, 2015; Haycock *et al.*, 2017). To address this, we studied the spontaneous tumor incidence of hyper-long telomere mice and control mice. We found that hyper-long telomere mice showed a reduction of almost 50% in the number of mice that developed tumors compared to the normal telomere length control mice, although this difference did not reach significance (**Figure 28B**). Of notice, the cause of death of tumor free mice was associated to general body degeneration associated to the aging process, as well as uterine infection in some female mice.

These findings clearly demonstrate that long telomeres *per se* do not lead to increased cancer, at least in mice. Instead, longer telomeres are clearly correlated with an increased mouse longevity.

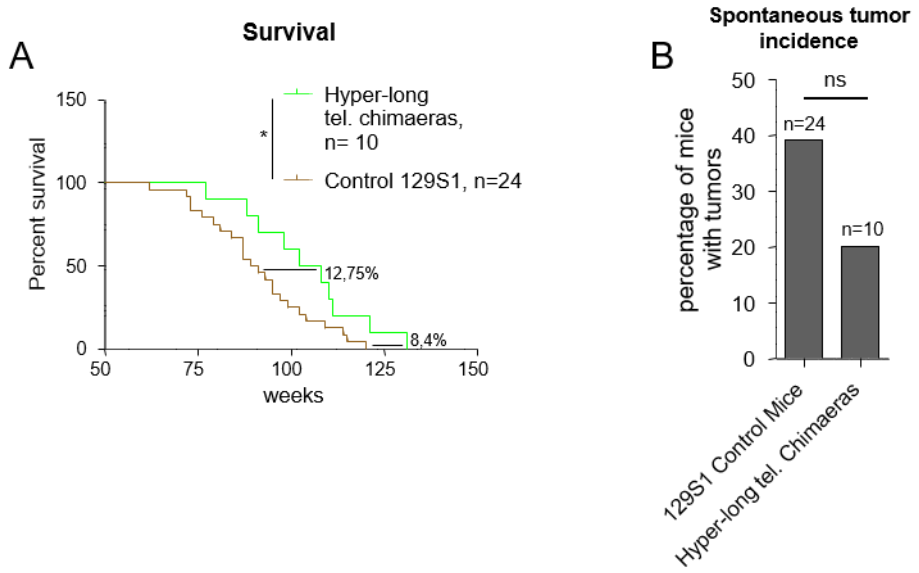

Figure 28. Hyper-long telomere mice live longer and have less spontaneous cancer. (A) survival proportions of 100% hyper-long chimeric mice compared to control mice from the same background. Hyper-long telomere mice show a 12,75% increase in median lifespan and an 8,4% increase in maximum lifespan. **(B)** Quantification of spontaneous tumor incidence in hyper-long telomere mice and controls. Hyper-long telomere mice show a decrease in almost 20% in tumor incidence compared to control mice from the same background. Error bars represent standard error. Mantel-Cox test was used for statistical analysis in survival curves and Chi-square test for spontaneous tumor incidence. The number of mice is indicated in each case. *, p<0.05. **, p<0,01. ***, p<0,001.

2.5 Hyper-long telomere mice show longer telomeres throughout their lifespan

In order to determine whether hyper-long telomere mice retained longer telomeres even at old age, we measured telomere length in different tissues at 100 weeks of age. Telomere length was determined in intestine and skin, as examples of proliferative tissues, and in brain as a non-proliferative tissue. We found that in all cases, 100- weeks old hyper-long telomere mice showed longer telomeres on average than the normal age-matched controls (**Figure 29A-F**). In agreement with longer telomeres, hyper-long telomere mice also showed a significantly lower accumulation of short telomeres at old age compared with the age-matched control mice (**Figure 29A-F**).

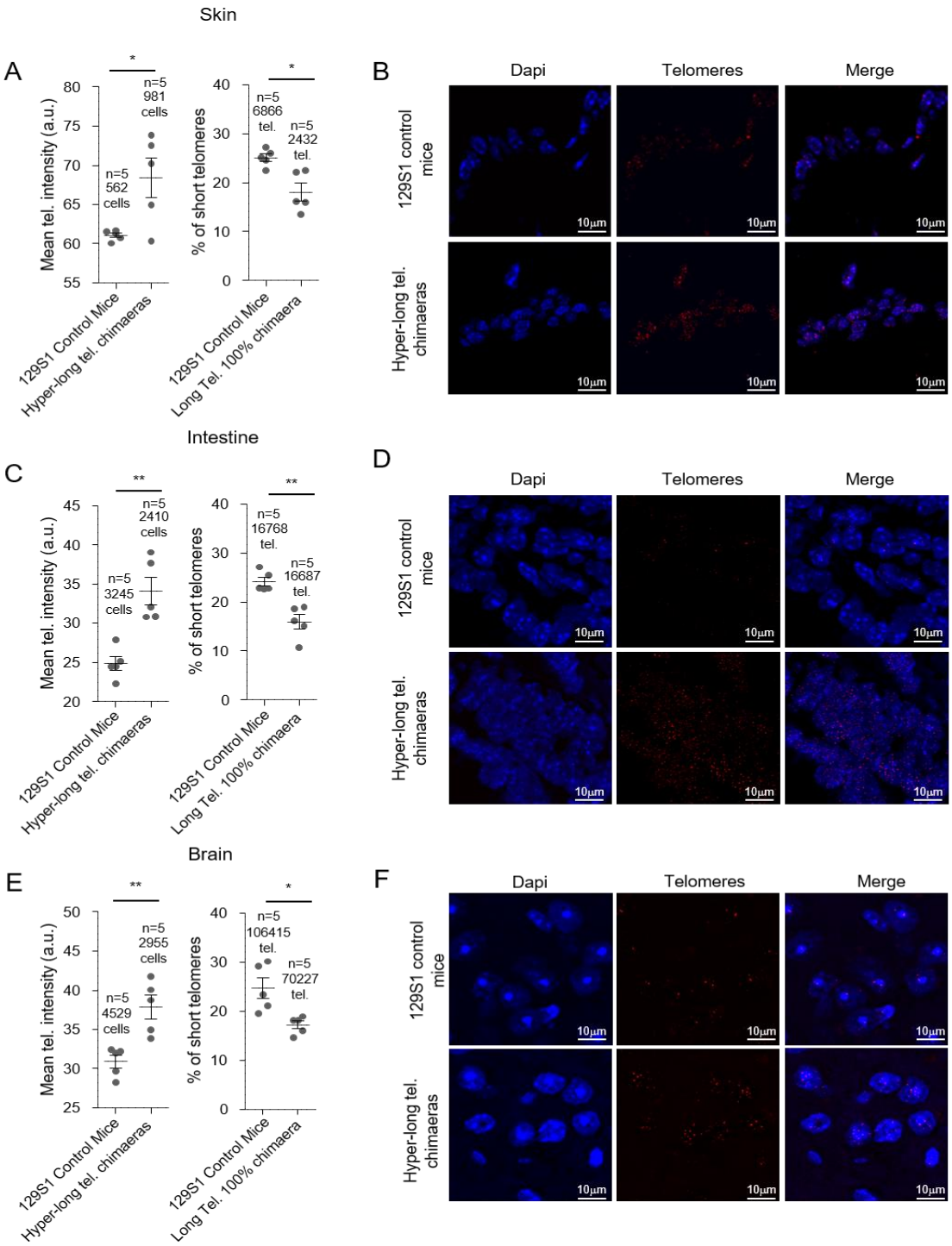

Figure 29. Hyper-long telomere mice show longer telomeres throughout their lifespan in both proliferative and non-proliferative tissues. (A-F) Mean telomere fluorescence and percentage of short telomeres in back skin **(A,B)**, intestine **(C,D)**, brain **(E,F)** in 100 weeks-old hyper-long telomere mice and age-matched controls. Error bars represent standard error. *t*-test was used for statistical analysis. The number of mice is indicated in each case. *, p<0.05. **, p<0,01. ***, p<0,001.

Importantly, as one of the main phenotypes in the hyper-long telomere mice is an improved metabolic profile, we measured telomere length and percentage of short telomeres in metabolically relevant tissues, such as the liver, white adipose tissue (WAT), and brown adipose tissue (BAT) at 100-110 weeks old. Interestingly, we found a very pronounced increase in telomere length in the hyper-long telomere mice in all three metabolic tissues compared to control mice from the same background (**Figure 30A-F**). Accordingly, we observed a significant decrease in the percentage of short telomeres in the hyper-long telomere mice compared to controls in all three tissues (**Figure 30A-F**).

To rule out that longer telomeres in the hyper-long telomere mice where the result of an altered telomerase expression in the adult organism we determined mRNA levels of the two essential telomerase components *Tert* and *Terc* in hyper-long telomeres and normal telomere mice at 100-110 weeks of age in the liver and the WAT. As expected, we found that *Tert* was not expressed in these tissues in agreement with previous reports showing that *Tert* expression is undetectable in the majority of adult mouse tissues after birth (Blasco *et al.*, 1998; Bernardes de Jesus *et al.*, 2012). Furthermore, we did not see any significant differences in the mRNA expression of *Terc* between the hyper-long telomere mice and the normal controls in the liver and the WAT (**Fig. 31A-D**).

Altogether, these results demonstrate that hyper-long telomere mice retain longer telomeres with aging, including metabolic tissues such liver, white adipose tissue and brown adipose tissue, in the absence of *Tert* overexpression.

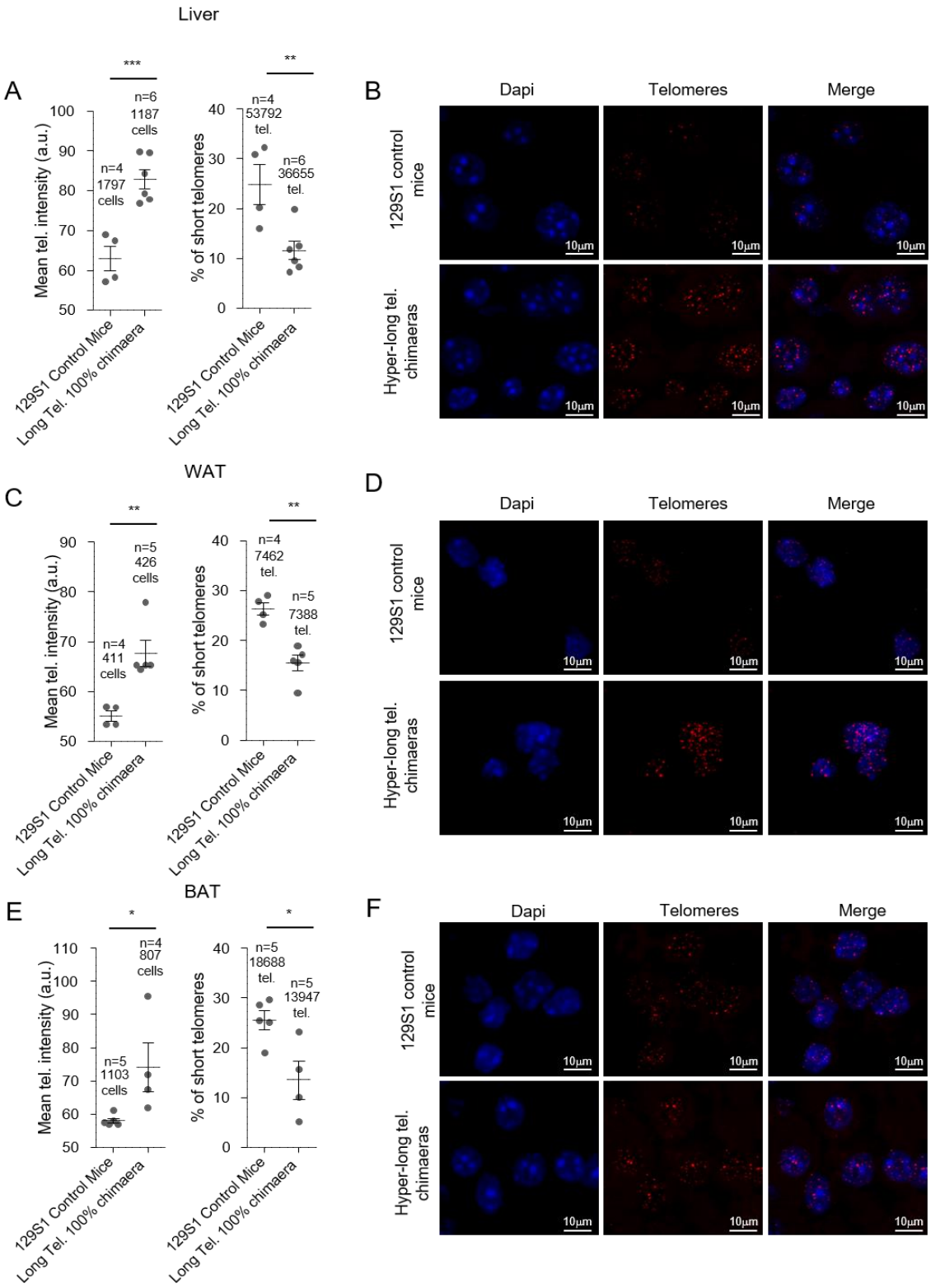

Figure 30. Hyper-long telomere mice show longer telomeres throughout their lifespan in metabolic related tissues. (A-F) Mean telomere fluorescence and percentage of short telomeres in liver **(A,B)**, white adipose tissue **(C,D)** and brown adipose tissue **(E,F)**, in 100 weeks-old hyper-long telomere mice and age-matched controls. Error bars represent standard error. *t*-test was used for statistical analysis. The number of mice is indicated in each case. *, p<0.05. **, p<0,01. ***, p<0,001.

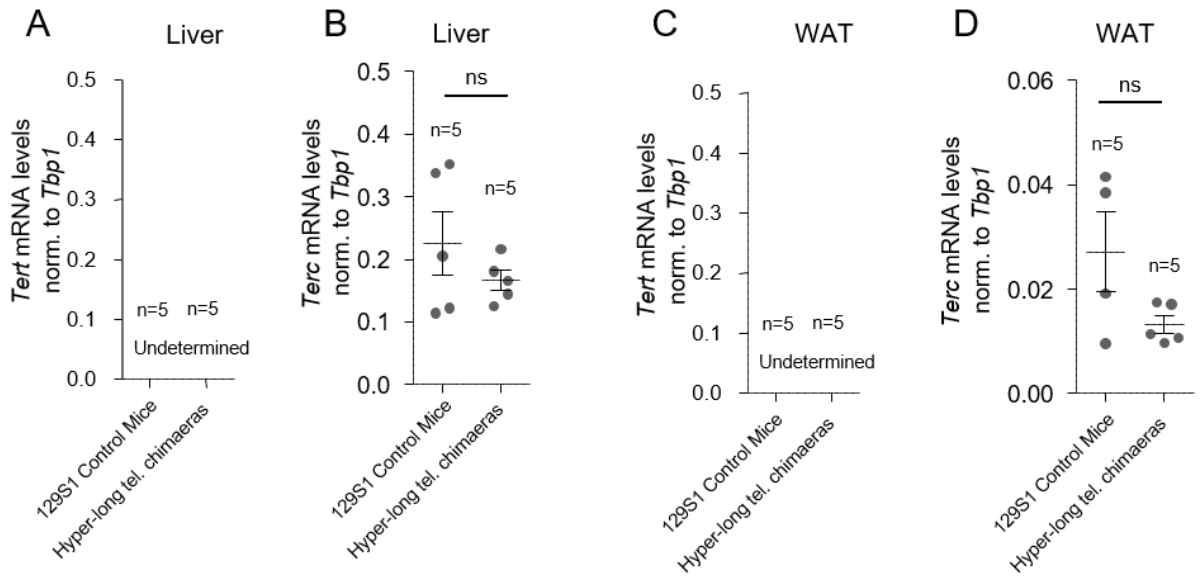

Figure 31. Hyper-long telomere mice does not present altered telomerase expression levels. (A-D) *Tert* and *Terc* mRNA expression levels as measured by Q-PCR in liver **(A,B)** and in white adipose tissue **(C,D)** in age-matched (100 weeks old) hyper-long telomere mice and control mice. Error bars represent standard error. *t*-test was used for statistical analysis. The number of mice is indicated in each case. *, p<0.05. **, p<0,01. ***, p<0,001.

2.6 Hyper-long telomere mice show less accumulation of cells with DNA damage and senescence markers

Next, we addressed whether longer telomeres than normal could be promoting or protecting from age-associated DNA damage. To this end, we performed a telomere Q-FISH to identify telomeres followed by an immunofluorescence against the DNA damage marker 53BP1 in liver of 100 weeks hyper-long telomere chimaeras and controls. To this end, we quantified the number of cells presenting ≥2 53BP1 foci (**Figure 32A,C**). Interestingly, hyper-long telomere mice showed an 8-fold decrease in 53BP1-positive cells compared to controls (**Figure 32A**). Importantly, the percentage of cells presenting ≥1 telomere induced foci (TIF) also showed a very significant 6-fold decrease in hyper-long telomere mice compared to controls (**Figure 32B,C**).To further investigate whether longer telomeres than normal were protective from DNA damage, we quantified the percentage of cells positive for the senescence marker, p21, in the liver of age matched (100 weeks of age) normal length and hyper-long telomere mice. Interestingly, we found a significant nine-fold decrease in the number of p21 positive cells in hyper-long mice compared with age-matched controls (**Figure 32D,E**).

Together, these results indicate that longer telomeres than normal in hyper-long telomere mice significantly reduce the global DNA damage and the telomeric DNA damage associated with aging in mice.

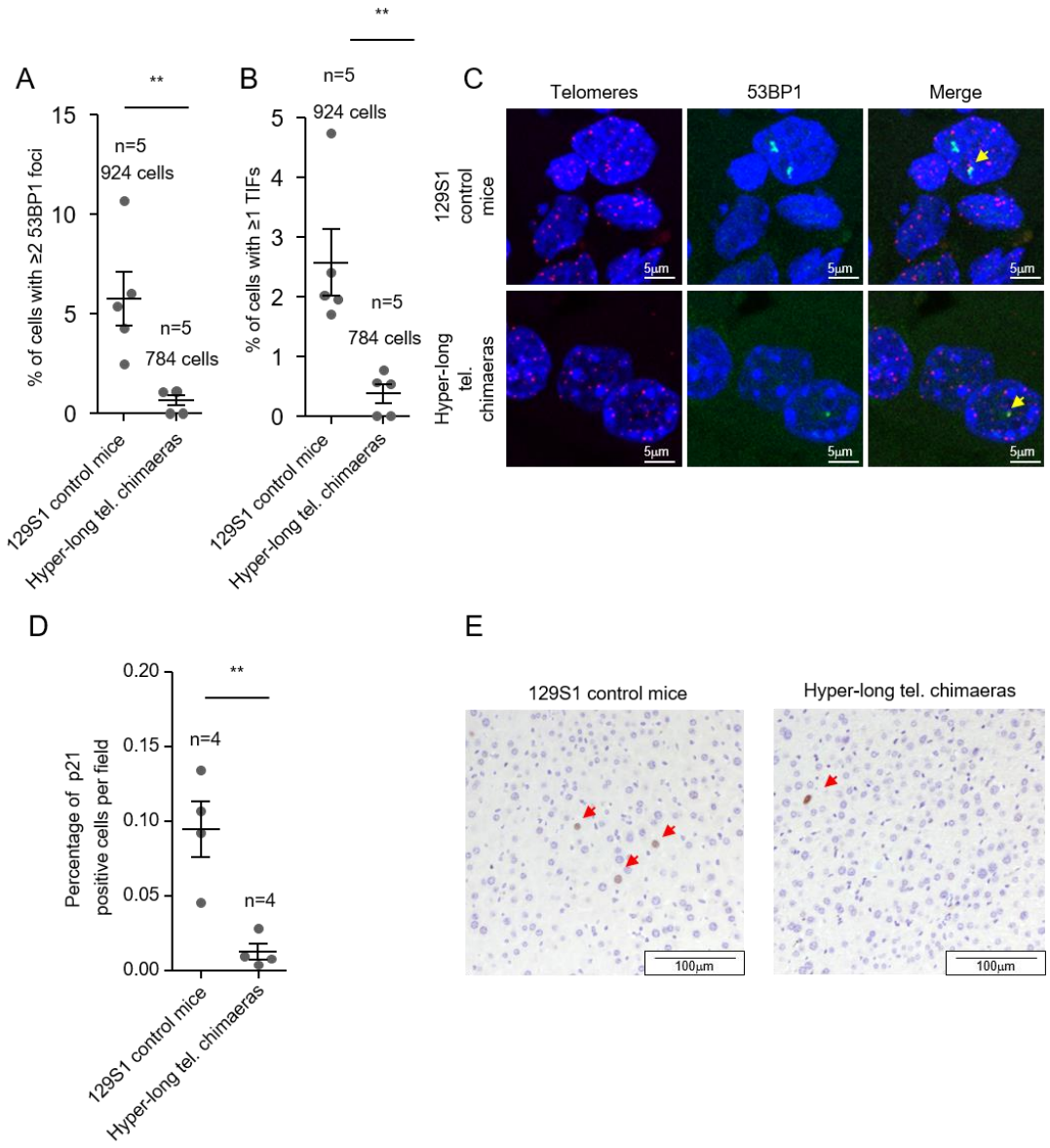

Figure 32. Hyper-long telomere mice show less DNA damage and less senescence. (A-B) Quantification of DNA damage in age-matched (100 weeks old) hyper-long telomere mice and control mice. Quantification of total damage as indicated by percentage of cells with ≥2 53BP1 foci as determined by immunofluorescence **(A)** and quantification of cells showing telomere-induced DNA damage as shown by percentage of cells with ≥1 TIF (telomere induced foci) as determined by telomere FISH followed by immunofluorescence with 53BP1 antibody. **(C)** Representative images of TIFs (yellow arrow). **(D)** Quantification of the percentage of p21 positive cells in liver of age matched (100 weeks old) hyper-long telomere mice and control mice. **(E)** Representative images of p21 (red arrows) positive cells. Error bars represent standard error. *t*-test was used for statistical analysis. The number of mice is indicated in each case. **, p<0,01.

2.7 Normal expression of shelterins in liver and fat of mice with hyper-long telomeres

It has been previously reported that mice deficient for the RAP1, a component of the shelterin telomere protective complex, showed an obese phenotype as well as signs of metabolic syndrome including abnormal fat accumulation, glucose intolerance and fatty liver (Martínez *et al.*, 2013). As we found here that hyper-long telomere mice are protected from age-associated metabolic syndrome, including fat accumulation, high cholesterol levels, liver damage and glucose intolerance, we set to address whether hyper-long telomeres were affecting the levels of the RAP1 protein. To this end, we first determined RAP1 protein levels by Western blot in the white adipose tissue (WAT). We found that RAP1 protein levels were similar in age-matched 100-110 weeks-old hyper-long telomere and normal telomere length controls (**Figure 33A,B**). Similarly, we detected similar RAP1 protein levels in the liver of hyper-long and normal telomere length mice as determined by immunofluorescence (IF) analysis at 100-110 weeks (**Figure 33C,D**). These findings suggest that protection from metabolic syndrome in mice with hyper-long telomeres does not seem to be related to altered levels of the RAP1 protein.

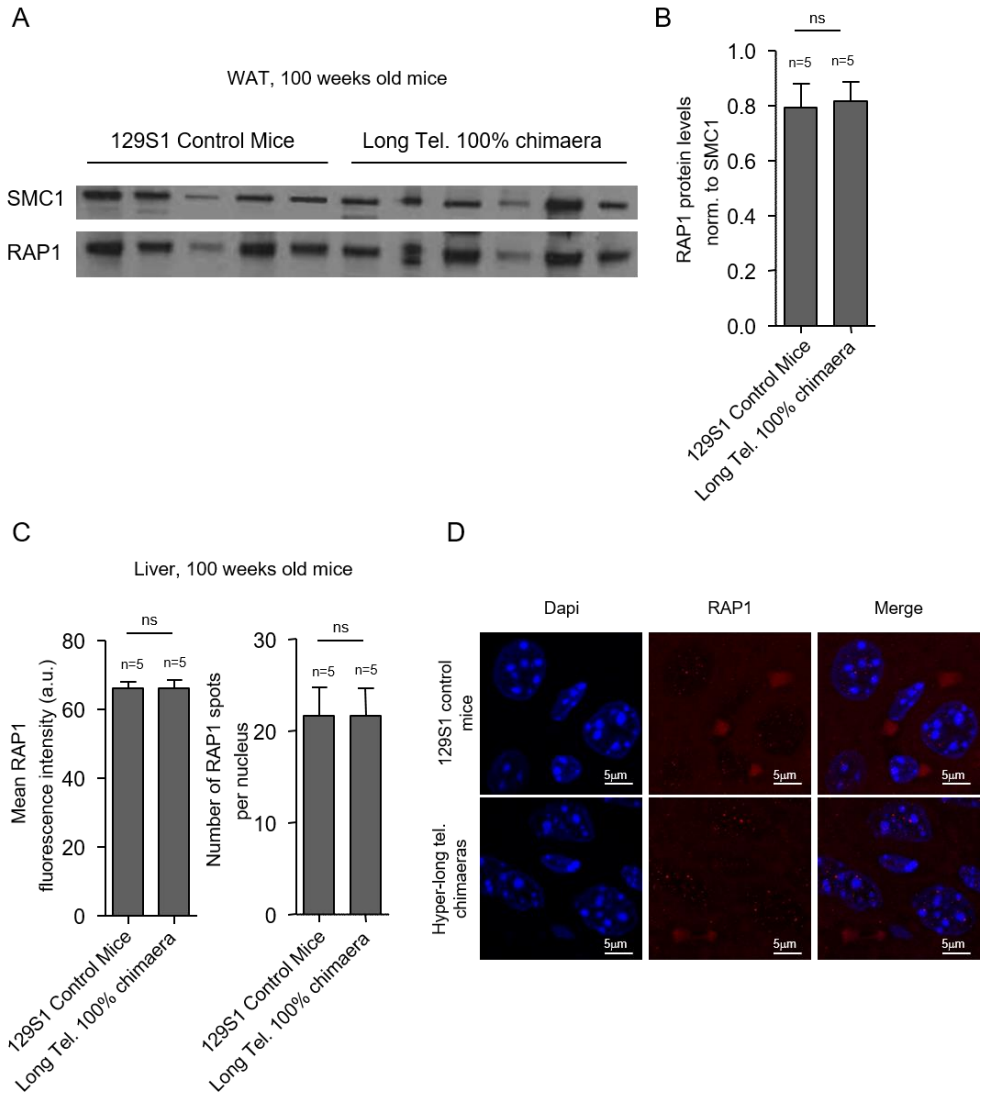

Figure 33. Hyper-long telomere mice show normal RAP1 levels. (A-B) Western Blot analysis shows RAP1 protein levels in white adipose tissue of age-matched (100 weels old) hyper-long telomere mice and control mice. **(C-D).** Immunofluorescence analysis of RAP1 protein levels in the liver of age-matched (100 weeks old) hyper-long telomere mice and control mice.

Next, we addressed whether hyper-long telomeres resulted in altered levels of the rest of the components of shelterin. To this end, we determined the mRNA expression levels of the different shelterin components in the liver and WAT of 100-110-week old mice. Again, although we observed a tendency to lower expression levels of the different shelterin components in hyper-long telomere mice compared to the controls both in the liver, this difference did not reach statistical significance (**Figure 34A-G**), similar findings were observed and in the white adipose tissue (**Figure 34H-N**). Thus, hyper-long telomeres in mice do not alter the mRNA expression of *Rap1* or the different shelterin components.

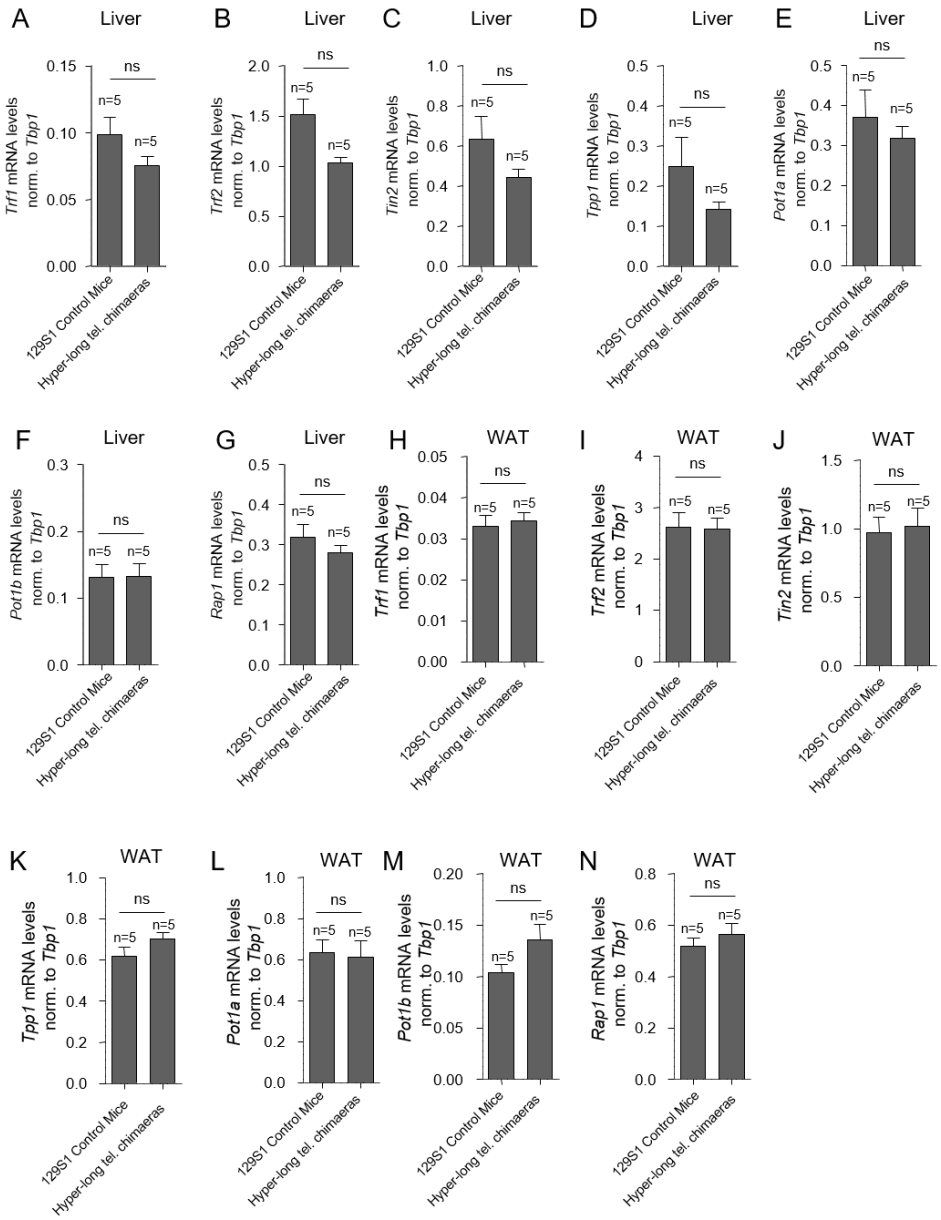

Figure 34. Hyper-long telomere mice show normal shelterin gene expression levels. (A-G) mRNA levels in the liver of shelterins *Trf1* **(A)**, *Trf2* **(B)**, *Tin2* **(C)**, *Tpp1* **(D)**, *Pot1a* **(E)**, *Pot1b* **(F)** and *Rap1* **(G)** in 100 weeks-old hyper-long telomere mice and age-matched controls as determined by qPCR. **(H-N)** mRNA levels in the WAT of shelterins *Trf1* **(H)**, *Trf2* **(I)**, *Tin2* **(J)**, *Tpp1* **(K)**, *Pot1a* **(L)**, *Pot1b* **(M)** and *Rap1* **(N)** in 100 weeks-old hyper-long telomere mice and age-matched controls measured by qPCR. Error bars represent standard error. *t*-test was used for statistical analysis. The number of mice is indicated in each case.

Discussion

PART 1. Effects of telomerase-based gene therapy in a cancer prone environment in mice

The majority of adult cell types in both humans and mice do not express telomerase and this results in progressive shortening of telomeres and increased telomere-associated DNA damage with aging (Harley, Futcher and Greider, 1990; Blasco *et al.*, 1995, 1998; Schaetzlein *et al.*, 2004; García-Cao *et al.*, 2006; Collado, Blasco and Serrano, 2007; Liu *et al.*, 2007; Flores *et al.*, 2008; Bernardes de Jesus *et al.*, 2012; Martínez and Blasco, 2017), a phenomenon that is proposed to be among the primary causes of organismal aging (López-Otín *et al.*, 2013). Mice are born with longer telomeres than humans but the rate of telomere shortening in blood cells from mice is 100-fold higher than in humans and telomeres do shorten very significantly during the mouse lifespan (Flores *et al.*, 2008; Vera *et al.*, 2012). Thus, although mice have on average longer telomeres than humans, they also suffer telomere shortening with aging, and indeed this shortening is relevant for aging (García-Cao *et al.*, 2006). In contrast to telomere shortening in healthy cells, the majority of cancer cells aberrantly reactivate telomerase to achieve unlimited proliferative potential, one of the hallmarks of cancer (Hanahan and Weinberg, 2011). Indeed, many different human cancer types show mutations in either the promotor region or coding regions of the telomerase catalytic subunit *Tert* gene (Ma *et al.*, 2014; Liu, Yuan and Xu, 2016). Also, a wide variety of mouse cancers activate telomerase (Bednarek *et al.*, 1995; Blasco *et al.*, 1996; Kiyozuka *et al.*, 1998) and this frequent re-activation of telomerase in cancer cells has led to the idea that the postnatal suppression of telomerase activity in the adult organism may have a role as a tumor suppression mechanism. However, there is mounting evidence that short telomeres can also lead to increased cancer, especially owing to accumulation of chromosome aberrations if DNA damage checkpoints are lost, such as p53 loss (Chin *et al.*, 1999; Shay, 2016; Martínez and Blasco, 2017). Indeed, cancer incidence increases with aging and it is also more elevated in the so-called telomere syndromes (Blackburn, Epel and Lin, 2015). Interestingly, constitutive telomerase expression in telomerase transgenic mouse models shows that telomerase does not act as an oncogene and only leads to slightly higher incidence of some spontaneous cancer at old ages (González-Suárez *et al.*, 2001; Artandi *et al.*, 2002). More recently, it has been demonstrated that telomerase activation using non-integrative gene therapy vectors (adeno associated vectors) does not lead to increased cancer both in the context of normal physiological aging (Bernardes de Jesus *et al.*, 2012) and in the context of mouse models of disease including heart infarct (Bär *et al.*, 2014), aplastic anemia associated to short telomeres (Bär *et al.*, 2016), and pulmonary fibrosis owing to short telomeres and low doses of a damaging agent to the lungs (Povedano *et al.*,

2018). However, whether telomerase activation can lead to more cancer in the context of tumor prone contexts remained to be formally addressed.

In line with this, here we demonstrate that telomerase gene therapy does not affect (either increasing or decreasing) tumorigenesis in a well-established mouse model of lung carcinogenesis induced by oncogenic K-Ras even in a p53-defficient background (Guerra *et al.*, 2003). We demonstrate this by using two independent strategies, one in which we over-express *Tert* before the induction of the oncogene and another in which we activate *Tert* at the same time that we induce the oncogenic *K-Ras* allele. This result suggests that endogenous telomerase activation associated to oncogene-induced tumorigenesis is sufficient to allow carcinogenesis and that extra telomerase activation provided by the gene therapy vectors does not affect tumor initiation or progression. Interestingly, when we treated mice with gene therapy vectors carrying a catalytically dead mutant allele of *Tert* that is unable to catalyze the addition of new telomeric repeats, we found a decreased cancer incidence but only when the vector carrying the catalytically dead *Tert* mutant was administered prior to oncogene activation. Furthermore, we show here that expression of *Tert* dominant negative prior to oncogene activation results in lower proliferation and increased DNA damage and apoptosis, thus contributing to block initiation of *K-Ras* carcinogenesis. Although we cannot rule out that AAV9-*Tert-DN* might also have some telomere-independent mechanism to suppress tumor growth, the fact that the tumors appearing in mice transduced with AAV9-*Tert-DN* showed a five-fold increase in telomere induced foci (TIFs) clearly indicates that *Tert-DN* expression suppress tumor growth by inducing telomere damage. Of note, this did not occur in the simultaneous treatment group, suggesting that telomerase inhibition once the tumor is already induced has less effect blocking tumorigenesis than when telomerase is inhibited prior to oncogene induction most likely owing to the fact that endogenous telomerase is activated with tumorigenesis.

The tumor suppressive effects observed with AAV9-*Tert-DN* treatment prior to oncogene induction are remarkable since telomerase activity is dispensable for transformation of cells with long telomeres (Seger *et al.*, 2002). Indeed, telomerase abrogation in the context of cancer-prone mouse models, including the *K-Ras*$^{+/G12D}$ lung tumorigenesis mouse model, only showed anti-tumorigenic activity after several mouse generations in the absence of telomerase when telomeres reached a critically short length (Chin *et al.*, 1999; Greenberg *et al.*, 1999; Gonzalez-Suarez *et al.*, 2000; Perera *et al.*, 2008). However, the fact that AAV9-*Tert-DN* treatment prior to oncogene activation significantly delays tumor onset and progression by increasing telomere-induced DNA damage and apoptosis suggests that telomere length is rate limiting in the early steps of

oncogene-induced lung tumorigenesis in mice. These results open new therapeutic opportunities using AAV9-*Tert-DN* gene therapy to prevent tumor induction in cancer prone settings.

Finally, we make here the very intriguing finding that AAV9-*Tert* treatment prior to oncogene induction significantly reduced the levels of the p16 senescence marker. It was previously proposed that DNA damage associated to oncogene-induced senescence is largely produced by short/dysfunctional telomeres (Suram *et al.*, 2012). These results support this notion as pre-treatment with telomerase is able to significantly decrease senescence in the early steps of lung carcinogenesis. Nevertheless, these results also indicate that senescence does not seem to correlate with tumor burden, as AAV9-*Tert* treatment does not impact on the final number of adenomas and carcinomas.

A limitation for any gene therapy as a treatment for human diseases is the potential immunogenic response elicited either by the viral particles or by the product encoded by the transgene. We use, however, AAV vectors that are weak immunogens (Nayak and Herzog, 2010). Our AAV9 vectors do not carry any viral gene and no immunogenic response against AAV9 have been reported in mice (Jimenez *et al.*, 2013). In line with this, we did not observe a significant difference in the tumor burden between the untreated and the AAV9-null treated mice, although there was a trend to lower tumor burden in the mice that received the AAV9 vectors in some of the parameters measured. Regarding the potential immune response against the AAV9-encoded transgene product, namely telomerase, we think it is unlikely since the transgene encodes the endogenous mouse telomerase. In agreement with this, we found no significant difference in the tumor burden between the AAV9-*Null* and the AAV9-*Tert* treated mice. However, the potential immunogenic response of human telomerase in humans deserves further clinical research. The experimental design of this work also poses the limitation that the delivery of the Cre recombinase to induce oncogenic K-Ras expression and of telomerase were performed using different viral vectors, adeno virus and adeno associated virus, respectively. Hence, there was no mechanism to select for cells that were infected with both viruses. Furthermore, owing to the packaging limit of AAV vectors to 5 kilobases (Wu, Yang and Colosi, 2010) , it was not possible to carry both the Cre and the *Tert* genes in the same AAV9-vector in the “simultaneous strategy”. Nevertheless, we observed that the K-Ras expressing tumors also expressed the AAV9-transduced *Tert*/*Tert-DN* genes, indicating that the majority of the tumors originated from cells transduced with the AAV9 vectors. Furthermore, we show that one week after co-infection with adeno-Cre and with AAV9-GFP the β-gal positive cells also expressed GFP, demonstrating that lung cells are susceptible to be co-infected with adeno and adeno-associated virus. However, we cannot rule out the possibility that some tumors arise from cells only infected by the adeno-Cre and not by the AAV9 vectors.

One could argue than in a long-lived specie like humans, the exogenous expression of *Tert* in a wild-type scenario may take several years/decades to facilitate cancer development, the time needed to acquire additional oncogenic mutations that eventually lead to malignant transformation and tumor development. To model the impact of AAV9-*Tert* in cancer in short lived mice, we forced oncogenic Ras expression to induce tumorigenesis both in wild-type and p53-null genetic backgrounds, thereby avoiding this lagging time. In addition, to avoid that long-term expression of telomerase could facilitate cancer development after several decades, we use non-integrative AAV9 vectors, which allow only for a transitory expression of telomerase due to the fact that as cells divide the virus load is progressively diluted until eventually cells lose the expression of the transgene (*Tert*).

In summary, the results shown here demonstrate that telomerase activation by adeno associated vectors does not increase lung carcinogenesis even in the context of an activated *K-Ras* oncogene, highlighting the safety of therapeutic strategies based on telomerase activation using AAV9 vectors.

PART 2. Effects of telomere elongation beyond the pre-established length in mice

It has been previously described that telomere elongation is only possible in certain adult stem cell compartment in which telomerase is partially active in both human and mouse and even in these cells telomerase expression is not enough to maintain telomere homeostasis throughout the lifespan of organisms (Blasco *et al.*, 1995, 1998; Flores *et al.*, 2008; Bernardes de Jesus *et al.*, 2012; Vera *et al.*, 2012). Indeed, although mice are born with longer telomeres than humans the rate of telomere shortening in mice is up to 100-folder higher (Flores *et al.*, 2008; Vera *et al.*, 2012) and both humans and mice show progressive telomere shortening with aging (Canela *et al.*, 2007; Bernardes de Jesus *et al.*, 2012; Vera *et al.*, 2012). In turn, telomere shortening with aging can trigger a number of secondary pro-aging phenomena such as increased DNA damage and genomic instability, cellular senescence and/or apoptosis, impaired ability of stem cells to regenerate tissues etc., and therefore it is considered one of the primary hallmarks of organismal aging (López-Otín *et al.*, 2013). In turn, telomere maintenance in the adult organisms by using different telomerase over-expression approaches, including gene therapy strategies, have been shown to delay aging and age-associated pathologies, as well as to increase lifespan in

mice (Blasco *et al.*, 1997; Blasco, 2005; González-Suárez *et al.*, 2005; Tomás-Loba *et al.*, 2008; Jaskelioff *et al.*, 2011; Bernardes de Jesus *et al.*, 2012).

However, telomerase has been found re-activated in the majority of human cancers (Hanahan and Weinberg, 2011) and this has generated a certain concern on potential negative long-term effects of telomerase reactivation in promoting tumorigenesis. In this regard, there is mounting evidence that telomerase re-activation in the adult organism by using non-integrative gene adeno associated vectors (AAV) does not lead to increased cancer in mice (Povedano *et al.*, 2015, 2018; Bär *et al.*, 2016). In humans, presence of longer telomeres than normal has been also associated to increased incidence of certain cancers such as lung cancer in large population studies (Wentzensen *et al.*, 2011; Horn *et al.*, 2013; Blackburn, Epel and Lin, 2015; Naxerova and Elledge, 2015; Haycock *et al.*, 2017). In addition, germinal mutations in the *Pot1* shelterin gene, which lead to longer telomeres than normal, have been also associated to various types of familial cancer, such as melanoma, Li-fraumeni like, and glioma (Hu *et al.*, 2010; Newey *et al.*, 2012; Ramsay *et al.*, 2013; Robles-Espinoza *et al.*, 2014; Shi *et al.*, 2014; Zhang *et al.*, 2014; Bainbridge *et al.*, 2015). Although in the latter case scenario, *Pot1* mutations not only lead to longer telomeres, but also increased telomere aberrations, which could be responsible of the increased cancer susceptibility (Hu *et al.*, 2010; Ramsay *et al.*, 2013; Robles-Espinoza *et al.*, 2014; Shi *et al.*, 2014; Zhang *et al.*, 2014; Bainbridge *et al.*, 2015). Thus, it is of relevance to address whether long telomeres *per se*, in the absence of telomerase activation or other telomere alterations, could be promoting tumorigenesis or not.

In this regard, it has been reported that telomeres lengthen during *in vitro* expansion of ES cells (Varela *et al.*, 2011). This telomere lengthening occurs simultaneously to the loss of heterochromatic marks at telomeres and in the absence of changes in the global DNA methylation (SINE elements) or subtelomeric methylation or telomerase activity (Varela *et al.*, 2011). This phenomenon is also recapitulated when differentiated cells are reprogrammed to induced pluripotent stem (iPS) cells and expanded *in vitro*, again associated to changes at telomeric heterochromatin (Marion *et al.*, 2009). Of note, in the absence of telomerase, differentiated cells can be reprogrammed to iPS cells, but telomeres do not lengthen (Marion *et al.*, 2009). These observations suggested that is possible to generate cells with hyper-long telomeres simply by *in vitro* passaging and, thus, in the absence of manipulation of the telomerase gene. However, it remained unknown whether cells derived from ESCs with hyper-long telomeres are maintained throughout embryonic and adult development in mice, and they retain longer telomeres and lower aging associated DNA damage in the adult organism.

The main challenge in this study was the successful generation of chimeric mice derived from ES cells with hyper-long telomeres (GFP-positive to allow lineage tracking),

which contain GFP-positive cells with longer telomeres than those of the unmodified species, both at the stem cell and more differentiated compartments. For this reason, we first demonstrated that maximum telomere length extension occurs at moderately passaged ES cells (up to passage 24). Of note, excessive passaging (ie, passage 60), resulted in accumulation of telomere damage as indicated by increased presence of telomere induced foci (TIFs) and multitelomeric signals (MTS), a telomere aberration associated with telomere fragility and indicative of telomere replication defects (Martínez *et al.*, 2009; Sfeir *et al.*, 2009). Furthermore, a moderate number of passages ensure a very similar genome-wide expression profile between ES cells at early passages as indicated by very few gene expression changes by RNA-seq. Importantly, we did not observe any changes in the expression of telomerase or shelterin proteins.

In this regard, we were able to obtain not only chimeric mice, but also fully contributed chimeric mice (100% chimaera) which show much longer telomeres than those of the unmodified species in the absence of changes in expression of telomerase or telomere-binding proteins. Importantly, chimeric mice and tissues were healthy and did not display any histopathological alterations. Interestingly, GFP-positive cells with hyper-long telomeres maintained longer telomeres and showed a lower abundance of cells with short telomeres at different times points up to 100 weeks of age. Accordingly, we also found a significantly decreased number of cells presenting global DNA damage, as well as telomere-induced DNA damage with aging in the hyper-long telomere mice compared to the normal telomere controls. Also, the levels of the p21 senescence marker were decreased in the 100% hyper-long telomere chimaeras. These results are in line with previous findings describing that transgenic over-expression of *TERT* in mice from a different genetic background (*C57BL6*), which also resulted in longer telomeres, also showed a lower accumulation of DNA damage with aging (Jaskelioff *et al.*, 2011). Similar results were obtained by *TERT* over-expression achieved by using a gene therapy strategy (Bernardes de Jesus *et al.*, 2012).

We next tested whether having hyper-long telomeres was advantageous or disadvantageous for mice. Interestingly, 100% hyper-long telomere mice showed a reduced body weight than normal from week 40 onwards. We further found that this reduced size is due to a lower accumulation of fat in the absence of changes in the lean mass. Furthermore, hyper-long telomere mice show signs of a “younger” metabolic phenotype, as indicated significantly reduced levels of LDL, ALT and cholesterol in serum throughout their lifespan. Moreover, they show an increased sensitivity to glucose and insulin intakes, even at old age, thus supporting a “younger” metabolic age in the case of hyper-long telomere mice compared to the normal telomere length controls.

Previous reports have shown decreased mitochondrial function associated to telomere dysfunction (Sahin *et al.*, 2011; Sahin and DePinho, 2012). In agreement with these previous findings, our current data suggest that mice with hyper-long telomeres have an improved mitochondrial function. In particular, we found that hyper-long telomere mice show increased expression of *Pgc1-*α/β as well as of their target genes *Err*α and *Ppar*α. Moreover, hyper-long telomere mice also show increased mitochondrial DNA copy number and increased expression levels of the OXPHOS mitochondrial genes Cytochrome C, ATP synthase, Cytochrome C subunit 6 and Cytochrome C subunit 5a compared to normal telomere controls. Together, these findings suggest that mitochondrial activity is enhanced in mice with hyper-long telomeres, and this could contribute to their improved metabolic performance.

Importantly, we did not see increased incidence of spontaneous tumors in the hyper-long telomere mice, which instead, showed a clear tendency to have reduced spontaneous tumors, compared to the normal telomere length control, thus indicating that long telomere per se do not increase tumorigenesis, instead, seem to be decreasing cancer risk in agreement with a younger state. Also in agreement with this, we found that 100% hyper-long mice lived longer than controls with a 12.75% increase in median survival and 8.4% in maximum survival. It could be argued that the 100% chimeric mice used in this study maybe derived from a donor trophoblast whose gender could impact in the survival of these mice. However, it is known (Prudhomme and Morey, 2016; Baines and Renaud, 2017) that trophoblast cells contribute entirely to form the placenta and the amniotic sac and are not likely to affect adult mice.

Overall, here we present a mouse model with delayed aging in the absence of genetic manipulations. This mouse model features anti-aging phenotypes that are also present in several genetically modified mouse models with delayed aging previously described. In particular, our model shows reduced body size, enhanced insulin sensitivity and even reduced incidence of fatal neoplastic disease, similar to the growth hormone (GH) mutant dwarf mice (Ikeno *et al.*, 2003, 2009; Bartke, 2011; Bartke and Quainoo, 2018), although there are notable differences such as lower body fat, which dwarf mice tend to accumulate (Bartke and Quainoo, 2018). In this regard, mice with hyper-long telomeres are more similar to insulin-like growth factor (IGF) mutant mice, which also feature decreased body fat accumulation (Bartke and Quainoo, 2018).

In summary, we demonstrate here that it is possible to generate mice that have telomeres which are much longer than those of the natural species by increasing the passage number of embryonic stem cells and in the absence of genetic modifications. These mice show a younger phenotype as indicated by improved mitochondrial function, improved metabolic parameters, decreased cancer, and increased longevity. These results also suggest that

there is not a negative selection for individuals with longer telomeres than normal in species, and therefore, one can envision that natural selection processes which favor individuals with longer telomeres within a given species, could potentially increase species longevity. Finally, these findings also suggest the intriguing possibility that a potential mechanism for rending individuals with longer telomeres could be regulation of the duration of pluripotency stages during embryonic development when telomeres are elongated.

Conclusions/Conclusiones

1. Effects of telomerase-based gene therapy in a cancer prone environment in mice

1.1 Telomerase activation mediated by AAV9 has no effect in tumor onset or in tumor development and does not increase the malignancy of oncogenic K-Ras lung tumorigenesis in mice.

1.2 AAV9-*Tert* treatment results in *Tert* mRNA over-expression in the lung and leads to reduced senescence associated to oncogene-activation.

1.3 AAV9-*Tert* treatment results in longer telomeres in lung cells.

1.4 AAV9-*Tert-DN* treatment induces DNA and specific telomeric damage, apoptosis and blocks proliferations in lung tumors.

2. Effects of telomere elongation beyond the pre-established length in mice

2.1 Mouse ES cells are able to elongate their telomeres in *vitro* with few passages maintaining a similar gene expression pattern, similar telomerase activity and without increasing DNA and specific telomere damage.

2.2 Hyper-long ES cells contribute to the formation of not only viable chimeric mice, but are also able to generate 100% contributing chimeric mice.

2.3 Hyper-long 100% chimeric mice present lower weight, improved metabolic parameters and enhanced mitochondrial functions and elongated telomeres does not affect cognitive capabilities.

2.4 100% Hyper-long telomere mice live longer and have less spontaneous cancer.

2.5 100% Hyper-long telomere mice show longer telomeres throughout their lifespan

2.6 100% Hyper-long telomere mice show less accumulation of cells with DNA damage and senescence markers.

2.7 100% Hyper-long telomere mice present normal expression of shelterin proteins.

1. Efectos de la terapia génica basada en telomerasa en un ambiente propenso a cáncer en ratones.

1.1 La activación de telomerasa mediada por AAV9 no tiene efectos en la aparición o desarrollo y no aumenta la malignidad en pulmones oncogénicos K-Ras en ratón.

1.2 El tratamiento con AAV9-*Tert* lleva a la sobreexpresión de los niveles de ARNm de *Tert* en pulmón y reduce la senescencia asociada a la activación oncogénica.

1.3 El tratamiento con AAV9-*Tert* resulta en telómeros más largos en los pulmones.

1.4 El tratamiento con AAV9-*Tert-DN* induce daño en el ADN y específicamente en el telómero, apoptosis y bloquea la proliferación en tumores de pulmón.

2. Effectos de la elongación telomérica más allá de la longitud pre-establecida en ratones.

2.1 Las células ES de ratón elongan sus telómeros mediante pocos pases de cultivo, manteniendo un patrón de expresión y una actividad telomerasa similares, y sin aumentar el daño en el ADN ni telomérico.

2.2 Las células ES con telómeros súper-largos no sólo contribuyen a la formación de ratones quiméricos viables, sino que son capaces de generar animales quiméricos 100% derivados de las mismas.

2.3 Los ratones quiméricos 100% presentan menor peso, mejores parámetros metabólicos y una mejorada función mitocondrial, y estos telómeros súper-largos no afectan a sus capacidades cognitivas.

2.4 Los ratones quiméricos 100% viven más y tienen menor incidencia de cáncer.

2.5 Los ratones quiméricos 100% tienen telómeros más largos a lo largo de su vida.

2.6 Los ratones quiméricos 100% muestran menor acumulación de células con daño en el ADN y marcadores de senescencia.

2.7 Los ratones quiméricos 100% presentan expresión normal de las selterinas.

Bibliography

Allsopp, R. C. *et al.* (2003) 'Telomerase is required to slow telomere shortening and extend replicative lifespan of HSCs during serial transplantation', *Blood*, 102(2), pp. 517–520. doi: 10.1182/blood-2002-07-2334.

Ambrogio, C. *et al.* (2014) 'Modeling lung cancer evolution and preclinical response by orthotopic mouse allografts', *Cancer Research*. doi: 10.1158/0008-5472.CAN-14-1606.

Aoi, T. *et al.* (2008) 'Generation of pluripotent stem cells from adult mouse liver and stomach cells', *Science*. doi: 10.1126/science.1154884.

Armanios, M. and Blackburn, E. H. (2012) 'The telomere syndromes.', *Nature reviews. Genetics*, pp. 693–704. doi: 10.1038/nrg3246.

Armanios, M. Y. *et al.* (2007) 'Telomerase Mutations in Families with Idiopathic Pulmonary Fibrosis', *New England Journal of Medicine*, 356(13), pp. 1317–1326. doi: 10.1056/NEJMoa066157.

Artandi, S. E. *et al.* (2002) 'Constitutive telomerase expression promotes mammary carcinomas in aging mice', *Proceedings of the National Academy of Sciences of the United States of America*. doi: 10.1073/pnas.112515399.

Artandi, S. E. and Attardi, L. D. (2005) 'Pathways connecting telomeres and p53 in senescence, apoptosis, and cancer', *Biochemical and Biophysical Research Communications*, pp. 881–890. doi: 10.1016/j.bbrc.2005.03.211.

Ayuso, E. *et al.* (2014) 'Manufacturing and characterization of a recombinant adeno-associated virus type 8 reference standard material', *Human Gene Therapy*. doi: 10.1089/hum.2014.057.

Bainbridge, M. N. *et al.* (2015) 'Germline mutations in shelterin complex genes are associated with familial glioma', *J Natl Cancer Inst*, 107(1), p. 384. doi: 10.1093/jnci/dju384.

Baines, K. J. and Renaud, S. J. (2017) 'Transcription Factors That Regulate Trophoblast Development and Function', in *Progress in Molecular Biology and Translational Science*. doi: 10.1016/bs.pmbts.2016.12.003.

Bär, C. *et al.* (2014) 'Telomerase expression confers cardioprotection in the adult mouse heart after acute myocardial infarction', *Nature Communications*. doi: 10.1038/ncomms6863.

Bär, C. *et al.* (2016) 'Telomerase gene therapy rescues telomere length, bone marrow aplasia, and survival in mice with aplastic anemia', *Blood*. doi: 10.1182/blood-2015-08-667485.

Barrientos, K. S. *et al.* (2008) 'Distinct Functions of POT1 at Telomeres', *Molecular and Cellular Biology*, 28(17), pp. 5251–5264. doi: 10.1128/MCB.00048-08.

Barthel, F. P. *et al.* (2017) 'Systematic analysis of telomere length and somatic alterations in 31 cancer types', *Nature Genetics*. Nature Research. doi: 10.1038/ng.3781.

Bartke, A. (2011) 'Single-gene mutations and healthy ageing in mammals', *Philosophical Transactions of the Royal Society B: Biological Sciences*. doi: 10.1098/rstb.2010.0281.

Bartke, A. and Quainoo, N. (2018) 'Impact of Growth Hormone-Related Mutations on Mammalian Aging', *Frontiers in Genetics*. doi: 10.3389/fgene.2018.00586.

Baumann, P. and Cech, T. R. (2001) 'Pot1, the putative telomere end-binding protein in fission yeast and humans', *Science*, 292(5519), pp. 1171–1175. doi: 10.1126/science.1060036.

Bednarek, A. *et al.* (1995) 'Increased Telomerase Activity in Mouse Skin Premalignant Progression', *Cancer Research*.

Benetti, R. *et al.* (2008) 'A mammalian microRNA cluster controls DNA methylation and telomere recombination via Rbl2-dependent regulation of DNA methyltransferases', *Nature Structural and Molecular Biology*. doi: 10.1038/nsmb.1399.

Bernardes de Jesus, B. *et al.* (2012) 'Telomerase gene therapy in adult and old mice delays aging and increases longevity without increasing cancer', *EMBO Molecular Medicine*, 4(8), pp. 691–704. doi: 10.1002/emmm.201200245.

Bianchi, A. *et al.* (1997) 'TRF1 is a dimer and bends telomeric DNA', *EMBO Journal*, 16(7), pp. 1785–1794. doi: 10.1093/emboj/16.7.1785.

Blackburn, E. H., Epel, E. S. and Lin, J. (2015) 'Human telomere biology: A contributory and interactive factor in aging, disease risks, and protection', *Science*. doi: 10.1126/science.aab3389.

Blackburn, E. H. and Gall, J. G. (1978) 'A tandemly repeated sequence at the termini of the extrachromosomal ribosomal RNA genes in Tetrahymena', *Journal of Molecular Biology*, 120(1), pp. 33–53. doi: 10.1016/0022-2836(78)90294-2.

Blasco, M. A. *et al.* (1995) 'Functional characterization and developmental regulation of mouse telomerase RNA', *Science*. doi: 10.1126/science.7544492.

Blasco, M. A. *et al.* (1996) 'Differential regulation of telomerase activity and telomerase RNA

during multi-stage tumorigenesis', *Nature Genetics*. doi: 10.1038/ng0296-200.

Blasco, M A, Lee, H. W., Rizen, M., *et al.* (1997) 'Mouse models for the study of telomerase', *Ciba Found Symp*.

Blasco, María A. *et al.* (1997) 'Telomere shortening and tumor formation by mouse cells lacking telomerase RNA.', *Cell*, 91(1), pp. 25–34. doi: S0092-8674(01)80006-4 [pii].

Blasco, M A, Lee, H. W., Hande, M. P., *et al.* (1997) 'Telomere shortening and tumor formation by mouse cells lacking telomerase RNA.', *Cell*, 91(1), pp. 25–34. doi: S0092-8674(01)80006-4 [pii].

Blasco, M. A. *et al.* (1998) 'Expression of mouse telomerase catalytic subunit in embryos and adult tissues.', *Proceedings of the National Academy of Sciences of the United States of America*. doi: 10.1073/pnas.95.18.10471.

Blasco, M. A. (2005) 'Mice with bad ends: Mouse models for the study of telomeres and telomerase in cancer and aging', *EMBO Journal*. doi: 10.1038/sj.emboj.7600598.

Bodnar, A. G. *et al.* (1998) 'Extension of life-span by introduction of telomerase into normal human cells', *Science*, 279(5349), pp. 349–352. doi: 10.1126/science.279.5349.349.

Broccoli, D. *et al.* (1997) 'Human telomeres contain two distinct Myb-related proteins, TRF1 and TRF2', *Nature Genetics*, p. 235. doi: 10.1038/ng1097-231.

Bryan, T. M. *et al.* (1995) 'Telomere elongation in immortal human cells without detectable telomerase activity', *EMBO J*, 14(17), pp. 4240–4248. doi: papers3://publication/uuid/E553EAC0-7D77-471F-A996-D41412778FFB.

Bryan, T. M. *et al.* (1997) 'Evidence for an alternative mechanism for maintaining telomere length in human tumors and tumor-derived cell lines', *Nat Med*, 3(11), pp. 1271–1274. doi: 10.1038/nm1197-1271.

Büning, H. *et al.* (2008) 'Recent developments in adeno-associated virus vector technology', *Journal of Gene Medicine*. doi: 10.1002/jgm.1205.

Calado, R. T. *et al.* (2009) 'A spectrum of severe familial liver disorders associate with telomerase mutations', *PLoS ONE*, 4(11). doi: 10.1371/journal.pone.0007926.

Calsou, P. *et al.* (2003) 'Coordinated assembly of Ku and p460 subunits of the DNA-dependent protein kinase on DNA ends is necessary for XRCC4-ligase IV recruitment', *Journal of Molecular Biology*, 326(1), pp. 93–103. doi: 10.1016/S0022-2836(02)01328-1.

Canela, A. *et al.* (2007) 'High-throughput telomere length quantification by FISH and its application to human population studies', *Proceedings of the National Academy of Sciences*. doi: 10.1073/pnas.0609367104.

Canela, A., Klatt, P. and Blasco, M. A. (2007) 'Telomere length analysis', *Methods in Molecular Biology*, 371, pp. 45–72. doi: 10.1385/1-59745-361-7:45.

Celli, G. B. and de Lange, T. (2005) 'DNA processing is not required for ATM-mediated telomere damage response after TRF2 deletion', *Nature Cell Biology*, 7(7), pp. 712–718. doi: 10.1038/ncb1275.

Chin, L. *et al.* (1999) 'p53 deficiency rescues the adverse effects of telomere loss and cooperates with telomere dysfunction to accelerate carcinogenesis', *Cell*, 97(4), pp. 527–538. doi: 10.1016/S0092-8674(00)80762-X.

Cimprich, K. A. and Cortez, D. (2008) 'ATR: An essential regulator of genome integrity', *Nature Reviews Molecular Cell Biology*, pp. 616–627. doi: 10.1038/nrm2450.

Cohen, S. B. *et al.* (2007) 'Protein composition of catalytically active human telomerase from immortal cells.', *Science (New York, N.Y.)*, 315(5820), pp. 1850–1853. doi: 10.1126/science.1138596.

Collado, M. *et al.* (2005) 'Tumour biology: Senescence in premalignant tumours', *Nature*. doi: 10.1038/436642a.

Collado, M., Blasco, M. A. and Serrano, M. (2007) 'Cellular Senescence in Cancer and Aging', *Cell*. doi: 10.1016/j.cell.2007.07.003.

Cristofari, G. and Lingner, J. (2006) 'Telomere length homeostasis requires that telomerase levels are limiting', *EMBO Journal*. doi: 10.1038/sj.emboj.7600952.

D'Adda Di Fagagna, F. *et al.* (2003) 'A DNA damage checkpoint response in telomere-initiated senescence', *Nature*. doi: 10.1038/nature02118.

Derevyanko, A. *et al.* (2017) 'Gene therapy with the TRF1 telomere gene rescues decreased TRF1 levels with aging and prolongs mouse health span', *Aging Cell*, 16(6), pp. 1353–1368. doi: 10.1111/acel.12677.

DiMauro, T. and David, G. (2010) 'Ras-Induced Senescence and its Physiological Relevance in Cancer', *Current Cancer Drug Targets*. doi: 10.2174/156800910793357998.

Djojosubroto, M. W. *et al.* (2003) 'Telomeres and telomerase in aging, regeneration and

cancer', *Molecules and Cells*.

Doksani, Y. *et al.* (2013) 'XSuper-resolution fluorescence imaging of telomeres reveals TRF2-dependent T-loop formation', *Cell*. doi: 10.1016/j.cell.2013.09.048.

Donate, L. E. and Blasco, M. A. (2011) 'Telomeres in cancer and ageing', *Philosophical Transactions of the Royal Society B: Biological Sciences*, 366(1561), pp. 76–84. doi: 10.1098/rstb.2010.0291.

Dunham, M. A. *et al.* (2000) 'Telomere maintenance by recombination in human cells', *Nature Genetics*, 26(4), pp. 447–450. doi: 10.1038/82586.

Duque, S. *et al.* (2009) 'Intravenous administration of self-complementary AAV9 enables transgene delivery to adult motor neurons', *Molecular Therapy*. doi: 10.1038/mt.2009.71.

Espejel, S., Franco, S., Sgura, A., *et al.* (2002) 'Functional interaction between DNA-PKcs and telomerase in telomere length maintenance', *EMBO Journal*, 21(22), pp. 6275–6287. doi: 10.1093/emboj/cdf593.

Espejel, S., Franco, S., Rodr??guez-Perales, S., *et al.* (2002) 'Mammalian Ku86 mediates chromosomal fusions and apoptosis caused by critically short telomeres', *EMBO Journal*, 21(9), pp. 2207–2219. doi: 10.1093/emboj/21.9.2207.

Flores, I. *et al.* (2008) 'The longest telomeres: A general signature of adult stem cell compartments', *Genes and Development*, 22(5), pp. 654–667. doi: 10.1101/gad.451008.

Flores, I., Cayuela, M. L. and Blasco, M. A. (2005) 'Effects of telomerase and telomere length on epidermal stem cell behavior.', *Science*, 309(5738), pp. 1253–1256. doi: 10.1126/science.1115025.

Foust, K. D. *et al.* (2009) 'Intravascular AAV9 preferentially targets neonatal neurons and adult astrocytes', *Nature Biotechnology*. doi: 10.1038/nbt.1515.

Franco, S. *et al.* (2002) 'Mammalian meiotic telomeres: Composition and ultrastructure in telomerase-deficient mice', *European Journal of Cell Biology*, 81(6), pp. 335–340. doi: 10.1078/0171-9335-00259.

García-Beccaria, M. *et al.* (2015) 'Therapeutic inhibition of TRF1 impairs the growth of p53-deficient K-RasG12V-induced lung cancer by induction of telomeric DNA damage.', *EMBO molecular medicine*, 7(7), pp. 930–949. doi: 10.15252/emmm.201404497.

García-Cao, I. *et al.* (2006) 'Increased p53 activity does not accelerate telomere-driven

ageing', *EMBO Reports*. doi: 10.1038/sj.embor.7400667.

García-Cao, M. *et al.* (2004) 'Epigenetic regulation of telomere length in mammalian cells by the Suv39h1 and Suv39h2 histone methyltransferases', *Nature Genetics*. doi: 10.1038/ng1278.

Gomez, M. (2006) 'PARP1 Is a TRF2-associated Poly(ADP-Ribose)Polymerase and Protects Eroded Telomeres', *Molecular Biology of the Cell*, 17(4), pp. 1686–1696. doi: 10.1091/mbc.E05-07-0672.

Gonzalez-Hunt, C. P. *et al.* (2016) 'PCR-Based Analysis of Mitochondrial DNA Copy Number, Mitochondrial DNA Damage, and Nuclear DNA Damage', *Current protocols in toxicology*. doi: 10.1002/0471140856.tx2011s67.

Gonzalez-Suarez, E. *et al.* (2000) 'Telomerase-deficient mice with short telomeres are resistant to skin tumorigenesis.', *Nature genetics*, 26(1), pp. 114–117. doi: 10.1038/79089.

González-Suárez, E. *et al.* (2001) 'Increased epidermal tumors and increased skin wound healing in transgenic mice overexpressing the catalytic subunit of telomerase, mTERT, in basal keratinocytes', *EMBO Journal*. doi: 10.1093/emboj/20.11.2619.

González-Suárez, E. *et al.* (2005) 'Antagonistic effects of telomerase on cancer and aging in K5-mTert transgenic mice', *Oncogene*. doi: 10.1038/sj.onc.1208413.

Goytisolo, F. A. *et al.* (2000) 'Short telomeres result in organismal hypersensitivity to ionizing radiation in mammals.', *The Journal of experimental medicine*, 192(11), pp. 1625–1636. doi: 10.1084/jem.192.11.1625.

Greenberg, R. A. *et al.* (1999) 'Short dysfunctional telomeres impair tumorigenesis in the INK4a(??2/3) cancer-prone mouse', *Cell*, 97(4), pp. 515–525. doi: 10.1016/S0092-8674(00)80761-8.

Greenberg, R. a *et al.* (1998) 'Expression of mouse telomerase reverse transcriptase during development, differentiation and proliferation.', *Oncogene*, 16(13), pp. 1723–1730. doi: 10.1038/sj.onc.1201933.

Greider, C. W. (1999) 'Telomeres do D-loop-T-loop', *Cell*, pp. 419–422. doi: 10.1016/S0092-8674(00)80750-3.

Greider, C. W. and Blackburn, E. H. (1985) 'Identification of a specific telomere terminal transferase activity in tetrahymena extracts', *Cell*, 43(2 PART 1), pp. 405–413. doi: 10.1016/0092-8674(85)90170-9.

Griffith, J. D. *et al.* (1999) 'Mammalian telomeres end in a large duplex loop', *Cell*, 97(4), pp. 503–514. doi: 10.1016/S0092-8674(00)80760-6.

Guerra, C. *et al.* (2003) 'Tumor induction by an endogenous K-ras oncogene is highly dependent on cellular context', *Cancer Cell*, 4(2), pp. 111–120. doi: 10.1016/S1535-6108(03)00191-0.

Hanahan, D. and Weinberg, R. A. (2011) 'Hallmarks of cancer: The next generation', *Cell*, pp. 646–674. doi: 10.1016/j.cell.2011.02.013.

Harley, C. B., Futcher, A. B. and Greider, C. W. (1990) 'Telomeres shorten during ageing of human fibroblasts', *Nature*, 345(6274), pp. 458–460. doi: 10.1038/345458a0.

Hastie, N. D. *et al.* (1990) 'Telomere reduction in human colorectal carcinoma and with ageing.', *Nature*, 346(6287), pp. 866–868. doi: 10.1038/346866a0.

Haycock, P. C. *et al.* (2017) 'Association between telomere length and risk of cancer and non-neoplastic diseases a mendelian randomization study', *JAMA Oncology*. doi: 10.1001/jamaoncol.2016.5945.

Hayflick, L. and Moorhead, P. S. (1961) 'The serial cultivation of human diploid cell strains', *Experimental Cell Research*, 25(3), pp. 585–621. doi: 10.1016/0014-4827(61)90192-6.

Hemann, M. T. *et al.* (2001) 'Telomere dysfunction triggers developmentally regulated germ cell apoptosis', *Molecular Biology of the Cell*. doi: 10.1091/mbc.12.7.2023.

Hemann, M. T. and Greider, C. W. (2000) 'Wild-derived inbred mouse strains have short telomeres.', *Nucleic acids research*, 28(22), pp. 4474–4478. doi: 10.1093/nar/28.22.4474.

Herrera, E. *et al.* (1999) 'Disease states associated with telomerase deficiency appear earlier in mice with short telomeres', *EMBO Journal*, 18(11), pp. 2950–2960. doi: 10.1093/emboj/18.11.2950.

Herrera, E. (1999) 'Telomere shortening in mTR-/- embryos is associated with failure to close the neural tube', *The EMBO Journal*, 18(5), pp. 1172–1181. doi: 10.1093/emboj/18.5.1172.

Herrera, E., Martínez-A, C. and Blasco, M. a (2000) 'Impaired germinal center reaction in mice with short telomeres.', *The EMBO journal*, 19(3), pp. 472–481. doi: 10.1093/emboj/19.3.472.

Hockemeyer, D. *et al.* (2006) 'Recent Expansion of the Telomeric Complex in Rodents: Two

Distinct POT1 Proteins Protect Mouse Telomeres', *Cell*, 126(1), pp. 63–77. doi: 10.1016/j.cell.2006.04.044.

Hoffmeyer, K. *et al.* (2012) 'Wnt/ -Catenin Signaling Regulates Telomerase in Stem Cells and Cancer Cells', *Science*, 336(6088), pp. 1549–1554. doi: 10.1126/science.1218370.

Horn, S. *et al.* (2013) 'TERT promoter mutations in familial and sporadic melanoma', *Science*. doi: 10.1126/science.1230062.

Houghtaling, B. R. *et al.* (2004) 'A dynamic molecular link between the telomere length regulator TRF1 and the chromosome end protector TRF2', *Current Biology*, 14(18), pp. 1621–1631. doi: 10.1016/j.cub.2004.08.052.

Hu, H. *et al.* (2010) 'Expression of TRF1, TRF2, TIN2, TERT, KU70, and BRCA1 proteins is associated with telomere shortening and may contribute to multistage carcinogenesis of gastric cancer', *Journal of Cancer Research and Clinical Oncology*, 136(9), pp. 1407–1414. doi: 10.1007/s00432-010-0795-x.

Huffman, K. E. *et al.* (2000) 'Telomere shortening is proportional to the size of the G-rich telomeric 3'-overhang', *Journal of Biological Chemistry*, 275(26), pp. 19719–19722. doi: 10.1074/jbc.M002843200.

Ikeno, Y. *et al.* (2003) 'Delayed occurrence of fatal neoplastic diseases in ames dwarf mice: correlation to extended longevity.', *The journals of gerontology. Series A, Biological sciences and medical sciences*.

Ikeno, Y. *et al.* (2009) 'Reduced incidence and delayed occurrence of fatal neoplastic diseases in growth hormone receptor/binding protein knockout mice', *Journals of Gerontology - Series A Biological Sciences and Medical Sciences*. doi: 10.1093/gerona/glp017.

Inagaki, K. *et al.* (2006) 'Robust systemic transduction with AAV9 vectors in mice: efficient global cardiac gene transfer superior to that of AAV8', *Molecular Therapy*. doi: 10.1016/j.ymthe.2006.03.014.

De Jager, M. *et al.* (2001) 'Human Rad50/Mre11 is a flexible complex that can tether DNA ends', *Molecular Cell*, 8(5), pp. 1129–1135. doi: 10.1016/S1097-2765(01)00381-1.

Jaskelioff, M. *et al.* (2011) 'Telomerase reactivation reverses tissue degeneration in aged telomerase-deficient mice', *Nature*. doi: 10.1038/nature09603.

Jimenez, V. *et al.* (2013) 'In vivo adeno-associated viral vector-mediated genetic engineering

of white and brown adipose tissue in adult mice', *Diabetes*. doi: 10.2337/db13-0311.

Joseph, I. *et al.* (2010) 'The telomerase inhibitor imetelstat depletes cancer stem cells in breast and pancreatic cancer cell lines', *Cancer Research*, 70(22), pp. 9494–9504. doi: 10.1158/0008-5472.CAN-10-0233.

Khadka, P. *et al.* (2014) 'DNA-PKcs-interacting protein KIP binding to TRF2 is required for the maintenance of functional telomeres.', *The Biochemical journal*, 463(1), pp. 19–30. doi: 10.1042/BJ20131395.

Kibe, T. *et al.* (2010) 'Telomere Protection by TPP1 Is Mediated by POT1a and POT1b', *Molecular and Cellular Biology*, 30(4), pp. 1059–1066. doi: 10.1128/MCB.01498-09.

Kim, N. *et al.* (1994) 'Specific association of human telomerase activity with immortal cells and cancer', *Science*, 266(5193), pp. 2011–2015. doi: 10.1126/science.7605428.

Kim, S. H. *et al.* (2004) 'TIN2 mediates functions of TRF2 at human telomeres', *Journal of Biological Chemistry*, 279(42), pp. 43799–43804. doi: 10.1074/jbc.M408650200.

Kim, S. H., Kaminker, P. and Campisi, J. (1999) 'TIN2, a new regulator of telomere length in human cells', *Nature Genetics*, 23(4), pp. 405–412. doi: 10.1038/70508.

Kiyozuka, Y. *et al.* (1998) 'Telomere length, telomerase activity and telomerase RNA expression during mouse mammary tumor progression.', *International journal of molecular medicine*. doi: 10.3892/ijmm.2.4.437.

Klobutcher, L. A. *et al.* (1981) 'All gene-sized DNA molecules in four species of hypotrichs have the same terminal sequence and an unusual 3' terminus.', *Proceedings of the National Academy of Sciences*, 78(5), pp. 3015–3019. doi: 10.1073/pnas.78.5.3015.

de Lange, T. *et al.* (1990) 'Structure and variability of human chromosome ends.', *Molecular and cellular biology*, 10(2), pp. 518–527. doi: 10.1128/MCB.10.2.518.Updated.

De Lange, T. (2002) 'Protection of mammalian telomeres', *Oncogene*, pp. 532–540. doi: 10.1038/sj/onc/1205080.

De Lange, T. (2005) 'Shelterin: The protein complex that shapes and safeguards human telomeres', *Genes and Development*, pp. 2100–2110. doi: 10.1101/gad.1346005.

De Lange, T. and DePinho, R. A. (1999) 'Unlimited mileage from tetomerase?', *Science*, pp. 947–948. doi: 10.1126/science.283.5404.947.

Lansdorp, P. M. *et al.* (1996) 'Heterogeneity in telomere length of human chromosomes',

Human Molecular Genetics, 5(5), pp. 685–691. doi: 10.1093/hmg/5.5.685.

Lee, H. W. *et al.* (1998) 'Essential role of mouse telomerase in highly proliferative organs', *Nature*, 392(6676), pp. 569–574. doi: 10.1038/33345.

Lee, J.-H. and Paull, T. T. (2007) 'Activation and regulation of ATM kinase activity in response to DNA double-strand breaks', *Oncogene*, 26(56), pp. 7741–7748. doi: 10.1038/sj.onc.1210872.

Lenain, C. *et al.* (2006) 'The Apollo 5′ Exonuclease Functions Together with TRF2 to Protect Telomeres from DNA Repair', *Current Biology*, 16(13), pp. 1303–1310. doi: 10.1016/j.cub.2006.05.021.

Li, B. (2003) 'Rap1 Affects the Length and Heterogeneity of Human Telomeres', *Molecular Biology of the Cell*, 14(12), pp. 5060–5068. doi: 10.1091/mbc.E03-06-0403.

Li, B., Oestreich, S. and De Lange, T. (2000) 'Identification of human Rap1: Implications for telomere evolution', *Cell*, 101(5), pp. 471–483. doi: 10.1016/S0092-8674(00)80858-2.

Li, L. *et al.* (2011) 'Defective nonhomologous end joining blocks B-cell development in FLT3/ITD mice', *Blood*, 117(11), pp. 3131–3139. doi: 10.1182/blood-2010-05-286070.

Lipps, H. J. and Rhodes, D. (2009) 'G-quadruplex structures: in vivo evidence and function', *Trends in Cell Biology*, pp. 414–422. doi: 10.1016/j.tcb.2009.05.002.

Liu, D. *et al.* (2004) 'Telosome, a mammalian telomere-associated complex formed by multiple telomeric proteins', *Journal of Biological Chemistry*, 279(49), pp. 51338–51342. doi: 10.1074/jbc.M409293200.

Liu, L. *et al.* (2002) 'An essential role for functional telomeres in mouse germ cells during fertilization and early development', *Developmental Biology*. doi: 10.1006/dbio.2002.0735.

Liu, L. *et al.* (2007) 'Telomere lengthening early in development', *Nature Cell Biology*. doi: 10.1038/ncb1664.

Liu, T., Yuan, X. and Xu, D. (2016) 'Cancer-specific telomerase reverse transcriptase (Tert) promoter mutations: Biological and clinical implications', *Genes*. doi: 10.3390/genes7070038.

Loayza, D. and De Lange, T. (2003) 'POT1 as a terminal transducer of TRF1 telomere length control', *Nature*, 423(6943), pp. 1013–1018. doi: 10.1038/nature01688.

Longhese, M. P. *et al.* (2010) 'Mechanisms and regulation of DNA end resection', *The*

EMBO Journal, 29(17), pp. 2864–2874. doi: 10.1038/emboj.2010.165.

López-Otín, C. *et al.* (2013) 'The hallmarks of aging', *Cell*. doi: 10.1016/j.cell.2013.05.039.

Ma, X. *et al.* (2014) 'Recurrent TERT promoter mutations in non-small cell lung cancers', *Lung Cancer*. doi: 10.1016/j.lungcan.2014.10.009.

Mainardi, S. *et al.* (2014) 'Identification of cancer initiating cells in K-Ras driven lung adenocarcinoma', *Proceedings of the National Academy of Sciences of the United States of America*. doi: 10.1073/pnas.1320383110.

Mantell, L. L. and Greider, C. W. (1994) 'Telomerase activity in germline and embryonic cells of Xenopus.', *The EMBO Journal*. doi: 10.1002/j.1460-2075.1994.tb06620.x.

Marcand, S. *et al.* (2000) 'Cell cycle restriction of telomere elongation', *Current Biology*, 10(8), pp. 487–490. doi: 10.1016/S0960-9822(00)00450-4.

Marcand, S., Gilson, E. and Shore, D. (1997) 'A protein-counting mechanism for telomere length regulation in yeast', *Science*, 275(5302), pp. 986–990. doi: 10.1126/science.275.5302.986.

Marion, R. M. *et al.* (2009) 'Telomeres Acquire Embryonic Stem Cell Characteristics in Induced Pluripotent Stem Cells', *Cell Stem Cell*, 4(2), pp. 141–154. doi: 10.1016/j.stem.2008.12.010.

Marion, R. M. and Blasco, M. A. (2010) 'Telomeres and telomerase in adult stem cells and pluripotent embryonic stem cells', *Advances in Experimental Medicine and Biology*. doi: 10.1007/978-1-4419-7037-4_9.

Martín-Rivera, L. and Blasco, M. A. (2001) 'Identification of Functional Domains and Dominant Negative Mutations in Vertebrate Telomerase RNA Using an in Vivo Reconstitution System', *Journal of Biological Chemistry*. doi: 10.1074/jbc.M008419200.

Martinez, P. *et al.* (2010) 'Mammalian Rap1 controls telomere function and gene expression through binding to telomeric and extratelomeric sites', *Nature Cell Biology*, 12(8), pp. 768–780. doi: 10.1038/ncb2081.

Martínez, P. *et al.* (2009) 'Increased telomere fragility and fusions resulting from TRF1 deficiency lead to degenerative pathologies and increased cancer in mice', *Genes and Development*, 23(17), pp. 2060–2075. doi: 10.1101/gad.543509.

Martínez, P. *et al.* (2013) 'RAP1 Protects from Obesity through Its Extratelomeric Role

Regulating Gene Expression', *Cell Reports*, 3(6), pp. 2059–2074. doi: 10.1016/j.celrep.2013.05.030.

Martínez, P. and Blasco, M. A. (2011) 'Telomeric and extra-telomeric roles for telomerase and the telomere-binding proteins', *Nature Reviews Cancer*, 11(3), pp. 161–176. doi: 10.1038/nrc3025.

Martínez, P. and Blasco, M. A. (2017) 'Telomere-driven diseases and telomere-targeting therapies', *Journal of Cell Biology*. doi: 10.1083/jcb.201610111.

McClintock, B. (1941) 'The Stability of Broken Ends of Chromosomes in Zea Mays.', *Genetics*, 26(2), pp. 234–282. doi: 10.1038/378739a0.

Meyne, J., Ratliff, R. L. and Moyzis, R. K. (1989) 'Conservation of the human telomere sequence (TTAGGG)n among vertebrates.', *Proceedings of the National Academy of Sciences of the United States of America*, 86(18), pp. 7049–7053. doi: 10.1073/pnas.86.18.7049.

Mitchell, J. R., Wood, E. and Collins, K. (1999) 'A telomerase component is defective in the human disease dyskeratosis congenita', *Nature*, 402(6761), pp. 551–555. doi: 10.1038/990141.

Montgomery, R. K. *et al.* (2011) 'Mouse telomerase reverse transcriptase (mTert) expression marks slowly cycling intestinal stem cells', *Proceedings of the National Academy of Sciences*, 108(1), pp. 179–184. doi: 10.1073/pnas.1013004108.

Muller, H. (1938) 'The remaking of chromosomes', *The Collecting Net - Woods Hole*.

Muntoni, A. and Reddel, R. R. (2005) 'The first molecular details of ALT in human tumor cells', *Human Molecular Genetics*, 14(SUPPL. 2). doi: 10.1093/hmg/ddi266.

Naxerova, K. and Elledge, S. J. (2015) 'Taking the brakes off telomerase', *eLife*. doi: 10.7554/eLife.09519.

Nayak, S. and Herzog, R. W. (2010) 'Progress and prospects: Immune responses to viral vectors', *Gene Therapy*. doi: 10.1038/gt.2009.148.

Newey, P. J. *et al.* (2012) 'Whole-exome sequencing studies of nonhereditary (sporadic) parathyroid adenomas', *Journal of Clinical Endocrinology and Metabolism*, 97(10). doi: 10.1210/jc.2012-2303.

Nussenzweig, A. and Nussenzweig, M. C. (2007) 'A Backup DNA Repair Pathway Moves to

the Forefront', *Cell*, pp. 223–225. doi: 10.1016/j.cell.2007.10.005.

Ohmura, H. *et al.* (1995) 'Restoration of the Cellular Senescence Program and Repression of Telomerase by Human Chromosome 3', *Japanese Journal of Cancer Research*, 86(10), pp. 899–904. doi: 10.1111/j.1349-7006.1995.tb02998.x.

Okazaki, R. *et al.* (1967) 'Mechanism of DNA replication possible discontinuity of DNA chain growth.', *Japanese Journal of Medical Science and Biology*.

Okita, K., Ichisaka, T. and Yamanaka, S. (2007) 'Generation of germline-competent induced pluripotent stem cells', *Nature*. doi: 10.1038/nature05934.

Olovnikov, A. M. (1973) 'A theory of marginotomy. The incomplete copying of template margin in enzymic synthesis of polynucleotides and biological significance of the phenomenon', *Journal of Theoretical Biology*, 41(1), pp. 181–190. doi: 10.1016/0022-5193(73)90198-7.

Opresko, P. L. *et al.* (2002) 'Telomere-binding protein TRF2 binds to and stimulates the Werner and Bloom syndrome helicases', *Journal of Biological Chemistry*, 277(43), pp. 41110–41119. doi: 10.1074/jbc.M205396200.

Perera, S. A. *et al.* (2008) 'Telomere dysfunction promotes genome instability and metastatic potential in a K-ras p53 mouse model of lung cancer', *Carcinogenesis*. doi: 10.1093/carcin/bgn050.

Povedano, J. M. *et al.* (2015) 'Mice with Pulmonary Fibrosis Driven by Telomere Dysfunction', *Cell Reports*, 12(2), pp. 286–299. doi: 10.1016/j.celrep.2015.06.028.

Povedano, J. M. *et al.* (2018) 'Therapeutic effects of telomerase in mice with pulmonary fibrosis induced by damage to the lungs and short telomeres', *eLife*. doi: 10.7554/eLife.31299.

Prudhomme, J. and Morey, C. (2016) 'Epigenesis and plasticity of mouse trophoblast stem cells', *Cellular and Molecular Life Sciences*. doi: 10.1007/s00018-015-2086-9.

Ramsay, A. J. *et al.* (2013) 'POT1 mutations cause telomere dysfunction in chronic lymphocytic leukemia', *Nature genetics*, 45(5), pp. 526–530. doi: 10.1038/ng.2584.

Riballo, E. *et al.* (2004) 'A pathway of double-strand break rejoining dependent upon ATM, Artemis, and proteins locating to $γ$-H2AX foci', *Molecular Cell*, 16(5), pp. 715–724. doi: 10.1016/j.molcel.2004.10.029.

Robles-Espinoza, C. D. *et al.* (2014) 'POT1 loss-of-function variants predispose to familial melanoma', *Nature Genetics*, 46(5), pp. 478–481. doi: 10.1038/ng.2947.

Rudolph, K. L. *et al.* (1999) 'Longevity, stress response, and cancer in aging telomerase-deficient mice', *Cell*, 96(5), pp. 701–712. doi: 10.1016/S0092-8674(00)80580-2.

Sachsinger, J. *et al.* (2001) 'Telomerase inhibition in RenCa, a murine tumor cell line with short telomeres, by overexpression of a dominant negative mTERT mutant, reveals fundamental differences in telomerase regulation between human and murine cells', *Cancer Research*.

Sahin, E. *et al.* (2011) 'Telomere dysfunction induces metabolic and mitochondrial compromise', *Nature*. doi: 10.1038/nature09787.

Sahin, E. and DePinho, R. A. (2012) 'Axis of ageing: Telomeres, p53 and mitochondria', *Nature Reviews Molecular Cell Biology*. doi: 10.1038/nrm3352.

Sallmyr, A., Tomkinson, A. E. and Rassool, F. V (2008) 'Up-regulation of WRN and DNA ligase III in chronic myeloid leukemia: consequences for the repair of DNA double-strand breaks', *Blood*, 112(4), pp. 1413–1423. doi: 10.1182/blood-2007-07-104257.

Samper, E. *et al.* (2002) 'Long-term repopulating ability of telomerase-deficient murine hematopoietic stem cells', *Blood*, 99(8), pp. 2767–2775. doi: 10.1182/blood.V99.8.2767.

San Filippo, J., Sung, P. and Klein, H. (2008) 'Mechanism of Eukaryotic Homologous Recombination', *Annual Review of Biochemistry*. doi: 10.1146/annurev.biochem.77.061306.125255.

Schaetzlein, Sonja *et al.* (2004) 'Telomere length is reset during early mammalian embryogenesis', *Proceedings of the National Academy of Sciences of the United States of America*. doi: 10.1073/pnas.0402400101.

Schaetzlein, S. *et al.* (2004) 'Telomere length is reset during early mammalian embryogenesis', *Proceedings of the National Academy of Sciences*. doi: 10.1073/pnas.0402400101.

Schepers, A. G. *et al.* (2011) 'Lgr5 intestinal stem cells have high telomerase activity and randomly segregate their chromosomes', *EMBO Journal*, 30(6), pp. 1104–1109. doi: 10.1038/emboj.2011.26.

Seger, Y. R. *et al.* (2002) 'Transformation of normal human cells in the absence of telomerase activation', *Cancer Cell*. doi: 10.1016/S1535-6108(02)00183-6.

Serrano, M. *et al.* (1997) 'Oncogenic ras provokes premature cell senescence associated with accumulation of p53 and p16(INK4a)', *Cell*. doi: 10.1016/S0092-8674(00)81902-9.

Sfeir, A. *et al.* (2009) 'Mammalian Telomeres Resemble Fragile Sites and Require TRF1 for Efficient Replication', *Cell*, 138(1), pp. 90–103. doi: 10.1016/j.cell.2009.06.021.

Sfeir, A. *et al.* (2010) 'Loss of Rap1 induces telomere recombination in the absence of NHEJ or a DNA damage signal', *Science*, 327(5973), pp. 1657–1661. doi: 10.1126/science.1185100.

Shay, J. W. (2016) 'Role of telomeres and telomerase in aging and cancer', *Cancer Discovery*. doi: 10.1158/2159-8290.CD-16-0062.

Shay, J. W. and Bacchetti, S. (1997) 'A survey of telomerase activity in human cancer.', *European journal of cancer (Oxford, England : 1990)*, 33(5), pp. 787–791. doi: 10.1016/S0959-8049(97)00062-2.

Shi, J. *et al.* (2014) 'Rare missense variants in POT1 predispose to familial cutaneous malignant melanoma', *Nat Genet*, 46(5), pp. 482–486. doi: 10.1038/ng.2941.

Smith, S. (1998) 'Tankyrase, a Poly(ADP-Ribose) Polymerase at Human Telomeres', *Science*, 282(5393), pp. 1484–1487. doi: 10.1126/science.282.5393.1484.

Smogorzewska, A. *et al.* (2000) 'Control of Human Telomere Length by TRF1 and TRF2', *Molecular and Cellular Biology*, 20(5), pp. 1659–1668. doi: 10.1128/MCB.20.5.1659-1668.2000.

Smogorzewska, A. *et al.* (2002) 'DNA ligase IV-dependent NHEJ of deprotected mammalian telomeres in G1 and G2', *Current Biology*, 12(19), pp. 1635–1644. doi: 10.1016/S0960-9822(02)01179-X.

Smogorzewska, A. and de Lange, T. (2002) 'Different telomere damage signaling pathways in human and mouse cells.', *The EMBO journal*, 21(16), pp. 4338–4348. doi: 10.1093/emboj/cdf433.

Sundquist, W. I. and Klug, A. (1989) 'Telomeric DNA dimerizes by formation of guanine tetrads between hairpin loops', *Nature*, 342(6251), pp. 825–829. doi: 10.1038/342825a0.

Suram, A. *et al.* (2012) 'Oncogene-induced telomere dysfunction enforces cellular senescence in human cancer precursor lesions', *EMBO Journal*. doi: 10.1038/emboj.2012.132.

Takahashi, K. and Yamanaka, S. (2006) 'Induction of Pluripotent Stem Cells from Mouse Embryonic and Adult Fibroblast Cultures by Defined Factors', *Cell*. doi: 10.1016/j.cell.2006.07.024.

Takai, H., Smogorzewska, A. and De Lange, T. (2003) 'DNA damage foci at dysfunctional telomeres', *Current Biology*. doi: 10.1016/S0960-9822(03)00542-6.

Tang, J. *et al.* (2008) 'G-quadruplex preferentially forms at the very 3′ end of vertebrate telomeric DNA', *Nucleic Acids Research*, 36(4), pp. 1200–1208. doi: 10.1093/nar/gkm1137.

Tejera, A. M. *et al.* (2010) 'TPP1 is required for TERT recruitment, telomere elongation during nuclear reprogramming, and normal skin development in mice', *Developmental Cell*, 18(5), pp. 775–789. doi: 10.1016/j.devcel.2010.03.011.

Tomás-Loba, A. *et al.* (2008) 'Telomerase Reverse Transcriptase Delays Aging in Cancer-Resistant Mice', *Cell*, 135(4), pp. 609–622. doi: 10.1016/j.cell.2008.09.034.

Tsakiri, K. D. *et al.* (2007) 'Adult-onset pulmonary fibrosis caused by mutations in telomerase', *Proceedings of the National Academy of Sciences*, 104(18), pp. 7552–7557. doi: 10.1073/pnas.0701009104.

Varela, E. *et al.* (2011) 'Different telomere-length dynamics at the inner cell mass versus established embryonic stem (ES) cells', *Proceedings of the National Academy of Sciences*, 108(37), pp. 15207–15212. doi: 10.1073/pnas.1105414108.

Vaziri, H. and Benchimol, S. (1998) 'Reconstitution of telomerase activity in normal human cells leads to elongation of telomeres and extended replicative life span', *Current Biology*, 8(5), pp. 279–282. doi: 10.1016/S0960-9822(98)70109-5.

Venegas, V. and Halberg, M. C. (2012) 'Measurement of mitochondrial DNA copy number', *Methods in Molecular Biology*. doi: 10.1007/978-1-61779-504-6_22.

Vera, E. *et al.* (2012) 'The Rate of Increase of Short Telomeres Predicts Longevity in Mammals', *Cell Reports*. doi: 10.1016/j.celrep.2012.08.023.

Wang, M. *et al.* (2006) 'PARP-1 and Ku compete for repair of DNA double strand breaks by distinct NHEJ pathways', *Nucleic Acids Research*, 34(21), pp. 6170–6182. doi: 10.1093/nar/gkl840.

Wentzensen, I. M. *et al.* (2011) 'The association of telomere length and cancer: A meta-analysis', *Cancer Epidemiology Biomarkers and Prevention*. doi: 10.1158/1055-9965.EPI-11-0005.

Williamson, J. R., Raghuraman, M. K. and Cech, T. R. (1989) 'Monovalent cation-induced structure of telomeric DNA: The G-quartet model', *Cell*, 59(5), pp. 871–880. doi: 10.1016/0092-8674(89)90610-7.

Wu, P., Takai, H. and De Lange, T. (2012) 'Telomeric 3′ overhangs derive from resection by Exo1 and apollo and fill-in by POT1b-associated CST', *Cell*, 150(1), pp. 39–52. doi: 10.1016/j.cell.2012.05.026.

Wu, Z., Yang, H. and Colosi, P. (2010) 'Effect of genome size on AAV vector packaging', *Molecular Therapy*. doi: 10.1038/mt.2009.255.

Xu, J. and Yang, X. (2000) 'Telomerase Activity in Bovine Embryos During Early Development1', *Biology of Reproduction*. doi: 10.1095/biolreprod63.4.1124.

Yamaguchi, H. *et al.* (2005) 'Mutations in TERT, the gene for telomerase reverse transcriptase, in aplastic anemia.', *The New England journal of medicine*, 352(14), pp. 1413–1424. doi: 10.1056/NEJMoa042980.

Yaneva, M., Kowalewski, T. and Lieber, M. R. (1997) 'Interaction of DNA-dependent protein kinase with DNA and with Ku: Biochemical and atomic-force microscopy studies', *EMBO Journal*. doi: 10.1093/emboj/16.16.5098.

Yang, J. *et al.* (1999) 'Human endothelial cell life extension by telomerase expression.', *The Journal of biological chemistry*, 274(37), pp. 26141–26148. doi: 10.1074/jbc.274.37.26141.

Yang, M. and Crawley, J. N. (2009) 'Simple behavioral assessment of mouse olfaction', *Current Protocols in Neuroscience*, (SUPPL. 48). doi: 10.1002/0471142301.ns0824s48.

Ye, J Z S *et al.* (2004) 'POT1-interaction protein PIP1: A telomere length regulator that recruits POT1 to the TIN2/TRF1 complex', *Genes and Development*, 18(14), pp. 1649–1654. doi: 10.1101/gad.1215404.

Ye, Jeffrey Zheng Sheng *et al.* (2004) 'TIN2 binds TRF1 and TRF2 simultaneously and stabilizes the TRF2 complex on telomeres', *Journal of Biological Chemistry*, 279(45), pp. 47264–47271. doi: 10.1074/jbc.M409047200.

Zhang, J. *et al.* (2014) 'The genomic landscape of mantle cell lymphoma is related to the epigenetically determined chromatin state of normal B cells', *Blood*, 123(19), pp. 2988–2996. doi: 10.1182/blood-2013-07-517177.

Zhu, X. D. *et al.* (2000) 'Cell-cycle-regulated association of RAD50/MRE11/NBS1 with TRF2 and human telomeres', *Nature Genetics*, 25(3), pp. 347–352. doi: 10.1038/77139.

Zhu, X. D. *et al.* (2003) 'ERCC1/XPF Removes the 3′ Overhang from Uncapped Telomeres and Represses Formation of Telomeric DNA-Containing Double Minute Chromosomes', *Molecular Cell*, 12(6), pp. 1489–1498. doi: 10.1016/S1097-2765(03)00478-7.

Zijlmans, J. M. *et al.* (1997) 'Telomeres in the mouse have large inter-chromosomal variations in the number of T2AG3 repeats.', *Proceedings of the National Academy of Sciences of the United States of America*, 94(14), pp. 7423–7428. doi: 10.1073/pnas.94.14.7423.

Acknowledgements

Thank you, Maria, for giving me the opportunity to be part of your laboratory during these years under your supervision. Thank you, Rosa, for all your help with the mice. Thanks to the CNIO units, thank you Diego, for giving us such an amazing support.

Thanks to all the members of the Telomeres and Telomerase group, past and present, for being like a family. Thanks to our ex-neighbors the Tumor Suppressors for all the good moments.

Gracias a mis padres, a mi hermana y al resto de mi familia por su apoyo incondicional y por estar siembre ahí.

Annexes

The present doctoral thesis has led to the elaboration of the following articles:

- Varela, E. *et al.* (2016) 'Generation of mice with longer and better preserved telomeres in the absence of genetic manipulations', *Nature Communications*, 7. doi: 10.1038/ncomms11739.

- Muñoz-Lorente, M. A. *et al.* (2018) 'AAV9-mediated telomerase activation does not accelerate tumorigenesis in the context of oncogenic K-Ras-induced lung cancer', *PLoS Genetics*. doi: 10.1371/journal.pgen.1007562.

- Muñoz-Lorente, M. A. *et al.* (2019) 'Mice with hyper-long telomeres show less metabolic aging and longer lifespans', *Nature Communications,* 10.doi: 10.1038/s41467-019-12664-x.